



Calhoun: The NPS Institutional Archive DSpace Repository

Theses and Dissertations

1. Thesis and Dissertation Collection, all items

1963

The performance of high power output axial flow turbines utilizing flows in the transonic regime

Howard, Robert E.

Monterey, California: U.S. Naval Postgraduate School

<http://hdl.handle.net/10945/12814>

Downloaded from NPS Archive: Calhoun



<http://www.nps.edu/library>

Calhoun is the Naval Postgraduate School's public access digital repository for research materials and institutional publications created by the NPS community.

Calhoun is named for Professor of Mathematics Guy K. Calhoun, NPS's first appointed -- and published -- scholarly author.

Dudley Knox Library / Naval Postgraduate School
411 Dyer Road / 1 University Circle
Monterey, California USA 93943

NPS ARCHIVE
1963
HOWARD, R.

THE PERFORMANCE OF HIGH POWER OUTPUT
AXIAL FLOW TURBINES UTILIZING FLOWS
IN THE TRANSONIC REGIME

ROBERT E. HOWARD

LIBRARY

U.S. NAVAL POSTGRADUATE SCHOOL
MONTEREY, CALIFORNIA

THE PERFORMANCE OF HIGH POWER OUTPUT AXIAL
FLOW TURBINES UTILIZING FLOWS IN THE TRANSONIC REGIME

Robert E. Howard, Jr.

THE PERFORMANCE OF HIGH POWER OUTPUT AXIAL
FLOW TURBINES UTILIZING FLOWS IN THE TRANSONIC REGIME

by

Robert E. Howard, Jr.

Major, United States Marine Corps

Submitted in partial fulfillment of
the requirements for the degree of

MASTER OF SCIENCE
IN
AERONAUTICAL ENGINEERING

United States Naval Postgraduate School
Monterey, California

1963

PS Archive
963
Howard, R.

42017

1963 - Project Report: The use of the 1000

1963 - Project Report: The use of the 1000

1963 - Project Report

1963 - Project Report: The use of the 1000

1963 - Project Report: The use of the 1000

1963 - Project Report

1963 - Project Report

1963 - Project Report: The use of the 1000

1963 -

THE PERFORMANCE OF HIGH POWER OUTPUT AXIAL
FLOW TURBINES UTILIZING FLOWS IN THE TRANSONIC REGIME

by

Robert E. Howard, Jr.

This work is accepted as fulfilling
the thesis requirements for the degree of
MASTER OF SCIENCE
IN
AERONAUTICAL ENGINEERING
from the
United States Naval Postgraduate School

ABSTRACT

The equations for estimating the performance of an axial flow turbine are examined to determine the efficiency and other parameters when very high power outputs per stage are required. It is indicated that turbine stages should be designed for peak efficiency or for high power output, but that compromise designs are not advisable.

A survey of the immediately available literature on losses in turbine stages at the U. S. Naval Postgraduate School is outlined. An attempt to find and correlate specific loss data with theoretical relations was not successful. Data is fragmentary, theoretical relations are few, and the correlation of the available data on profile losses, tip clearance losses, effect of trailing edge thickness and secondary losses is poor.

An axial flow single stage turbine was designed for transonic flows and a digital computer program was written to evaluate the off-design performance of this turbine. The particular relations for supersonic expansion after a blade row are included in the program as well as the effects of entry shocks into the rotor. Initial indications are that the program should be useful for evaluating turbines designed by the procedure shown.

The computer programs included are written in FORTRAN language for the CDC 1604 Digital Computer.

ACKNOWLEDGEMENT

The assistance, teaching and encouragement of Dr. M. H. Vavra of the U. S. Naval Postgraduate School are gratefully acknowledged. The lines of investigation in this thesis were prompted by him, and it has been a pleasure to study under his instruction.

Table of Contents

<u>Section</u>	<u>Title</u>	<u>Page</u>
I.	Introduction	1
II.	Development of High Head Coefficient Data	3
	A. Basic Equations	3
	B. Computer Program	5
	C. Results	6
III.	Loss Investigation	9
	A. Loss Components	9
	B. Survey of the Literature	12
	C. Results of Loss Investigation	30
	1. Profile Loss	30
	2. Tip Clearance Loss	31
	3. Trailing Edge Loss	32
	4. Secondary Loss	32
	5. Comparison of Methods Quantitatively	33
IV.	Design of Turbine	36
	A. Loss Coefficient Data	36
	B. Flow Function	37
	C. Geometry and Velocity Triangles	39
	D. Dimensionless Parameters	40
	E. Design Computations	41
V.	Computer Program	
	A. General Considerations	53
	B. Main Program	53
	C. Subroutines	56
	1. Subroutine for Velocity Triangle Computation	56
	2. Subroutine to Compute After-expansion	56
	3. Subroutine to Compute Flow Function	56
	4. Subroutine to Compute Entry Shocks in Rotor	57
	5. Subroutine to Find Data Points for Losses	57
	D. Results of Computer Program	57

<u>Section</u>	<u>Title</u>	<u>Page</u>
VI.	Conclusions and Recommendations	63
	A. Conclusions	63
	B. Recommendations	65
Appendix I.	Development of Flow Function Relations	104
Appendix II.	After-expansion from a Blade Row	109
Appendix III.	Computer Programs and Flow Charts	117
Appendix IV.	Critical Mach Number of Flow Undergoing Polytropic Expansion	157
Appendix V.	Computer Program Printouts	Separate Cover

List of Illustrations

<u>Figure</u>		<u>Page</u>
1	Efficiency vs. Head Coefficients	70
2	High Head Coefficient Data, $\alpha_1 = 60^\circ$	71
3	High Head Coefficient Data, $\alpha_1 = 65^\circ$	72
4	High Head Coefficient Data, $\alpha_1 = 70^\circ$	73
5	High Head Coefficient Data, $\alpha_1 = 75^\circ$	74
6	Flow Between Two Blades of an Arbitrary Cascade	10
7	Flow in the Boundary Layer of a Cascade Channel	12
8	Flow Coefficient ψ as a Function of Turning Angle in a Cascade	14
9	Tip Clearance Loss Coefficients	75
10	Profile Loss Coefficients	76
11	Secondary Loss According to Markov	77
12	Vector Diagram of Flow Through an Arbitrary Cascade	78
13	Vector Diagram of Lift and Drag Forces on One Blade	79
14	H-s Diagram for the Relative Flow in a Rotor	80
15	Secondary Loss According to Meldahl	81
16	Profile Loss Coefficients for Conventional Section Blades at Zero Incidence	82
17	Secondary Losses in Turbine Blade Rows	83
18	Secondary Losses According to Ainley	84
19	Effect of Trailing Edge Thickness on Blade Loss Coefficients	83
20	Trailing Edge Thickness Loss Coefficients	85
21	Stator Loss Coefficients	86
22	Rotor Loss Coefficients	87
23	Effect of Blade Height on Loss Coefficients	88
24	T-s Diagram of Expansion Process Through a Turbine	89
25	Stator and Rotor Blade Design at Mean Diameter	90
26	Velocity Triangles of Turbine Flow	91
27	Flow Function for $\gamma = 1.37$	92

<u>Figure</u>		<u>Page</u>
28	After-expansion at $\gamma = 1.37$ and $\alpha_1 = 75^\circ$	93
29	Blading for Rotor Design	94
30	Dimensions of Rotor Blades	95
31	Design Computations for Turbine from Computer Program	96
32	H-s Diagram for Polytropic Expansion	97
33	Relations for After-expansion from Cascade	109
34	H-s Diagram for After-expansion Process	98
35	Turbine Efficiency vs. Pressure Ratio	99
36	Power Coefficient vs. Turbine Efficiency	100
37	Power Coefficient vs. Pressure Ratio	101
38	Turbine Performance Map	102
39	Power Coefficient vs. Turbine Efficiency, Referred to Design Point	103

List of Tables

<u>Table</u>		<u>Page</u>
I.	Head Coefficients and Other Parameters from High Efficiency Down to 40% Efficiency	Separate Cover
II.	Head Coefficients for Peak Efficiency, and Other Parameters	Separate Cover
III.	Flow Function and Polytropic Loss Coefficients	Separate Cover
IV.	Turbine Physical Dimensions	34
V.	Stator Loss Coefficient Comparison	34
VI.	Rotor Loss Coefficient Comparison	35
VII.	Choked Flow Values of Flow Function and Pressure Ratio	Separate Cover
VIII.	Turbine Performance Printout	Separate Cover
IX.	Comparison of Theoretical and Turbine Design Values	61

Symbols and Units

<u>Symbol</u>	<u>Definition</u>	<u>Units</u>
a	Minimum distance between blades	inches
A	Area	in ²
b	Minimum distance between blades, Appendix II	inches
b	Blade width in axial direction	inches
B	Constant, used in equation (38)	
c	Chord of blade	inches
C	Constant	
c_o	Theoretical velocity for isentropic expansion from stagnation pressure ahead of stator to static pressure behind rotor	ft/sec
c_L	Lift coefficient	
c_D	Drag coefficient	
c_p	Specific heat at constant pressure	Btu/lbm °R
(d)	Discharge plane	
D	Drag	lbs
D_m	Mean diameter	inches
(e)	Exit plane	
f	Reheat factor	
F	Force	lbs
g	Acceleration of gravity, used as a conversion factor, 32.174	lbf-ft/lbm-sec ²
h	Blade height	inches
h	Static enthalpy	Btu/lbm
I.D.	Inner diameter of turbine annulus flow area	inches

J	Mechanical equivalent of heat, 778.17	ft-lbf/Btu
k	Radial clearance	inches
k_E	Leaving loss coefficient	
k_{is}	Head coefficient	
K	Constant	
K_2	Form factor, Meldahl	
K_h	Blade height correction factor	
L	Lift	lbs
m_S	Mass flow rate	lbm/sec
M	Mach number (subscripted with appropriate velocity)	
n	Polytropic exponent	
O. D.	Outer diameter of turbine annulus flow area	inches
p	Static pressure	lbf/in ² abs
P	Total pressure	lbf/in ² abs
r	Pressure ratio, P/p in Appendix I	
r^*	Degree of reaction	
R	Gas constant	ft-lbf/lbm $^{\circ}$ R
R	Mean radius	inches
s	Spacing of blades	inches
s	Entropy	inches
t	Maximum blade thickness	inches
t_e	Trailing edge blade thickness	inches
T	Temperature	$^{\circ}$ R
U	Peripheral velocity at mean blade diameter	ft/sec
v	Specific volume	ft ³ /lbm

\dot{w}	Mass flow rate	lbm/sec
W	Relative flow velocity	ft/sec
(W)	Wall	
X	An algebraic relation defined by eq.(5a)	
Y	Loss coefficient, Ainley	
z	Number of blades	
α	Absolute flow angles	deg., radians
β	Relative flow angles	deg., radians
γ	Ratio of specific heats	
γ_E	End quantity, Meldahl	
δ_E	End loss, Meldahl	
Δ	A small finite interval	
ξ	End loss, Markov	
ζ	Loss coefficient	
η	Efficiency	
Γ	Circulation	ft ³ /sec
λ	Parameter for secondary flow, Ainley eq. (41)	
λ	Power coefficient, eq. (54)	
π	Conversion factor, 3.1415927/180	radians/ deg
ρ	Density	lbm/ft ³
ϕ	Flow function	
ϕ_E	Carryover coefficient of kinetic energy into next turbine stage	
ϕ_R	Carryover coefficient of kinetic energy from stator to rotor	
ψ	Velocity coefficient in rotor	
ψ	Velocity coefficient in stator	
ψ_T	Aerodynamic load coefficient, Zweifel	

Subscripts

a	"Flow" loss coefficient
a	Axial velocity component
A	Computed according to eq. (3)
A	After-expansion loss coefficient
cr	Critical, at choked flow condition
d	Discharge plane
e	Edge, losses
e	Exit plane
i	Internal
is	Isentropic
m	Meridional velocity component
o	Stagnation or total
o	Initial or reference value, when used with ψ and ζ
opt	Optimum
P	Polytropic
p	Profile
R	Relative
R2	Rotor blade
S1	Stator blade
s	Secondary loss
te	Trailing edge
th	Theoretical
n	Peripheral velocity component
(2-dim)	Two-dimensional
0	Station ahead of stator in a turbine stage
1	Station between stator and rotor in a turbine stage
2	Station behind rotor in a turbine stage
∞	Infinity, velocity field infinitely far from blade row

Superscript

* Explained where used.

Note: Computer program names and their meanings given in Appendix III.

Note: Velocity and flow angle relations measured as shown in Fig. 26, with sign convention as given on page 39.

Note: Physical dimensions of the turbine design are as shown in Fig. 25 with numerical values given in Table IV.

THE PERFORMANCE OF HIGH POWER OUTPUT AXIAL
FLOW TURBINES UTILIZING FLOWS IN THE TRANSONIC REGIME

I. Introduction

The increasing need in space applications for turbines of high power output from a minimum physical volume and weight requires more knowledge of efficiency, losses and performance estimation of these turbines.

If the required power output and space limitations are predominant then efficiency must suffer. As a means of showing the degree of efficiency sacrificed, the equations which determine the power output and efficiency of an arbitrary turbine were programmed for digital computer solution in terms of the head coefficient. The head coefficient for peak efficiency was determined and then the head coefficient was increased in increments and various parameters affecting the turbine performance were computed at each increment until the efficiency dropped to an arbitrary cutoff point. The data are plotted in non-dimensional form and simple equations are found to represent the data.

Of paramount importance in the design of a turbine is the estimation of the losses due to boundary layer formation, mixing effects, clearances and secondary flows. This area is explored in the hope of finding a more accurate and precise method of presenting these losses. A survey of the immediately available literature is included.

A particular single-stage turbine is designed for supersonic flow leaving the stator blade row and a relative subsonic flow as seen by the rotor. The equations for determining the effects of after-expansion behind a blade row and entry shocks entering a blade row are programmed for the computer in addition to the regular performance parameters. The rpm and pressure ratio across the turbine are then varied to show the effects of demanding extreme power outputs from a turbine so designed. A performance map of the turbine is developed.

II. Development of High Head Coefficient Data

A. Basic Equations

In Ref. 1 the equations are developed to establish the design parameters for turbine stages. These equations are obtained by assuming that the flow through the turbine is represented by the conditions on a mean stream surface and the primary parameter is taken to be the "head coefficient". The head coefficient relates the total isentropic drop of the stage from the inlet stagnation pressure to the discharge static pressure to the kinetic "energy" of the peripheral speed at the rotor entrance and is defined as

$$k_{is} = \frac{\Delta h_{is}}{U_1^2/2} = \left(\frac{C_0}{U_1} \right)^2 \quad (1)$$

In order to relate the theoretical expressions to values found in engineering use, some expression for the losses involved must be used. A velocity coefficient (ψ) is used as a measure of rotor efficiency and is defined as

$$\psi = \frac{W_2}{W_{2th}} \quad (2)$$

This velocity coefficient has been found through experience to depend primarily on the deflection of the flow in the rotor ($\Delta\beta$). Vavra has established a mean curve through data from a variety of sources to be

$$\psi = 0.99 - \frac{2.28}{10^4} \Delta\beta - \frac{4.97}{180 - \Delta\beta} \quad (3)$$

and this equation is used to represent the losses for purposes of evaluating the efficiency at each step of the calculation.

Following the procedure outlined in Ref. 1, arbitrary values were chosen for the angle of the flow leaving the stator (α_1), reheat factor (f), and the carryover coefficient of kinetic energy into the next stage (ϕ_E), the radius ratio (R_2/R_1), the meridional velocity ratio (V_{m2}/V_{m1}), the velocity coefficient in the stator (ψ), and the carryover coefficient of kinetic energy from the stator into the rotor (ϕ_R). Then the degree of reaction (r^*) is selected and the head coefficient is increased in increments. The degree of reaction is the fraction of the isentropic enthalpy change through the turbine stage which occurs in the rotor. At each increment of head coefficient the particular values of velocity coefficient (ψ), internal efficiency (η_i), leaving loss coefficient (k_E), ratio of meridional absolute velocity to peripheral speed (V_{m1}/U_1), relative velocity ratio (W_2/W_1), and the relative and absolute angles (α_2 , β_1 , β_2) are computed.

A similar computer program using the same equations was written to find the peak efficiency for a given entering angle and degree of reaction, and then all the other parameters are computed. The values are also found for higher head coefficients such that the efficiency is 0.5% less than optimum and then 1.0% less than optimum.

B. Computer Program

The equations to be solved by iteration until $\psi_A = \psi$ are;

$$1. \quad \tan \beta_1 = \tan \alpha_1 - \frac{1}{\varphi \cos \alpha_1 \sqrt{1-r^*} \sqrt{k_{is}}} \quad (4)$$

$$2. \quad \tan \beta_2 = - \frac{\psi}{\varphi (V_{m2}/V_{m1})} \frac{X}{\cos \alpha_1 \sqrt{1-r^*}} \quad (5)$$

where $X^2 = (1+f)r^* + \varphi^2 \left[\phi_R - \left(\frac{V_{m2}/V_{m1}}{\psi} \right)^2 \cos^2 \alpha_1 \right] \left[1-r^* \right]$

$$-2\phi_R \varphi \sin \alpha_1 \sqrt{\frac{1-r^*}{k_{is}}} + \frac{1}{k_{is}} \left[\phi_R + \left(\frac{R_2}{R_1} \right)^2 - 1 \right] \quad (5a)$$

$$3. \quad \psi_A = 0.99 - \frac{2.28}{10^4} \Delta \beta - \frac{4.97}{180} \frac{\Delta \beta}{\Delta \beta} \quad (3)$$

Once this condition ($\psi_A = \psi$) is satisfied the values of the other parameters are found from

$$1. \quad \eta_i = \frac{2}{\sqrt{k_{is}}} \left[\varphi \sin \alpha_1 \sqrt{1-r^*} - \frac{1}{\sqrt{k_{is}}} \left(\frac{R_2}{R_1} \right)^2 + \varphi X \left(\frac{R_2}{R_1} \right) \right] \quad (6)$$

$$2. \quad k_E = k_{is} \left[\varphi^2 (1-r^*) \cos^2 \alpha_1 \left(\frac{V_{m2}}{V_{m1}} \right)^2 + \varphi^2 X^2 - \frac{2}{\sqrt{k_{is}}} \varphi X \left(\frac{R_2}{R_1} \right) + \frac{1}{k_{is}} \left(\frac{R_2}{R_1} \right)^2 \right] \quad (7)$$

$$3. \quad \frac{V_{m1}}{U_1} = \varphi \sqrt{1-r^*} \sqrt{k_{is}} \cos \alpha_1 \quad (8)$$

$$4. \quad \tan \alpha_2 = \frac{(R_2/R_1)/\sqrt{k_{is}} - \varphi X}{\varphi (V_{m2}/V_{m1}) \cos \alpha_1 \sqrt{1-r^*}} \quad (9)$$

$$5. \quad \frac{W_2}{W_1} = \sqrt{\frac{(W_2/U_1)^2}{(W_1/U_1)^2}} \quad (10)$$

$$\left(\frac{W_2}{U_1}\right)^2 = \varphi^2 k_{is} \left[(1+f) r^* + \phi_R \varphi^2 (1-r^*) - \frac{2}{\sqrt{k_{is}}} \phi_R \varphi \sqrt{1-r^*} \sin \alpha_1 + \frac{1}{k_{is}} \left(\phi_R + \frac{R_2^2}{R_1^2} - 1 \right) \right]$$

$$\left(\frac{W_1}{U_1}\right)^2 = 1 + \varphi^2 k_{is} (1-r^*) - 2 \sqrt{k_{is}} \varphi \sqrt{1-r^*} \sin \alpha_1$$

The equations were coded in Fortran language, Ref. 2, and solved on the Control Data Corporation 1604 computer at the U. S. Naval Postgraduate School. A copy of the program is presented in Appendix III. The resulting data printouts are included in Appendix V as Table I.

The program finding the peak efficiencies, efficiencies 0.5% less than optimum and efficiencies 1.0% less than optimum is also in Appendix III, with data in Appendix V as Table II. It should be noted here that all equations are completely coded in Fortran language so that any selected numerical values may be introduced in the beginning of the program. Any of these arbitrarily chosen values may be changed and the equations of the main program remain unchanged.

C. Results

Representative data from Tables I and II are presented in Fig. 1. The regularity and progression of the data curves indicate that non-dimensionalizing the efficiency and head coefficient parameters might

be profitable. When all the efficiencies for one entering angle and one degree of reaction are divided by the optimum efficiency for that set of conditions (η/η_{opt}) and the head coefficients are divided by the optimum head coefficient ($k_{is}/k_{is\ opt}$) the curves of Figs. 2, 3, 4 and 5 result.

A closer inspection of these plots reveals that for each degree of reaction, one curve suffices for all four entering angles.

The cubic equation

$$(\eta/\eta_{opt}) = -.000223 \left(\frac{k_{is}}{k_{is\ opt}} \right)^3 + .008345 \left(\frac{k_{is}}{k_{is\ opt}} \right)^2 - .12068 \left(\frac{k_{is}}{k_{is\ opt}} \right) + 1.125$$

represents all the data for $r^* = 0.0$ for all entering angles from 60° to 75° .

Similarly as an approximation to all the data at $r^* = 0.25$, the equation is

$$(\eta/\eta_{opt}) = -.000223 \left(\frac{k_{is}}{k_{is\ opt}} \right)^3 + .00770 \left(\frac{k_{is}}{k_{is\ opt}} \right)^2 - .1098 \left(\frac{k_{is}}{k_{is\ opt}} \right) + 1.1$$

and for $r^* = 0.50$

$$(\eta/\eta_{opt}) = -.000125 \left(\frac{k_{is}}{k_{is\ opt}} \right)^3 + .00554 \left(\frac{k_{is}}{k_{is\ opt}} \right)^2 - .09414 \left(\frac{k_{is}}{k_{is\ opt}} \right) + 1.097$$

The maximum error in the range of entering angles presented here is approximately 8 parts in 130. This is probably accurate enough for preliminary engineering estimates based on the equations in Ref. 1

used in the computer programs. As will be seen later, the loss data is not known to this accuracy.

The curves show that, roughly speaking, increasing the head coefficient to five times the optimum causes a reduction of 30% of the obtainable peak efficiency. Increasing the head coefficient to ten times the optimum causes a reduction of 45% of the obtainable peak efficiency. This indicates that if it is necessary to go to very high head coefficients to obtain a certain required work output, the rate of change of efficiency with increasing head coefficient is greatest from optimum to five times optimum head coefficient. The rate of change of efficiency decreases as the head coefficient is further increased.

Table I of Appendix V can be used to establish the other stage parameters after the head coefficient range of interest is chosen.

Figs. 1 through 5 are not the off-design performance of a particular turbine, but they are the locus of points of an infinite number of different turbine designs. Each point on each curve represents a turbine designed for that condition. Therefore, if the requirement is that the turbine be designed for a high head coefficient, the loss in efficiency need not be the absolute controlling factor, and the design may as well be based on extreme high values of head coefficient. These investigations show that it is advisable to either design the turbine for peak efficiency of maximum output but do not compromise both by operating at only two or three times the optimum head coefficient.

III. Loss Investigation

Since the design of a turbine depends on the loss assumptions made, the use of an average velocity coefficient based on general considerations of flow deflection in the rotor is not a very precise method of estimating the losses. This was the method used in the preceding section of this thesis. A better way should be found and the following considerations are basic to the problem.

A. Loss Components

It seems logical to class the losses encountered in turbines into four particular categories;

- 1) Profile loss -- the friction loss associated with the formation of the boundary layer on the blades of the cascade.
- 2) Tip clearance loss -- the pressure and energy loss associated with the leakage flow between the tips of the blades and the casing of the rotor, including the effects of trailing vortices at the hub where there is zero clearance.
- 3) Trailing edge loss -- the loss due to mixing effects behind the blades of the row as caused by the finite thickness of the blade trailing edge.
- 4) Secondary loss -- the loss due to the vortices which are set up in the flow in the curved channel between blades giving a velocity component normal to the desired direction.

In the axial flow turbine, the closely packed blades and large flow deflections usually require the flow through the turbine to be considered from the point of view of "channel flow" between blades instead of using airfoil theories. As will be seen in the subsequent discussion, this secondary flow causes the principal problem preventing the accurate assessment of the losses.

Looking at the flow between two blades of an arbitrary cascade, Fig. 6, the velocity distribution is as shown for the mid-span of the blade channel and it can be seen that a static pressure gradient is developed between surfaces 0-1-2 and 0'-1'-2'. The centrifugal forces on the fluid being turned cause an increase in the static pressure near the 0'-1'-2' wall and decrease the static pressure near the 0-1-2 wall.

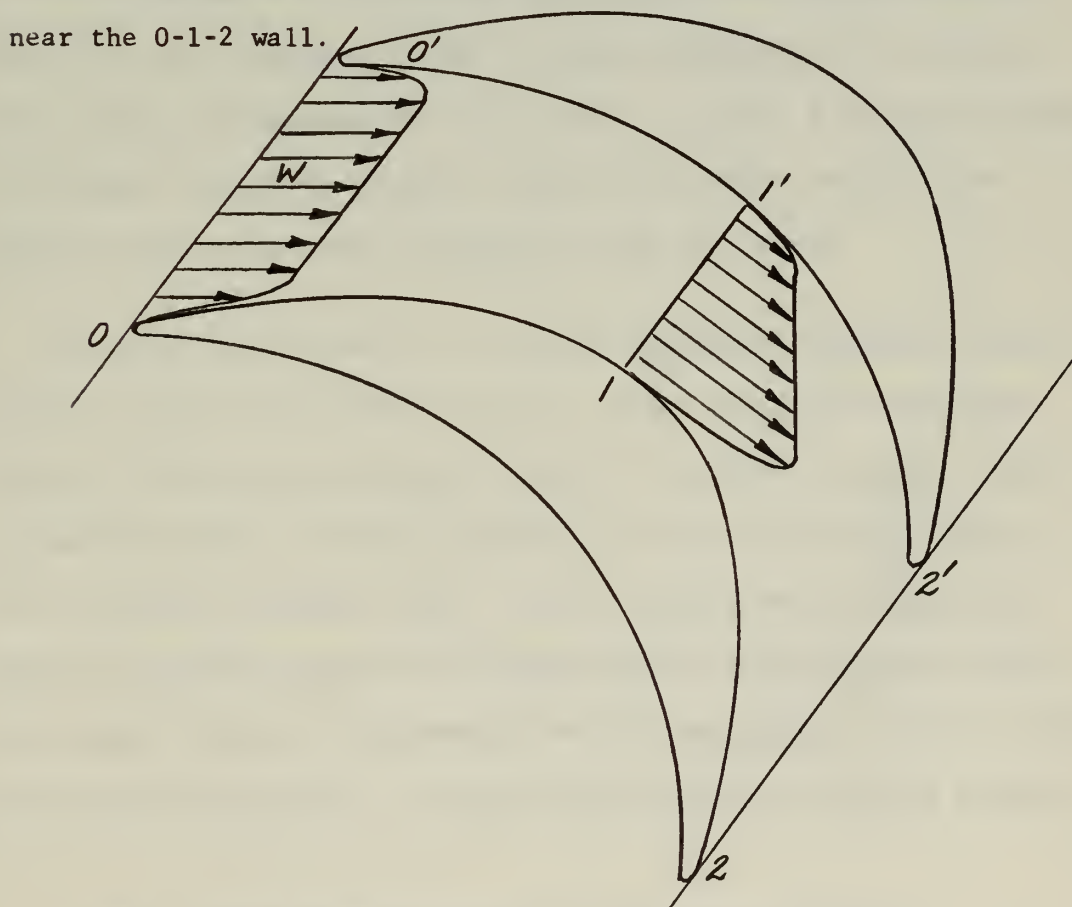


Fig. 6 Flow Between Blades of an Arbitrary Cascade

Assuming non-viscous flow outside the boundary layer requires the flow to increase velocity near the 0-1-2 convex wall to maintain the total pressure a constant ($P = p + \frac{1}{2} \rho W^2$). Conversely, the flow velocity must decrease near the 0'-1'-2' concave wall outside the boundary layer. In the boundary layer at the top and bottom of the channel, the loss of velocity (and total pressure) due to friction causes the flow direction to be dominated by the pressure gradient imposed (assuming the static pressure is constant through the boundary layer). Therefore, as the flow progresses from station 0-0' to station 1-1' to station 2-2', the fluid in the upper and lower boundary layers tends to flow from 0' toward 1 and from 1' toward 2.

This change of direction of the flow in the boundary layers results in the formation of two vortices superimposed on the main flow leaving the channel at station 2-2'. In Fig. 7 the flow patterns in the upper and lower boundary layers are shown as well as the induced vortices rotation direction at the exit plane.

This vorticity results in velocity components developed perpendicular to the desired exit velocity. Since a velocity component normal to the desired direction cannot be recovered usually, most of the useful energy in these components is lost in friction. This is the so-called "secondary loss". For a rotating row of blades, the blade tip clearance also has a marked effect on the secondary flow. The leakage from the high pressure to the low pressure side of a blade encourages an additional trailing vortex to form a reaction blading.

For impulse blading the flow over the tips which is not deflected also enhances vortex formation. For cascades of infinite blade height (two-dimensional only) there is no secondary flow since the mechanism depends principally on the annulus boundary layers.

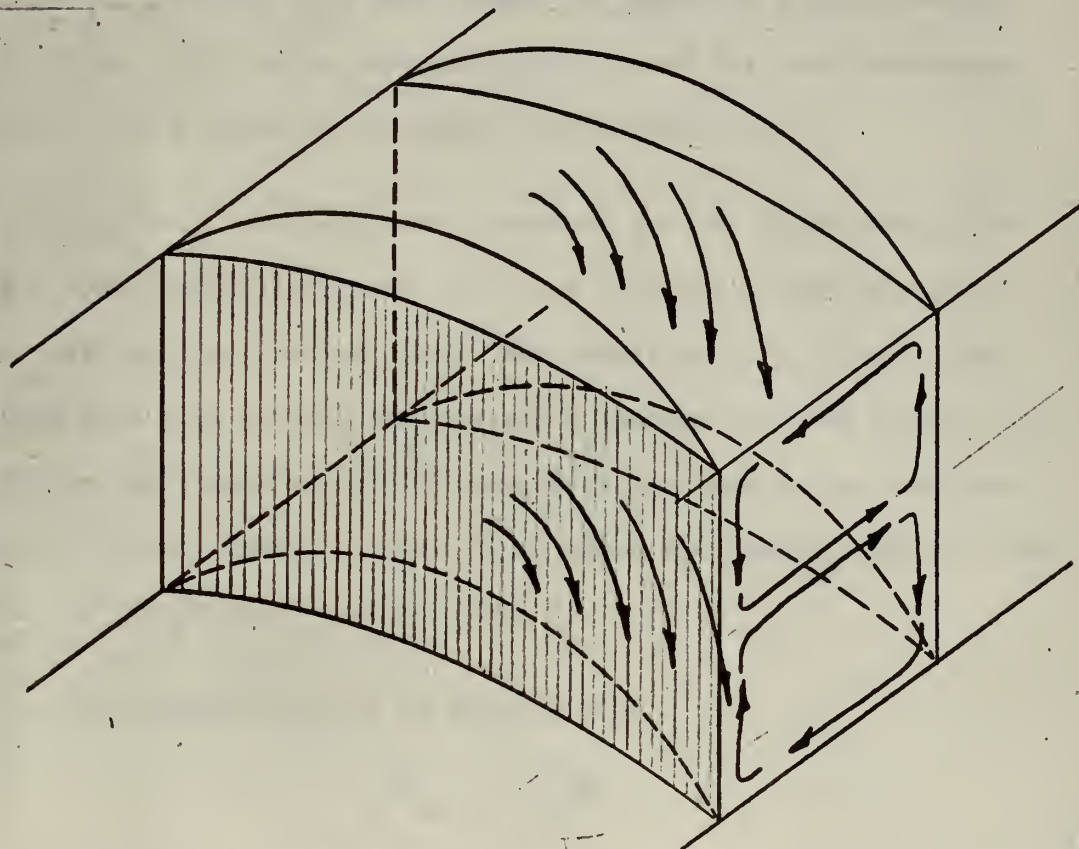


Fig. 7 Flow in the Boundary Layer of a Cascade Channel

With the physical parameters of blade height, trailing edge thickness, tip clearance, profile shape, and spacing given, it should be possible to make a reasonably exact estimate of losses.

B. Survey of the Literature

The immediately available literature at the U. S. Naval Post-graduate School was surveyed to find the particular loss breakdown

used by the various sources, the theory and representations offered, and any precise loss data published. The survey is limited in scope and critical since the particular desire is to locate specific loss theories and data. The results of this survey are presented here in the order of reference books, general texts, and then periodicals and reports. The NACA/NASA reports provide a wealth of data on the efficiency, or total loss coefficient, of specific turbine designs from tests. Very little information was found for loss components, however, in the frame of reference considered here.

1. In Ref. 1 an equation is derived for the determination of a flow coefficient in a rotor (ψ) as a function of the change in flow angle of the relative flow. This equation is a fitted curve through data from several sources and a variety of blade shapes and operating conditions and is the same equation used in the preceding section of this thesis. In Fig. 8 is shown the general shape of the curve and the derived equation (3).

A loss coefficient can be defined as

$$\zeta = 1 - \psi^2 \quad (11)$$

Considering the case of $\Delta\beta = 0$, we see the loss coefficient $\zeta_0 = 1 - \psi_0^2$ represents those losses in the cascade which are present when the flow is not deflected. As the flow is deflected an amount $\Delta\beta$, the reduction in ψ indicates an additional loss. The additional loss will be taken as the secondary loss. The secondary loss coefficient is then

$$\zeta_s = \zeta - \zeta_0 = \psi_0^2 - \psi^2 \quad (12)$$

Curves shown in subsequent discussions of secondary losses will now show a loss coefficient curve based on this equation plotted as a dashed line and labeled "VAVRA". This curve will act as a general reference and will show "average" conditions so a comparison of each method can be made.

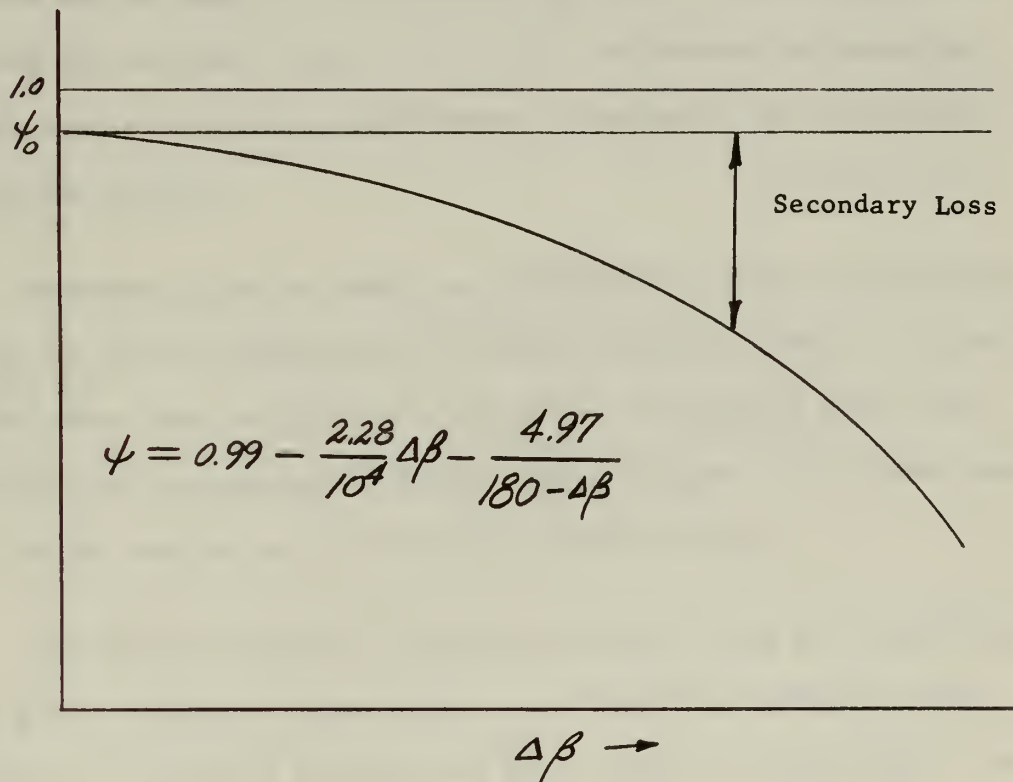


Fig. 8 Flow Coefficient ψ as a Function
of Turning Angle in a Cascade

2. A veritable fountainhead of theory, design and ideas are presented in Ref. 3. This basic work by Stodola touches on almost all the subjects considered important now. The important works of

others up until 1927 are included to show their measurements and developments. The losses through fixed rows of blades are given in the form of the so-called velocity coefficient φ ; the ratio of actual velocity to theoretical velocity. The measurements of the Institution of Mechanical Engineers of England and others all show good correlation for flows up to sonic speed for stators with an axial entering angle and an exiting angle of 70° - 78° from the axial. For supersonic speeds the data show some scatter due to difference in measuring apparatus and some basic differences in design of the convergent-divergent passage.

Secondary flows in bends are explained but there is wide variation in the available data for friction losses in bends. No published data were available for the losses in rotating blade rows. The data and experiments on fixed rows of impulse rotor blades were of limited application and only show general trends.

For design purposes, velocity coefficients and loss coefficients are given in general terms only, i.e., "velocity coefficient for stators = 0.975-0.92 for long and short nozzles respectively". The curve presented by Stodola for the velocity coefficient for rotating blade rows as a function of turning angle is included in the data used for the determination of the equation (3) by Vavra.

The tip clearance losses had been explored in a limited fashion. These losses were accounted for by an empirical formula for the decrease in internal work as a function of clearance and blade height,

$$\zeta = 6.27 k^{1.4} / h \quad (13)$$

where k = radial clearance and h is the blade height corresponding to zero clearance. This relation, credited to Anderhub, is plotted on Fig. 9 and noted as (A).

The steam turbine design procedures presented are strongly dependent on making the new design a small modification of an already designed unit which is in service and for which the efficiency is known. The peak efficiencies were recognized to be in the regions of k _{is} from 1.0 to 5.0, as shown in the previous section of this paper.

3. The axial turbine section of Ref. 4 gives a lucid and brief explanation of the flows in such machines but the loss data and secondary flow considerations are based completely on Ref. 22, 23 and 24 which are considered later in this paper.

4. Since books written to be used as school texts of necessity try to cover the complete spectrum of fluid mechanics, theory, and design, only the most cursory reference is made to specific losses in turbine stages. Refs. 5, 6 and 7 are representative of books of this type. Ref. 5 defines a work recovery coefficient as the ratio of useful work extracted by the rotor to the total kinetic energy of the flow leaving the stator, times the stator flow efficiency. This work-recovery coefficient variation with the velocity ratio (U/V_1) is shown for impulse and reaction conditions and no other explanation of the nature of the losses is offered. The charts

presented are based on data from Ref. 16, in which report the losses in a blade row are presented only as a function of stagger angle and incidence.

In Ref. 6 the author makes the statement that no adequate criterion is available for the difference in the flow conditions between an efficient and an inefficient hydrodynamic machine of a given type. Any losses and efficiencies of turbines offered are tied to airfoil theory or definitions of losses by Stodola and others. Secondary flows and radial flow of the boundary layer are mentioned only from Ref. 17 where the measurements were made on widely spaced blades on a rotating blade row at low speed.

A large list of references on the work in gas turbines is given in Ref. 7 for the data available at that time. Principally the work in Ref. 16 below is mentioned in connection with turbines but only general terms are offered and no specific loss derivations are offered.

5. The most comprehensive effort to make a breakdown of losses and show specific data found in a textbook is that of Ref. 8. This book takes selected data from Refs. 15, 16 and 23, discussed later in this paper, and presents plots of the losses due to leakage, profile losses, losses from turbulence and wall friction (including secondary loss effects) and incidence losses. The discussion is brief, however, and no new data or theory are presented.

6. An attempt to mathematically tackle the problem of the secondary flows in bends is presented in Ref. 9. The equations of motion of an ideal fluid are used and frictional effects are ignored. An induced drag pressure drop coefficient is defined to account for the power loss due to secondary flow. The method is applied to the flow in the corner of a 3' x 4' wind tunnel which has two turning vanes to simulate a blade row and the method shows the proper trends. A quantitative value derived for the loss is computed and found to be about twice the measured loss. No other example of the theory being applied is available.

7. A qualitative investigation of the flow in boundary layers and wakes of blade rows is offered in Ref. 10. An excellent discussion of the general nature of these flows is accompanied by the statement that a quantitative theory for these effects is not available.

8. An analytical method of estimating turbine performance described in Ref. 11 is based on losses due to incidence angle and losses due to flow of the fluid through the blade row. A blading loss parameter is used to represent the losses but only a general range of values of the parameter are given. No method is presented for determining the magnitude of the blading loss parameter before the turbine is built.

9. The general state of the art to 1948 is described in Ref. 12. The paper is not intended to be used as a basis for other than general design considerations, however, and some empirical relations presented

were attempts to cover both axial turbines and compressors. This necessarily limited the worth of such relations for large flow deflection turbine loss estimations. Those relations presented for strictly turbine use are repeated in Refs. 24 and 25 which will be covered in more detail later in this thesis.

10. The losses in stators are, of course, easier to measure than the losses in rotors. Some excellent tests and measurements are presented in Refs. 13 and 14. These show that, in general, a properly designed nozzle for a turbine will have a velocity coefficient (ratio of actual velocity to isentropic velocity) value of .96. This single value is found to be uniform over a considerable range of designs and conditions. Off-design values do fluctuate, particularly in the case of supersonic nozzles but the reasons do not seem obscure and loss estimations for stator rows should be on relatively firm ground.

11. Ref. 15 is mentioned as a reference work in many textbooks on turbomachinery. This compilation of the then current design practices only shows the losses as a function of axial length of the blades of the rotor, turning angle in the rotor and incidence angle. The curves for loss as a function of turning angle are included in the data used for the determination of the equation (3) by Vavra. Specific detailed loss breakdowns or data are not available.

12. The systematic investigations into secondary loss presented in Refs. 18 and 19 are of real interest although the test data is too

limited to permit any universal application. An attempt is made to define the two-dimensional loss by theory, measure the end loss at the blade root and the clearance loss at the tip, and subtract these from the total pressure loss measured to arrive at the secondary loss. The tests are performed on a particular airfoil shape in three solidity arrangements and three flow deflections. The inaccuracies and errors discussed should help any further investigator in this subject.

13. A comparable breakdown of the losses into components as assumed here is offered in Ref. 20. This work by Markov also includes the experimental results of some other Russians in the field. Without attempting to completely describe the development of equations and data presented, the pertinent data for the present consideration is extracted.

The profile loss, or two-dimensional loss which would be caused by blades of infinite length is shown on Fig. 10 along with other data to be described later. The basis of the Ref. 20 data is a whole series of experimental measurements of widely used cascades for turbines in Russia. For stators, the profile loss coefficient is almost constant at .03 over a wide range of conditions.

The tip clearance loss is shown on Fig. 9 as represented by two plots in Ref. 20. One plot is shown as the loss for a reaction stage and one plot is based on experimental data for the efficiency of stages with a small degree of reaction. The magnitudes of the degree of

reaction are not specified but the trend is correct. Stages with a high degree of reaction have a higher loss across the tip, as would be expected due to the pressure difference across the rotor from entrance to exit.

The trailing edge loss for cases where the pressure gradient is small along the surface of the trailing edges of the blades is computed by

$$\zeta_{te} = 0.41 \frac{t_e}{s \cos \beta_2} \quad (14)$$

Where such a pressure gradient is present the use of boundary layer thickness parameters is required. The trailing edge loss coefficient according to eq. (14) is shown in Fig. 20.

The energy lost due to the secondary flow is treated as a function of the mass flow rate in the cascade. The efficiency of a cascade of blades with finite length is defined as

$$\gamma = \gamma_{(2\text{-dim})} \left[1 - \frac{\text{Energy lost due to secondary flow}}{\text{Energy available flowing through cascade}} \right] \quad (15)$$

The loss coefficient is defined as

$$\zeta = 1 - \gamma \quad (16)$$

and so

$$\zeta = \zeta_{(2\text{-dim})} + \left[1 - \zeta_{(2\text{-dim})} \right] \left[\frac{\text{Energy lost}}{\text{Energy available}} \right]$$

$$\zeta = \zeta_{(2\text{-dim})} + \left[\gamma_{(2\text{-dim})} \right] \left[\zeta_{\epsilon} \right]$$

The secondary flow loss coefficient ζ_{ϵ} is converted to the ζ_s used for comparison in this thesis by

$$\zeta_s = \zeta_{\epsilon} \gamma_{(2\text{-dim})}$$

An expression for ζ_{ϵ} is developed that is a function of the circulation around the blades, the blade width, and incompressible flow, namely

$$\zeta_{\epsilon} = K \frac{\tan \beta_2 - \tan \beta_1}{(h/c)}$$

where the coefficient K depends on the expansion of the flow in the cascade. The value of K is determined from experimental data to be

$$K = 0.01 \frac{\cos \beta_2}{\cos \beta_1}$$

Thus

$$\zeta_{\epsilon} = 0.01 \frac{\cos \beta_2}{\cos \beta_1} \left[\frac{\tan \beta_2 - \tan \beta_1}{h/c} \right] \quad (17)$$

In Fig. 11 the function ζ_s is shown for the two-dimensional efficiency of Ref. 1,

$$\gamma_{(2\text{-dim})} = \psi_o^2 = 0.9262$$

Values of h/c plotted are chosen arbitrarily but Ref. 20 specifies that the derivation holds for blades that are not excessively short. There is assumed to be some two-dimensional flow in the channel between the blades at the center section. Experimental data are shown

for short blades, and these data commence at $\left(\frac{h}{c}\right) = 2.0$ and go to smaller values. So the plot in Fig. 11 is based on eq. (17) and is shown for a value of $\left(\frac{h}{c}\right) = 2.0$, the lower limit permitted. For $\left(\frac{h}{c}\right) = 1.33$ and 1.25 the mean coefficients are about 10% of the representative values based on the Vavra equation (3), but these are specific data for short blades not arrived at using the equation above. The secondary loss as computed by Markov is low compared to any other available data. When complete loss coefficients are computed in Ref. 20 the values are comparable to any other method however, since the tip clearance losses, trailing edge losses, blade height corrections, etc., used bring the total loss to the proper level. Any use of the Ref. 20 data must take account of this fact.

Of interest also in Ref. 20 is a relation for the discharge flow angle of a turbine blade row. The relation is

$$\cos \alpha_1 = \frac{a}{s - (t_e / \cos \alpha_{B1})} \quad (18)$$

and it gives more accurate results than the other widely-used equation

$$\cos \alpha_1 = \frac{a}{s} \quad (19)$$

which does not take account of trailing edge thickness.

14. The tip clearance loss as represented by Ref. 21 is also shown in Fig. 9. The equation derived is

$$\zeta = \frac{\delta_E}{(h/b) + \gamma_E} \quad (20)$$

where

$$\delta_E = .1011 + 4.667 (k/b)$$

$$\gamma_E = -.0422 + 2.790 (k/b)$$

h = blade height

b = blade width

k = clearance

and the results are shown for two values of (h/b) .

Also given in Ref. 21 is the equation for the minimum induced drag due to flow in a clearance gap at the tip of an airfoil (as derived by Betz) to be

$$D = K_2 \frac{L^2}{\frac{1}{2} \rho W_\infty^2 h^2} \quad (21)$$

where K_2 is a form factor depending on the clearance, blade spacing and relative exit angle of the flow.

Assuming the axial component of velocity to remain constant and drawing an arbitrary turbine stage velocity triangle (such that all angles are positive), Fig. 12a, the circulation (Γ) can be computed by integrating around the closed curve in Fig. 12b to give

$$\left(\frac{\Gamma}{h} \right) = s (W_{u2} - W_{u1}) \quad (22)$$

Then the lift per blade is

$$L = \rho \left(\frac{r}{h} \right) W_{\infty} h = \rho s h W_{\infty} (W_{u2} - W_{u1}) \quad (23)$$

The lift and drag forces exerted on a blade can be seen in Fig. 13 as well as the axial and peripheral components of the resultant force F . It can be seen that for each blade channel

$$F_a = s h (p_1 - p_2) \quad (24)$$

$$F_u = \frac{m_s}{g} (W_{u2} - W_{u1}) \quad (25)$$

The secondary flow loss will be associated with the loss from the pressure drop in the axial direction.

To arrive at a loss coefficient expression for the axial force component, it is necessary to define the loss coefficient in terms of the pressure loss, as shown in Fig. 14. The loss coefficient is defined as

$$\zeta_s = \frac{P_{R1} - P_{R2}}{\frac{1}{2} \rho W_{2th}^2} \quad (26)$$

Substituting

$$P_{R1} - P_{R2} = \zeta (P_{R1} - p_2)$$

and for incompressible flow,

$$P_{R1} = p_1 + \frac{1}{2} \rho w_1^2 \quad (27)$$

$$P_{R2} = p_2 + \frac{1}{2} \rho w_2^2$$

and collecting terms,

$$(p_1 - p_2) = \frac{1}{2} \rho \frac{w_2^2}{1 - \zeta} - \frac{1}{2} \rho w_1^2 = \frac{F_a}{sh} \quad (28)$$

Then from Fig. 13,

$$F_a = L \sin \beta_\infty + D \cos \beta_\infty \quad (29)$$

Using the above derived expressions for L and D and equating

$$sh(p_1 - p_2) = L \sin \beta_\infty + D \cos \beta_\infty \quad (30)$$

gives

$$\zeta_s = 1 - \frac{1}{\cos^2 \beta_2} \left[1 / \left\{ 2 (\tan \beta_2 - \tan \beta_1) \tan \beta_\infty + \frac{1}{\cos^2 \beta_1} \right. \right. \\ \left. \left. + 4 K_2 \left(\frac{s}{h} \right) (\tan \beta_2 - \tan \beta_1)^2 \cos \beta_\infty \right\} \right]$$

For an arbitrary value of $K_2 \left(\frac{s}{h} \right)$, this secondary loss is plotted in Fig. 15. The value of $K_2 \left(\frac{s}{h} \right)$ can be adjusted to change the general inclination of the family of curves shown to any desired value. That is, a lower value of $K_2 \left(\frac{s}{h} \right)$ raises the curves and vice versa.

15. In Ref. 22 an attempt is made to find a mathematical solution to the problem of secondary flows in particular. The approximate relations derived are not able to satisfy the boundary conditions. One conclusion drawn from the derivations is that the secondary flows are a direct consequence of a non-uniform approach velocity, and, if the lift is assumed proportional to the square of the local velocity, then the secondary flow is independent of aspect ratio. These conclusions are counter to the ideas of most investigators in the field.

The tests and measurements made showed odd discrepancies and it was felt that rotor-stator induced effects may have been the cause. No relation was deduced which is directly useful here.

16. The ideas and relations presented in Ref. 23 and 24 were carried through and refined and elaborated in Ref. 25. All three references have the same authors. Therefore, Ref. 25 will be discussed here as being most useful, and parts of Ref. 23 and 24 will be extracted as necessary.

By far the most detailed method presently available for determining loss coefficients is presented in Ref. 25. The loss is broken into component parts similar to those assumed at the begining of this discussion and the quantitative data offered are based on tests of turbines.

The loss coefficients of Ref. 25 are

$$\gamma = \frac{P_{R1} - P_{R2}}{P_{R2} - P_2} = \frac{\text{Loss of total head pressure}}{\text{Total pressure at blade outlet} - \text{static pressure at blade outlet}} \quad (32)$$

The loss coefficients used in this thesis are

$$\zeta = 1 - \gamma = \frac{P_{R1} - P_{ez}}{P_{ez} - P_2} \quad (33)$$

and the necessary conversion is

$$\zeta = \frac{\left[\frac{P_{R1} - P_{ez}}{P_{ez} - P_2} \right]}{1 + \left[\frac{P_{R1} - P_{ez}}{P_{ez} - P_2} \right]} = \frac{\gamma}{1 + \gamma} \quad (34)$$

For profile losses, two figures are presented, one for nozzle blades and one for impulse blades. These are reproduced here as Fig. 16a and Fig. 16b. An interpolation method is proposed for rotors with reaction and a method of extending the profile loss to conditions of other than zero incidence is also shown.

A number of relations for the loss due to tip clearance are presented in Ref. 25 as

$$\zeta = 3.1 \left(\frac{k}{h} \right) \quad (\text{Stodola, Reaction turbine}) \quad (35)$$

$$\zeta = 3.5 \left(\frac{k}{h} \right) \quad (\text{Meldahl}) \quad (36)$$

$$\zeta = 2.6 \left(\frac{k}{h} \right) \quad (50\% \text{ Reaction turbine}) \quad (37)$$

These relations are shown in Fig. 9.

Expressions are also derived for tip clearance loss based on C_D and C_L if the ratio spacing/blade height is small and the gas turning angle is small. For our uses here, the gas turning angles are large. The loss relation arrived at is

$$Y_k = 4B \left(\frac{h}{d} \right) \left[\cos^2 \alpha_2 / \cos \alpha_\infty \right] \left[\tan \alpha_1 - \tan \alpha_2 \right]^2 \quad (38)$$

where $B = 0.5$ for blades with clearance and $B = 0.25$ for blades with shrouds.

Equation (38) is used to find the range of loss coefficients for the impulse conditions of $\cos \alpha_\infty = 1.00$ and $\alpha_1 = \alpha_2$. Shown in Fig. 9 is the band of values corresponding to $\alpha_1 = \alpha_2 = 60^\circ$ to 75° .

The data available to Ainley and Mathieson led them to the conclusion that the effect of area ratio is more important to secondary flows than is the magnitude of the gas deflection. The area ratio used is

$$\frac{A_2}{A_1} = \frac{(\text{annulus area at outlet from blade row}) (\cos \alpha_2)}{(\text{annulus area at inlet to blade row}) (\cos \beta_1)} \quad (39)$$

where α_2 = gas outlet angle measured from the axial and β_1 = blade inlet angle measured from the axial. The hub ratio (inner diameter/outer diameter) was also felt to exert a strong influence. This led to the plot of $(A_2/A_1)^2 / [1 + (\text{ID.OD})]$ versus a parameter λ used in defining the drag coefficient due to the secondary flow as

$$C_{D_S} = \lambda C_L^2 / (4/c) \quad (40)$$

This plot is reproduced here as Fig. 17. Ultimately then, a loss coefficient for secondary flows is presented as

$$Y_s = 4\lambda \left[\cos^2 \alpha_2 / \cos \alpha_\infty \right] \left[\tan \alpha, \tan \alpha_2 \right]^2 \quad (41)$$

Converting these values of Y_s to ζ_s , a plot is presented as Fig. 18 for a wide span of inlet and outlet angles.

For trailing edge thickness losses, the assumption is made that the previously derived losses are for a blade of trailing edge thickness which is 2% of the blade pitch. For other trailing edge thicknesses a correction is applied according to a plot which is reproduced here as Fig. 19.

C. Results of Loss Investigation

The results of the loss investigation will be discussed according to the original breakdown of loss components mentioned at the beginning of this section of this thesis. The specific turbine design used in the last section of this report will be used as the object of a quantitative comparison of the loss relations shown here.

1. The profile loss estimation method presented by Ainley in Ref. 25 is straightforward and complete and should give good data for the "conventional" blade shapes from which the data is derived. An anomaly presents itself in Fig. 10 however, when a comparison is made between the profile loss coefficient data of Ainley and the data of Markov. The blade shapes from which the Markov data are derived

are very similar to those of Fig. 25. It would appear that such blade shapes would have higher profile losses than those based on airfoil designs which usually are used for lower flow deflections. The data comparison shows this is not the case.

Of special interest in the Markov data in Fig. 10 is the fact that an optimum solidity of $(s/c) \cong .625$ to $.650$ is evident. Higher solidities apparently block the flow thereby increasing the profile loss, and lower solidities encounter separation effects since the blades act more like individual airfoils. The low point in the curve corresponds to guiding the flow in a channel, retarding separation onset, but not blocking the flow.

Variable solidity

2. The tip clearance losses shown in Fig. 9 seem to give a large range of values depending on which curve is chosen. The situation is perhaps more reasonable when the ratio of radial clearances to blade height is restricted to realistic values less than .03. The loss estimate from the Ainley equation is obviously outside the flow deflection range intended for that relation. The other curves for tip clearance loss for reaction blading could be based on different degrees of reaction corresponding to the fan aspect of the curves, i.e., high reaction blading would use the highest curve. Some reasonable estimate could be made. The only relation for impulse blading available is that of Markov. The Meldahl relation is the only one which accounts for the trailing vortex inducing a loss even though the tip clearance is zero, but the dependence on blade aspect ratio appears unreasonably strong for this data as a

whole. For $(h/b) = 1.00$, the loss at $(k/h) = .02$ is greater than the highest ordinate shown.

3. The Markov data is all that is available for making an estimate of trailing edge thickness loss directly. The plots in Fig. 20 indicate the trends which would be expected.

The Ainley method of modifying the complete loss coefficient depending on the relative trailing edge thickness seems an unfortunate way to present the data. The system is workable but indirect. It would be more useful for comparison and design purposes to have the trailing edge thickness data presented directly.

4. The situation regarding secondary flow loss coefficients is the most confused of all. The general equation by Vavra is not very precise but certainly indicates the proper trend if the model presented in Fig. 7 is correct. None of the other presently available methods investigated will even show the proper trends for high flow deflections.

The Ainley relation plotted in Fig. 18 seems to have depended too heavily on stator data with an axial entering angle and low flow deflections in the rotor. Otherwise, the curves indicate that for a given entering angle, increasing the flow deflection decreases the loss.

In Fig. 15 the relation derived from Meldahl and Betz indicates the proper trend for low flow deflections only. Taking the plot for

$\beta_1 = -45^\circ$ as an example, it can be seen that for flow deflections greater than $\Delta\beta = 90^\circ$ the indication is that increasing the flow deflection decreases the loss.

The Markov relation plotted in Fig. 11 suffers the same deficiency pointed out for the Ainley and Meldahl curves plus abnormally low secondary loss coefficients throughout for reasonable blade aspect ratios. The data is of no value unless used specifically with Markov relations for all losses. In Ref. 20, when sample loss estimations are carried out, the total loss coefficients compare well with the measured values. Apparently the profile, tip clearance and trailing edge loss coefficients with the blade height corrections used in the complete method counter the low secondary loss estimates.

5. The relations now available can be used to make a quantitative comparison of the component losses. The turbine designed in the following section will be used as a model to show the comparisons. The physical dimensions of the stator and rotor are as listed in Table IV and these are used in the relations and plots so far developed. The numerical results are shown in Table V for the stator and Table VI for the rotor.

Table IV
TURBINE PHYSICAL DIMENSIONS

	Stator	Rotor
Entering angle	0°	69.60°
Exiting angle	75°	-71.57°
Blade height, h	1.165 in	1.465 in
Trailing edge thickness, t_e	.036 in	.025 in
Blade chord, c	3.16 in	1.355 in
Blade width, b	1.60 in	1.375 in
Spacing, s	1.80 in	.9415 in
Blade thickness, t	.69 in	.6485 in
Tip clearance assumed, (k/h)	.00	.02

Table V
STATOR LOSS COEFFICIENT COMPARISON

Author	Profile Loss	Tip Clearance Loss	Trailing Edge Loss	Secondary Loss
Vavra, Ref.1				.070
Ainley, Ref.23	.067			
Ainley, Ref.25	.047			.041
Markov, Ref.20	.030		.032	<.005
Meldahl, Ref.21		.106		
Stodola, Ref.3	.040			.022

Table VI
ROTOR LOSS COEFFICIENT COMPARISON

Author	Profile Loss	Tip Clearance Loss	Trailing Edge Loss	Secondary Loss
Vavra, Ref.1				.231
Ainley, Ref.23	~ .12			
Ainley, Ref.25	.148	.13		.168
Markov, Ref.20	.068	.025	.032	.025
Meldahl, Ref.21		.223*		.2601
Stodola, Ref.3		.05*		

* reaction

As can be seen, the component losses presented in Tables V and VI can be combined selectively to obtain almost any desired answer.

The loss investigation is disappointing in that no clear-cut answers are provided. The complete Ainley method, or the complete Markov method, may produce a reasonable estimate but the correlation is poor at best for component losses.

Any desire to find a way of basing a new design on component loss considerations is presently thwarted. A need is evident for an orderly testing program to find the magnitude and interaction of component losses.

IV. Design of Turbine

As a further investigation into the characteristics of a turbine being used for maximum work output, a single stage turbine is designed for a slightly supersonic velocity leaving the stator and a relative Mach number of 0.8 as seen by the rotor. Then the overall pressure ratio is increased and the off-design performance evaluated. The number of calculations required are prohibitive for hand calculations so the equations necessary for the performance evaluation are also programmed in Fortran language for the CDC 1604 Digital Computer.

A. Loss Coefficient Data

A set of loss coefficients for the design were provided by Vavra from some unpublished data. These loss coefficients are shown in Figs. 21, 22 and 23 and will be used for the design and the performance evaluations.

The abscissa of the plot of stator loss coefficients, M_{is} , is the Mach number for an isentropic expansion from the total pressure at the inlet to the static pressure at the discharge of the blade row. This can be seen in the T-s diagram of the expansion through a turbine shown in Fig. 24 to be the isentropic velocity V_{th} divided by the acoustic velocity based on T_1 is. When reduced, the result is

$$M_{is} = \sqrt{\frac{2}{\gamma-1} \left[\left(\frac{P}{P_0} \right)^{\frac{\gamma-1}{\gamma}} - 1 \right]} \quad (42)$$

To properly determine the flow area through the stator, the loss coefficient in Fig. 20 noted "for flow rates" and shown in Fig. 24 as γ_{a1} is used. This loss coefficient is intended to represent the losses encountered by the flow in the channel between blades, but is not intended to account for the mixing losses and separation losses encountered by the flow leaving the blade row. These additional losses are included in the higher loss coefficients which are applied to velocity determinations. These loss coefficients are noted "for velocities" in Fig. 21 and as γ_1 in Fig. 24. Similar considerations are used for the loss coefficients through the rotor.

The loss coefficients are corrected for blade height according to the curves given in Fig. 23.

B. Flow function

For steady adiabatic flow the stagnation enthalpy remains constant along a streamline. For stators, the stagnation enthalpy is

$$H = H_0 = h_1 + \frac{V_1^2}{2} \quad (43)$$

and in Fig. 24, to a different scale, H_0 would be represented by T_0 and h_1 would be represented by T_1 . A similar situation pertains to a relative stagnation enthalpy defined as

$$H_R = h_1 + \frac{W_1^2}{2} = h_2 + \frac{W_2^2}{2} \quad (44)$$

for the condition such that the peripheral velocity at the entrance

of the rotor equal to the peripheral velocity at the exit of the rotor. As shown in Appendix I, the mass flow rate for a given set of inlet conditions can be expressed by

$$\dot{m} = \frac{P_0 A_1}{\gamma R T_0} \sqrt{\frac{2g\gamma}{\gamma-1} \left[\left(\frac{P_1}{P_0}\right)^{\frac{2}{\gamma}} - \left(\frac{P_1}{P_0}\right)^{\frac{\gamma+1}{\gamma}} \right]} \quad (45)$$

where n is the polytropic exponent, P_0 is the total pressure ahead of the stator blade row and p_1 is the static pressure behind the blade row.

As shown in Fig. 24, a relative total temperature and relative total pressure can be defined as

$$T_{R1} = T_1 + \frac{W_1^2}{2g\gamma C_p} \quad (46)$$

$$P_{R1} = P_1 \left(\frac{T_{R1}}{T_1} \right)^{\frac{\gamma}{\gamma-1}} \quad (47)$$

The mass flow rate through the rotor is then

$$\dot{m} = \frac{P_{R1} A_2}{\gamma R T_{R1}} \sqrt{\frac{2g\gamma}{\gamma-1} \left[\left(\frac{P_2}{P_{R1}}\right)^{\frac{2}{\gamma}} - \left(\frac{P_2}{P_{R1}}\right)^{\frac{\gamma+1}{\gamma}} \right]} \quad (45a)$$

Rearranging the above expressions for flow rate in non-dimensional terms defines a flow function,

$$\phi = \frac{\dot{m} \sqrt{T_0}}{P_0 A_1} \sqrt{\frac{R}{g}} = \sqrt{\frac{2\gamma}{\gamma-1} \left[\left(\frac{P_1}{P_0}\right)^{\frac{2}{\gamma}} - \left(\frac{P_1}{P_0}\right)^{\frac{\gamma+1}{\gamma}} \right]} \quad (48)$$

and

$$\phi = \frac{\dot{m} \sqrt{T_{e1}}}{P_{e1} A_2} \sqrt{\frac{R}{g}} = \sqrt{\frac{2\gamma}{\gamma-1} \left[\left(\frac{P_2}{P_{e1}} \right)^{\frac{2}{\gamma}} - \left(\frac{P_2}{P_{e1}} \right)^{\frac{\gamma+1}{\gamma}} \right]} \quad (48a)$$

It will be necessary to investigate whether this flow function can be satisfied for each set of conditions imposed across a blade row. The choked flow condition corresponds to the maximum value of P/p which the blade row can accomodate. The development of the critical values of the flow function and pressure ratio can also be found in Appendix I to be

$$\phi_{cr} = \left(\frac{2}{m+1} \right)^{\frac{1}{m-1}} \sqrt{\frac{2\gamma}{\gamma-1} \left(\frac{m-1}{m+1} \right)} \quad (49)$$

$$\left(\frac{P}{P} \right)_{cr} = \left(\frac{2}{m+1} \right)^{\frac{m}{m-1}} \quad (50)$$

A computer program to do these computations is explained in section E below.

C. Geometry and Velocity Triangles

The final design of the stator and rotor blade rows is as shown in Fig. 25 for the mean diameter. The velocity triangles of the average flow velocities at each station are as shown in Fig. 26.

The sign convention chosen is that positive angles and positive peripheral velocity components point in the same direction as U , the rotor peripheral velocity.

It is convenient to define an "exit plane" and a "discharge plane" leaving each blade row as shown in Fig. 25 by the (e) and (d) designations. The design of the stator and rotor is such that the minimum cross-sectional area of the channel between blades occurs at the exit plane (e). For maximum work output, the pressure drop across the stator is great enough to cause choked flow at the exit plane plus an additional expansion of the flow from the exit plane to the discharge plane. The conditions for such after-expansions are as shown in Appendix II based on the treatment in Ref. 26.

In Ref. 1 a similar development is shown for a supersonic flow entering a blade row. Since the flow leaving the stator is supersonic, it is possible under certain conditions for the rotor to see a supersonic flow also and proper account must be taken of the shock losses involved.

D. Dimensionless Parameters

As has already been mentioned, the number of variables to be handled is greatly reduced if the mass flow expression is non-dimensionalized to form a flow function depending only on pressure ratio, specific heat ratio and the polytropic exponent of the expansion process.

In Ref. 27 can be found a complete development of dimensionless parameters and referred values for minimizing the number of variables necessarily handled in presenting the data for a turbine performance

analysis. Those used in the present analysis are referred rpm, overall pressure ratio, referred flow rate, and a power coefficient. The necessary coefficient forms are computed from

$$\text{Referred RPM} = \text{RPM} / \sqrt{T_o} \quad (51)$$

$$\text{Overall pressure ratio} = P_o / p \quad (52)$$

$$\text{Referred flow rate} = \dot{w} / \sqrt{T_o / P_o} \quad (53)$$

$$\text{Power coefficient} = \text{HP} / P_o \sqrt{T_o} \quad (54)$$

The referred flow rate and power coefficient are constant in this evaluation. It is useful to refer all the conditions at any point in the turbine to inlet conditions. For this reason, velocities are carried as $V / \sqrt{T_o}$ and $W / \sqrt{T_o}$ and pressures as p / P_o and P_R / P_o .

E. Design Computations

In order to design the stator for choked flow at the exit plane, the flow function must be known for the imposed conditions. A computer program was written to compute the flow function for a given specific heat ratio, γ , pressure ratio, P/p , and loss coefficient, ξ . As a by-product the program also computes the polytropic loss coefficient, ξ_p . This information is presented in Appendix V as Table III, Flow Function and Polytropic Loss Coefficients, for γ from 1.25 to 1.40, ξ from 0.0 to 0.25 and P/p from 1.02 to 6.00. The particular flow function data to be applied here for $\gamma = 1.37$ are also included as Fig. 27. The computer program is included in Appendix III.

The following data were assumed given for the design:

Mass flow rate	= 100. lbm/sec
Total pressure at inlet	= 1000 psia
Total temperature at inlet	= 1460°R
Specific heat ratio	= 1.37
Gas constant, R	= 421.5 ft lbf/lbm °R
Mean diameter of stator	= 23.0 in
Mean diameter of rotor	= 23.0 in
Design rpm	= 13000

The stator blade design was provided by Vavra from unpublished data and is as shown in Fig. 25. It is now necessary to select the blade height and number of blades so the choked flow condition at the exit is satisfied.

A blade height of 1.16 inches is taken as a first estimate. Then, from Fig. 21 the loss coefficient for flow areas at $M_{is} = 1.00$ is found to be $\zeta_{ao} = .053$. From Fig. 23 the blade height correction is $K_h = 0.872$ and so

$$\zeta_a = .872 (.053) = .0462$$

Using linear interpolation on Fig. 27 for this loss coefficient between the maximum values of ϕ , i.e., ϕ_{cr} , it is found that

$$\phi_{cr} = .65811$$

$$\left(\frac{P}{P}\right)_{cr} = 1.86$$

Recalling the flow function equation (48), it is found that

$$A_{THROAT} \phi_{cr} = \frac{\dot{m} \sqrt{T_0}}{P_0} \sqrt{\frac{R}{g}} = 13.82$$

$$A_{THROAT} = \frac{13.82}{.65811} = 21.0 \text{ in}^2$$

From Fig. 25 the measured minimum distance between blades at the exit plane is $a = .448 \text{ in.}$ and $s = 1.8 \text{ in.}$ is given. The number of blades is then

$$z = \frac{\pi D_m}{a} = 40.2 \quad (55)$$

In order to prevent harmonics in the wake pattern from the stator as seen by the rotor, a prime number of stator blades is chosen. In this case, $z = 41$ blades will suffice. For 41 blades,

$$a = \frac{\pi (23.0)}{41} = 1.763$$

so all measured values from Fig. 25 must be scaled by the scale factor,

$$\text{Scale Factor} = \frac{1.763}{1.8} = 0.9794$$

The blade height must now be

$$h_{S1} = \frac{A}{za} = \frac{21.0}{41.0 (.448 \times .9794)} = 1.165 \text{ in} \quad (56)$$

Recomputing ϕ_{cr} with a new loss coefficient based on this new blade height makes no measurable difference in exit area required so the

stator row design is now fixed. To simplify the iteration on ϕ a computer program was written to find the choked flow values of ϕ_{cr} , $(P/p)_{cr}$ and γ_p . This computer program is included in Appendix III and the computed data are presented as Table VII in Appendix V.

The flow conditions at the stator exit plane are determined from Fig. 24 as follows:

$$\frac{P_e}{P_0} = \frac{1}{1.86} = .538$$

$$\frac{T_{eis}}{T_0} = \left(\frac{P_e}{P_0} \right)^{\frac{\gamma-1}{\gamma}} = .8458$$

$$\frac{\Delta T_e}{T_0} = \left(\frac{T_0}{T_0} - \frac{T_{eis}}{T_0} \right) (1 - \gamma_a) = .1470$$

$$\frac{V_e}{T_0} = \sqrt{\frac{2\gamma g R}{\gamma-1} \frac{\Delta T_e}{T_0}} = 121.52$$

When a check is now made of the Mach number at the exit plane in order to check for choked flow it is found that

$$M_{V_e} = \frac{V_e}{\sqrt{2\gamma g R T_e}} = 0.97$$

This computed Mach number is the average Mach number of the flow at the minimum area. The highest Mach number at this area is equal to 1.00 but it is averaged with the Mach number of the flow in the boundary layer as accounted for by the loss coefficient. In

Appendix IV the derivation of the Mach number for choked flow in a polytropic expansion is presented. The "critical average" Mach number is found to be

$$M_{cr} = \sqrt{\frac{1-\gamma_p}{1+\gamma_p(\gamma-1)}} = \sqrt{\frac{n-1}{\gamma-1}} \quad (IV, 9)$$

This condition will also be encountered later in the computer program for the flow through the rotor and proper account must be taken of it there.

Using the relation from Ref. 20 for flow exit angle and the measured blade exit angle from Fig. 25 of $\alpha_{B1} = 73.9^\circ$ gives

$$\cos \alpha_1 = \frac{a}{a - (t_e / \cos \alpha_{B1})} = .268$$

$\alpha_1 = 75^\circ$

(18)

For the rotor, the blade height is permitted to be approximately 0.30 inches greater than the stator blade height in order to permit the streamlines to expand and offer no resistance to flow leaving the stator but not have dead areas above and below the useful flow area of the rotor blade. The rotor blade height will be taken then as

$$h_{R2} = 1.465 \text{ in.}$$

In order to satisfy the requirement for the rotor to see a relative Mach number of 0.8, some after-expansion is required. In order to evaluate the proper amount of after-expansion, the equations in Appendix II were coded for the computer to solve for any applied pressure ratio between the exit and discharge planes for a given γ ,

Mach number and blade angle. This computer program is included in Appendix III and the solution for $\gamma = 1.37$ and $\alpha_1 = 75^\circ$ over a range of pressure ratios is presented here as Fig. 28. The computer program can be used for any specific heat ratio, blade angle, Mach number and pressure ratio range.

After some iteration, it is determined that $p_1/p_0 = 0.460$ should give approximately the correct pressure ratio across the expansion area from the exit plane to the discharge plane,

$$\frac{p_1}{p_e} = \frac{p_d}{p_e} = \frac{.460}{.538} = 0.855$$

Now from Fig. 28 it is found that $\Delta\alpha \approx 0.2^\circ$ and $\zeta_A \approx .0008$. The total loss coefficient to be applied is based on a blade height of 1.165 inches for the stator. There is $\gamma = .1045$ from Fig. 21 and $K_h = .838$ from Fig. 23 for velocity computations. Therefore

$$\zeta_1 = \zeta(K_h) + \zeta_A = .0883$$

Now the velocity leaving the stator is determined with Fig. 24 as reference

$$\frac{T_{1,ss}}{T_0} = \left(\frac{p_1}{p_0} \right)^{\frac{\gamma-1}{\gamma}} = \left(\frac{460}{1000} \right)^{.2701} = .8108$$

$$\frac{\Delta T_1}{T_0} = \left(\frac{T_0}{T_0} - \frac{T_{1,ss}}{T_0} \right) (1 - \zeta_1) = .1892 (.9117) = .1725$$

$$\frac{V_1}{\sqrt{T_0}} = \sqrt{\frac{2\pi g R}{\gamma-1} \frac{\Delta T_1}{T_0}} = 131.60$$

and the corresponding boundary term. Applying the same procedure to the term $\int_{\partial\Omega} \phi \partial_\nu \phi \, d\sigma$ we get the corresponding boundary term. Since ϕ is zero on $\partial\Omega$ and $\partial_\nu \phi$ is zero on $\partial\Omega$ we have $\int_{\partial\Omega} \phi \partial_\nu \phi \, d\sigma = 0$.

Since ϕ is zero on $\partial\Omega$ and $\partial_\nu \phi$ is zero on $\partial\Omega$ we have $\int_{\partial\Omega} \phi \partial_\nu \phi \, d\sigma = 0$.

$$\int_{\Omega} \phi \partial_\nu \phi \, dx = \int_{\Omega} \phi \partial_\nu \phi \, dx$$

Since ϕ is zero on $\partial\Omega$ and $\partial_\nu \phi$ is zero on $\partial\Omega$ we have $\int_{\Omega} \phi \partial_\nu \phi \, dx = 0$. Since ϕ is zero on $\partial\Omega$ and $\partial_\nu \phi$ is zero on $\partial\Omega$ we have $\int_{\Omega} \phi \partial_\nu \phi \, dx = 0$. Since ϕ is zero on $\partial\Omega$ and $\partial_\nu \phi$ is zero on $\partial\Omega$ we have $\int_{\Omega} \phi \partial_\nu \phi \, dx = 0$.

$$\int_{\Omega} \phi \partial_\nu \phi \, dx = \int_{\Omega} \phi \partial_\nu \phi \, dx$$

Since ϕ is zero on $\partial\Omega$ and $\partial_\nu \phi$ is zero on $\partial\Omega$ we have $\int_{\Omega} \phi \partial_\nu \phi \, dx = 0$.

Since ϕ is zero on $\partial\Omega$ and $\partial_\nu \phi$ is zero on $\partial\Omega$ we have $\int_{\Omega} \phi \partial_\nu \phi \, dx = 0$.

$$\int_{\Omega} \phi \partial_\nu \phi \, dx = \int_{\Omega} \phi \partial_\nu \phi \, dx$$

$$\int_{\Omega} \phi \partial_\nu \phi \, dx = \int_{\Omega} \phi \partial_\nu \phi \, dx$$

$$\int_{\Omega} \phi \partial_\nu \phi \, dx = \int_{\Omega} \phi \partial_\nu \phi \, dx$$

To find the relative angle and relative velocity of the flow, it is necessary to construct the velocity triangle as shown in Fig. 26.

$$\frac{U_r}{\sqrt{T_0}} = \frac{\pi (RPM / \sqrt{T_0}) D_m}{720} = 34.18$$

$$\alpha_r = 75^\circ - 0.2^\circ = 74.8^\circ$$

$$\frac{V_{m1}}{\sqrt{T_0}} = \frac{V_r \cos 74.8^\circ}{\sqrt{T_0}} = 34.5$$

$$\frac{V_{u1}}{\sqrt{T_0}} = \frac{V_r \sin 74.8^\circ}{\sqrt{T_0}} = 127.0$$

$$\frac{W_{u1}}{\sqrt{T_0}} = \frac{V_{u1}}{\sqrt{T_0}} - \frac{U_r}{\sqrt{T_0}} = 92.82$$

$$\beta_r = \arctan (W_{u1} / V_{m1}) = 69.60^\circ$$

$$\frac{W_r}{\sqrt{T_0}} = \frac{W_{u1}}{\sqrt{T_0}} \frac{1}{\sin \beta_r} = 99.07$$

As a check on the requirement of a relative Mach number of 0.8 as seen by the rotor

$$M_{W_r} = \frac{W_r / \sqrt{T_0}}{\sqrt{\gamma g R T_r / T_0}} = \frac{99.07}{123.9} = 0.80$$

To design the rotor, several considerations must be kept in mind. The flow deflection should be as great as is practicable for maximum work output. The trailing edge thickness will be arbitrarily selected as .025 inches, and the spacing and blade design will be chosen so the minimum cross section area of the flow passage between

blades will occur at the "exit" plane. The rotor blade width is selected as 1.375 inches and impulse conditions only will be used for unchoked flow, i.e., $p_1 = p_2$.

Recalling that a relative total temperature and relative total pressure are defined as

$$\frac{T_{R1}}{T_0} = \frac{T_1}{T_0} + \frac{W_1^2}{2gJ\gamma T_0} = \frac{T_1}{T_0} + \frac{W_1^2(\gamma-1)}{2gJ\gamma R} = .9253 \quad (46)$$

$$\frac{P_{R1}}{P_0} = \frac{P_1}{P_0} \left(\frac{T_{R1}}{T_0} \right)^{\frac{1}{\gamma-1}} = .6955 \quad (47)$$

The flow function as applied to the rotor is

$$\phi = \frac{i\sqrt{T_{R1}}}{A_2 P_{R1}} \sqrt{\frac{R}{g}} \quad (48a)$$

and this expression will be used to determine the exit area of the rotor. For the prescribed impulse conditions

$$\frac{P_{R1}}{P_2} = \frac{.6955}{.4600} = 1.515$$

and the value to be used on the abscissa of the plots for rotor loss coefficients in Figs. 22 and 23

$$\frac{U_1}{V_1} = \frac{34.18}{131.61} = .2598$$

and the other for the same reason. The first is the
natural state of the tree, and the second is the
state of the tree when it is cut down.

It is evident that the tree is cut down.

It is evident that the tree is cut down.

It is evident that the tree is cut down.

It is evident that the tree is cut down.

It is evident that the tree is cut down.

It is evident that the tree is cut down.

It is evident that the tree is cut down.

It is evident that the tree is cut down.

It is evident that the tree is cut down.

It is evident that the tree is cut down.

It is evident that the tree is cut down.

It is evident that the tree is cut down.

With this value the rotor loss coefficient for flows is found to be

$$\zeta_2 = .819 (.192) = .1572$$

Now using Fig. 27 for this pressure ratio and loss coefficient and using linear interpolation the flow function is

$$\phi = .58953$$

and from eq. (48a) above

$$\phi A_2 = 19.13$$

$$A_2 = 32.44 \text{ in}^2$$

An impulse rotor operating under conditions as these should have a ratio

$$\left(\frac{s}{b}\right) \cong 0.7$$

and so

$$s = 0.7 (1.375) = 0.962$$

For the mean diameter of 23.0 inches, the number of blades on the rotor is then

$$z_2 = \frac{\pi(23.0)}{.962} = 75.1 \text{ blades}$$

Since an odd number of blades was chosen for the stator the rotor should have an even number of blades to reduce the possibility of resonance induced vibrations and the resulting metal fatigue.

Arbitrarily choosing 76 blades

$$s = \frac{\pi(23.0)}{76} = .9415 \text{ in}$$

and the distance between blades, a , to obtain the required area of 32.44 square inches is

$$a = \frac{A_2}{\frac{z_2}{2} \frac{h}{R^2}} = .273 \text{ in}$$

The exiting blade angle can be seen from Fig. 25 to be

$$\cos \beta_{82} = \frac{a + t_e}{s} = .3162$$

$$\beta_{82} = 71.57^\circ$$

The blade design itself is based on a circular arc contour of the concave face. The geometric relations of the design have been programmed by Vavra for computer solution. Using this computer program and requiring solutions for 74, 76, 78, 80 and 82 blades, the printout of the computer solution is presented as Fig. 29. The values necessary to draw the blade design are shown in Fig. 30 and have been used to draw Fig. 25.

The solution for 76 blades appears valid and so the other solutions are not used. The resulting $\left(\frac{s}{b}\right) = 0.691$. A check on this spacing can be made by Brilings Rule, an early rule-of-thumb for steam turbines which is found in Ref. 3 to be

$$\left(\frac{b}{s}\right) = 2.5 \sin 2 \beta^* \text{ where } \beta^* = 90 - \beta_{B2} \quad (57)$$

$$\left(\frac{b}{s}\right) = 2.5 \sin 36.86^\circ = 1.5$$

$$\left(\frac{s}{b}\right) = \frac{1}{1.5} = .6667$$

Also Ref. 28 presents a relation for spacing and blade angles based on an aerodynamic load coefficient ψ_T which is found to have a nearly constant value over a wide range of turbine designs. The relation is

$$\psi_T = 2 \cdot \frac{\sin \beta_2^*}{\sin \beta_1^*} \sin(\beta_1^* - \beta_2^*) \left(\frac{s}{b}\right) = 0.8 \quad (58)$$

and so, using proper angles as defined in Ref. 28 for this case

$$\left(\frac{s}{b}\right) = \frac{0.8}{2.0} \frac{\sin 20.40^\circ}{\sin 18.43^\circ \sin 38.83^\circ} = .704$$

The relations by Briling and Zweifel show at least that the choice of 76 blades is reasonable for this design. The relation of Zweifel in particular is based on two-dimensional considerations and does not account for blade height. Some unpublished test data available to Vavra indicates the value of 0.691 is a good one for this size turbine.

To complete the computations necessary to determine the power output of the turbine for a given set of conditions, the velocity triangle after the rotor is computed.

and other biological systems. It appears that the cell membrane is a complex system, consisting of a number of different components, and that the membrane is not a simple barrier to the passage of molecules. The membrane is a complex system, consisting of a number of different components, and that the membrane is not a simple barrier to the passage of molecules.

$$\left(1 - \frac{1}{2} \left(\frac{1}{2} \right)^{n-1} \right) \frac{1}{2} \left(\frac{1}{2} \right)^{n-1} = \frac{1}{2} \left(\frac{1}{2} \right)^{n-1}$$

consists of all cells having a single membrane, the membrane

$$= \frac{1}{2} \left(\frac{1}{2} \right)^{n-1} = \frac{1}{2} \left(\frac{1}{2} \right)^{n-1}$$

consists of all cells having a single membrane, the membrane is not a simple barrier to the passage of molecules. The membrane is a complex system, consisting of a number of different components, and that the membrane is not a simple barrier to the passage of molecules.

consists of all cells having a single membrane, the membrane is not a simple barrier to the passage of molecules.

consists of all cells having a single membrane, the membrane is not a simple barrier to the passage of molecules.

For no after-expansion, $\beta_2 = \beta_{B2} = -71.57^\circ$, and finding loss coefficients in the manner previously described,

$$\frac{T_{2is}}{T_0} = \frac{T_{R1}}{T_0} \left(\frac{P_2}{P_{R1}} \right)^{\frac{r-1}{r}} = .9263 \left(\frac{.460^\circ}{.6955} \right)^{.2701} = .8275$$

$$\frac{\Delta T_2}{T_0} = \left(\frac{T_{R1}}{T_0} - \frac{T_{2is}}{T_0} \right) (1 - \beta_2) = .0710$$

$$\frac{T_2}{T_0} = \frac{T_{R1}}{T_0} - \frac{\Delta T_2}{T_0} = .8543$$

$$\frac{W_2}{\sqrt{T_0}} = \sqrt{\frac{2\pi g R}{r-1} \frac{\Delta T_2}{T_0}} = 84.39$$

Using relations as before with Fig. 26 as reference, it is found

$$\frac{V_{u2}}{\sqrt{T_0}} = -45.93$$

and the power output, with the proper conversion factors is

$$HP = \frac{\dot{W}}{gJ} (U_1 V_{u1} - U_2 V_{u2}) (1.414) = 48,682 \text{ HP} \quad (59)$$

These computations are verified by the computer program. The first page of the printout of the computer program is presented as Fig. 31.

and $\sin \theta = \frac{1}{2}$. The condition $\sin \theta \neq 0$ is equivalent to $\theta \neq 0$ and $\theta \neq \pi$.

$$\begin{aligned} \text{Condition 1: } & \left(\theta \neq 0 \right) \cap \left(\theta \neq \pi \right) \cap \left(\frac{\partial f}{\partial x} \neq 0 \right) \cap \left\{ \frac{\partial f}{\partial x} \neq 0 \right\} \\ \text{Condition 2: } & \left(\theta \neq 0 \right) \cap \left(\theta \neq \pi \right) \cap \left(\frac{\partial f}{\partial x} \neq 0 \right) \cap \left\{ \frac{\partial f}{\partial x} \neq 0 \right\} \\ \text{Condition 3: } & \left(\theta \neq 0 \right) \cap \left(\theta \neq \pi \right) \cap \left(\frac{\partial f}{\partial x} \neq 0 \right) \cap \left\{ \frac{\partial f}{\partial x} \neq 0 \right\} \end{aligned}$$

Since $\theta \neq 0$ and $\theta \neq \pi$ are the same condition, Condition 1 is the same as Condition 2.

$$\text{Condition 1: } \left(\theta \neq 0 \right) \cap \left(\theta \neq \pi \right) \cap \left(\frac{\partial f}{\partial x} \neq 0 \right) \cap \left\{ \frac{\partial f}{\partial x} \neq 0 \right\}$$

Condition 1 is equivalent to $\theta \neq 0$ and $\theta \neq \pi$ and $\frac{\partial f}{\partial x} \neq 0$.

$$\text{Condition 1: } \left(\theta \neq 0 \right) \cap \left(\theta \neq \pi \right) \cap \left(\frac{\partial f}{\partial x} \neq 0 \right) \cap \left\{ \frac{\partial f}{\partial x} \neq 0 \right\}$$

Condition 1 is equivalent to $\theta \neq 0$ and $\theta \neq \pi$ and $\frac{\partial f}{\partial x} \neq 0$. The condition $\frac{\partial f}{\partial x} \neq 0$ is equivalent to $\frac{\partial f}{\partial x} \neq 0$. The condition $\frac{\partial f}{\partial x} \neq 0$ is equivalent to $\frac{\partial f}{\partial x} \neq 0$.

V. Computer Program

A. General Considerations

The computer program for the evaluation of the turbine performance is intended to be as general as possible within the framework of the turbine design method used. Any single stage turbine so designed can be evaluated by entering new physical dimensions, entrance conditions and loss coefficient data. The static pressures to be imposed ahead of and behind the rotor must be programmed by the user within the main program. The loss data must be of the same format as Figs. 21, 22 and 23.

B. Main Program

1. The main program is intended to make the major computations and comparisons and provide control. The subroutines are provided to do the lengthy iterative processes and repetitive calculations. The flow charts for the main program and the subroutines are included with the program listings found in Appendix III.

The basic concept of the computer program is as follows:

- a. With the input data given, compute the design condition including the after-expansion at stator discharge.
- b. Reduce the static pressure through the impulse rotor in increments, computing velocity triangles and power at each pressure increment. The shock condition for supersonic flow entering the rotor is computed. Also the flow function through the rotor is checked for the choked condition.

c. When the choked condition through the rotor is attained, the static pressure at the rotor discharge is lowered in increments and the after-expansion condition computed. The resulting power and velocity and thermodynamic conditions are computed for each pressure increment.

d. The process is terminated when the loss coefficient due to the rotor after-expansion is reduced to zero.

The program will also terminate if the loss coefficient due to after-expansion out of the stator goes to zero or if the loss coefficient due to an entry shock into the rotor goes to zero. Any continuation of the program beyond these limiting conditions would lead to conditions which violate the Second Law of Thermodynamics, as explained in Ref. 1.

The loss coefficient reaches a maximum and then declines to zero or negative values as the imposed pressure ratio across the control area is decreased in increments for the after-expansion case. The exact reason for this is not known. A check was made to see if the axial component of the Mach number of the flow leaving the blade row reached $M = 1.00$ when the loss coefficient reduced to zero. It is found this is not exactly the case but that the axial component of the Mach number is less than one. Further work is needed on this point.

2. Some pertinent comments may be useful about the main decision points in the main program. The flow chart in Appendix III shows that the first check is for the magnitude of the static pressure between

the stator and rotor compared to the static pressure in the exit plane of the stator. For a stator designed as a converging-diverging nozzle, the Mach number at the exit plane may be greater than $M_{Ve} = 1.00$. If the static pressure between the stator and rotor is greater than the static pressure at the stator exit plane, the shock condition is computed at the stator exit. If the pressures are equal, there is no flow deflection, and if the static pressure between the stator and rotor is lower than the exit plane pressure, the after-expansion case is computed.

The next decision is based on the relative Mach number as seen by the rotor. For the supersonic case, the shock of the flow in the rotor entry is computed. For subsonic flow the component of relative velocity in the direction of the rotor blade entering angle is used to compute flow conditions.

The flow function and critical pressure ratios are used to determine choked conditions in the rotor. As can be seen in Appendix IV the Mach number of the flow at the rotor exit plane is an average value, and the critical Mach number varies with the loss coefficient as shown there. Since the impulse conditions for the rotor are specified, some care is taken by an iteration process to find the $P_1 = P_2$ condition for choked flow before the program continues.

Once the choked condition in the rotor is attained, the conditions forward of the rotor exit plane remain fixed. The Mach number of the flow at the rotor exit plane is set at $M_{We} = 1.00$ and the

static pressure behind the rotor is lowered in increments. The after-expansion behind the rotor is then computed until the limiting condition is reached.

C. Subroutines

1. The subroutine called TRNGL computes the velocity triangle based on rpm, absolute velocity and direction or based on rpm, relative velocity and direction.

2. The subroutine called AFTER computes the deflection of the flow due to shock or expansion of the flow out of a blade row. The flow angle is incremented from the blade angle and the pressure ratio is computed and compared to the imposed value. The process continues until the flow deflection is found which corresponds to the pressure ratio imposed. The detailed equations are derived in Appendix II, based on Ref. 26.

3. The subroutine for computing the flow function for a pressure ratio imposed across the blade row is named CPHI. The polytropic loss coefficient corresponding to the design flow loss coefficient is determined by iteration. Then the flow function to satisfy the imposed conditions, critical flow function, and critical pressure ratio are computed from the equations developed in Appendix I. The pressure ratio was found to be more sensitive in fewer significant figures than the flow function itself so decisions in the main program are based on pressure ratio comparisons.

4. Subroutine BEFORE is used to compute rotor entry shocks based on the relations in Ref. 1 which in turn are based on considerations similar to those of Ref. 26 for after-expansion. Since the flow deflection is known, an iteration process is not required and the computations are straightforward. For cases which are not directly solvable by the basic equations, the component of the velocity in the direction of the blade angle is taken as the useful resultant.

5. The CURVE subroutine is written as a means of finding a data point on a curve. The loss coefficient curves "for velocities" from Figs. 21, 22 and 23 are stored in the computer in the form of arrays. The subroutine writes the second-order equation of the appropriate three stored data points nearest to the input abscissa, and then finds the ordinate on the curve with the input abscissa. The subroutine is arranged in such a manner that the stored data must have equal abscissa increments and the first abscissa point must be zero. This means arbitrarily extending a curve such as Fig. 21 to $M_{is} = 0.0$ whether the data at low values of M_{is} will be used or not.

D. Results of Computer Program

1. The turbine design data given in the preceding section of this thesis were entered into the computer program and the resulting printout for the design condition only is presented as Fig. 31. The pressure ratio across the turbine was then increased in increments (by lowering p_1 and p_2 while holding P_0 constant) and the resulting computations are included as Table VIII in Appendix V. The rpm was

also decreased from 13000 to 9000 in 1000 rpm increments and the complete pressure range imposed at each rpm. These results are also included in Table VIII.

2. The non-dimensional parameters previously discussed were then plotted in order to make cross plots which ultimately result in a portion of the turbine performance map.

3. The data immediately available from the computer printout permits the direct plotting of Fig. 35, Turbine Efficiency vs. Pressure Ratio, with the rpm as a parameter. The anticipated gradual loss of efficiency with increasing pressure ratio is evident. Of interest is the change in slope of the curve at the point where rotor after-expansion commences. The indication is that the increase in velocity due to after-expansion causes the peripheral component of the velocity to increase, even though a deflection of the flow toward the axial direction also occurs. Therefore, the rate of loss of efficiency is decreased, although the change is very small. A reduction in rpm contributes to a large loss in efficiency at any given pressure ratio.

4. In Figs. 36 and 37 the most important indication is as follows: Fig. 37 shows that for a fixed design at a pressure ratio of $(P_o/p_2) = 2.174$, the increase in power for an increase in overall pressure ratio is direct and marked up to a pressure ratio of about 4.5 or 5.0. Further large increases in pressure ratio net very small gains. In Fig. 36 the corollary is shown for efficiency. The

initial increase in pressure ratio and power output causes a certain loss of efficiency but the remaining increase in pressure ratio and power output causes a drastic loss of efficiency.

An interesting comparison can now be made with the high head coefficient data from the first section of this thesis. In that section, each point on each curve represents a different turbine design. The conclusion was that if a required high power output transcends the need for high efficiency, then a very high head coefficient should be used for the turbine design. The initial increase of head coefficient from the optimum value causes a large loss of efficiency. Once this initial efficiency loss is accepted, further increase in head coefficient require little more loss of efficiency. Now in this section concerned with the off-design performance of a particular fixed turbine design, the conclusion is: additional power can be obtained at a higher pressure ratio than design but only in the initial increase of pressure ratio. The extremely high loss in efficiency is encountered if the last possible increment of power is demanded.

5. The turbine performance map presented as Fig. 38 serves to indicate the pertinent trends for the parameters investigated. The lines of constant efficiency form only a portion of the elliptical curves they become over the complete range of referred rpm and power coefficient. The only conditions investigated in this thesis are at high power coefficients. The peak efficiency for this turbine would occur in the lower right hand corner of Fig. 38, i.e., in a

lower power coefficient range than shown here and in the referred rpm range of about 350.

6. This turbine designed for high head coefficients can now be compared to the theoretical values predicted in the first section of this thesis. The head coefficient is defined in eq. (1). The isentropic velocity C_o is given by reference to the ΔT_{is} of Fig. 24 as

$$\frac{C_o^2}{2gJ\zeta_p} = T_o \left[1 - \left(\frac{P_2}{P_o} \right)^{\frac{\gamma-1}{\gamma}} \right] \quad (60)$$

For pressures and temperatures at the design point

$$k_{is} = \left[\frac{C_o / \sqrt{T_o}}{U_1 / \sqrt{T_o}} \right]^2 = \left(\frac{137.839}{34.144} \right)^2 = 16.2 \quad (1)$$

Referring now to Table I at $\alpha_1 = 75^\circ$, $r^* = 0.0$ and $k_{is} = 16.0$ the values determined from the theoretical conditions can be compared to the turbine design. The comparison is shown in Table IX in the columns Theoretical #1 and Turbine Design.

The ratio V_{m2}/V_{m1} was arbitrarily selected equal to one for the theoretical development. This was not a selected parameter for the turbine design and the discrepancy between the two values of V_{m2}/V_{m1} are the basis for the differences seen in Table IX. Since the ratio V_{m2}/V_{m1} was not required to be equal to one in the turbine design, the flow is deflected more in the rotor. This results in higher absolute values for β_2 and α_2 . Since the flow deflection is greater, the peripheral component of the absolute velocity (V_{u2}) is greater and the power output and efficiency are increased. Otherwise,

the theoretical predictions are good. The v_{m2}/v_{m1} value from the turbine design can be entered into the equations and the correspondence should be more exact. This was done and the resulting data is the column headed Theoretical #2 in Table IX.

Table IX
COMPARISON OF THEORETICAL AND TURBINE DESIGN VALUES

	Theoretical #1	Turbine Design	Theoretical #2
α_1	75°	74.8° (after-expansion)	75° *
ϕ_E	0 *	0	0 *
R_2/R_1	1.0 *	1.0	1 *
v_{m2}/v_{m1}	1.0 *	.784	.784 *
ψ	.95 *	.955	.95 *
ϕ_R	.95 *	1.00	.95 *
ψ	.849	.852	.833
r^*	0.0 *	0.0	0.0 *
k_{is}	16. *	16.2	16.2 *
γ	.60111	.723	.60358
k_E	2.263	2.42	2.031
v_{m1}/U_1	.984	.998	.990
W_2/W_1	.827	.852	.812
β_1	69.78°	69.60°	69.82°
β_2	-65.30°	-71.57°	-70.54°
α_2	-49.17°	-59.84°	-57.02°

* selected, not computed

7. The curves of Fig. 26 are shown again in Fig. 39 with all values referred to the design point. All values are then shown as a percent of the design point values. Fig. 39 demonstrates the strong effect of rpm on power output and efficiency. At 70% design rpm, it is not possible to develop design power output. At about 90% design rpm, the design power can be developed at 95% of design efficiency. A maximum power of about 125% of the design value is the maximum which can be developed at 90% design rpm. At the design rpm, 125% design power can be developed with a loss of efficiency of 10%. When greater power increments are required, the efficiency loss becomes increasingly large. A 40% increase in power can be developed but at only 72.5% of design efficiency.

At design rpm, 125% design power requires an overall pressure ratio of 3.5, and 140% design power requires an overall pressure ratio of 8.5.

8. As this thesis was being published, it was determined that the computer program finds the off-design performance of a turbine in which impulse conditions are maintained until choked flow occurs in the rotor. A rotor blade height of 1.648 inches is required to satisfy such a condition. When this new rotor blade height is introduced into the computer program, the only direct influence is on the blade height correction factor for loss coefficients. The performance computations change is negligibly small.

VI. Conclusions and Recommendations

A. Conclusions

1. If a requirement for a high shaft power output turbine is encountered for which weight, size and space limitations preclude having several stages operating at peak efficiency, then a slightly higher head coefficient and slightly lower efficiency compromise design should not be made. Designing for power outputs higher than optimum should be based on extreme power output per stage. The initial loss of efficiency is great when a slightly higher than optimum head coefficient is considered. Not much more efficiency is lost by imposing extreme values of head coefficient.

2. From the available literature, no straightforward method of computing losses is found which correlates well with the available data. This appears to be a fruitful area for future research and testing.

a. The available data indicates the tip clearance loss is not zero even for impulse conditions and no clearance gap. The trailing vortices induced at the ends of the blades introduce velocity components which do no useful work. Clearance gaps within the annulus boundary layers should give tip clearance loss values about the same as zero clearance. As the clearance gap is increased, the loss increases. Also the loss increases as the degree of reaction is increased. A high degree of reaction means a high pressure drop across the blade row and such a pressure differential is conducive to high leakage across the blade tips.

The loss due to tip clearance is also affected by the relative size of the gap to the blade height. The effect of leakage across the tips of the blades on the secondary flow will make measurements difficult to separate into tip clearance and secondary flow losses.

b. The profile loss is a function of blade thickness to chord ratio, spacing, flow deflection and probably general blade shape. This loss offers the most possibilities for simple and accurate measurements in a cascade test rig.

c. The trailing edge thickness losses are probably insensitive below a certain ratio of trailing edge thickness and spacing, and then assume a real importance at higher values. These losses, too, should be relatively simple to measure.

d. The secondary loss measurement offers the most difficulty. No known theory accurately predicts the loss. Indications are that the secondary loss is primarily dependent on the flow turning angle and ratio of blade height to the chord or axial width of the blade. The tip clearance effect is also of primary importance and will be difficult to divorce in the measurements.

e. Once the four component losses mentioned above have a firm basis in measurements, it will be appropriate to consider Reynolds number and Mach number effects as they affect the losses in turbine blade rows.

3. The computer program for the turbine performance analysis yields results as accurate as the loss data available. The program only requires inputs of loss coefficients in the specified form and

a design based on the flow function ϕ for area determinations.

The analysis of the off-design performance of this particular turbine indicates that large gains in power output can be obtained at pressure ratios two or three times the design value if a 15% drop in efficiency can be accepted. Attempting to obtain the last possible increment of power, however, requires extreme values of pressure ratio and another large loss in efficiency.

4. Further investigation into the after-expansion behind a blade row is needed. A cursory examination of the magnitude of the axial component of the Mach number of the flow leaving an after-expansion showed it to be less than one when the loss coefficient decreased to zero. The exact reason for this loss coefficient behavior is not known.

B. Recommendations

1. That an organized effort be made to measure and define component losses in blade rows in a form useful for design purposes.

a. It would appear that trailing edge thickness effects and profile losses could be measured in cascade test rigs with a limited number of profiles, solidities and blade heights. Some correlation of these measurements could be made with Ainley and Markov.

b. The tip clearance loss should be measured in a rotating turbine test stand. The direct effects would not be hard to measure if the effect on secondary loss was not present. Since this effect

is present, it will require study to obtain quantitative correlation and isolate the tip clearance loss from the secondary flow effects.

c. The secondary loss will probably have to be deduced by subtracting the outer component losses from the overall efficiency as measured for the complete turbine blade row. No method is presently known for measuring the secondary loss directly.

2. Tests on the after-expansion behind a blade row should be made. Physical measurements may shed some light on the reason for the loss coefficient reaching a peak and then decreasing to negative values as the expansion is increased. Further theoretical study is also required, especially to consider three-dimensional effects. The testing program should include this variable.

References

1. Vavra, M. H., "Aero-Thermodynamics and Flow in Turbomachines", John Wiley and Sons, Inc., 1960.
2. McCracken, D. D., "A Guide to FORTRAN Programming", John Wiley and Sons, Inc., 1961.
3. Stodola, A. and L. C. Loewenstein, "Steam and Gas Turbines", Vol. I and II, McGraw-Hill Book Co., Inc., 1927.
4. Cox, Sir Harold Roxbee (Editor), "Gas Turbine Principles and Practice", D. Van Nostrand Co., Inc., 1955.
5. Godsey, F. W. Jr., and Lloyd A. Young, "Gas Turbines for Aircraft", McGraw-Hill Book Co., Inc., New York and London, 1949.
6. Wislicenus, George F., "Fluid Mechanics of Turbomachinery", McGraw-Hill Book Co., Inc., New York and London, 1947.
7. Vincent, E. T., "The Theory and Design of Gas Turbines and Jet Engines", McGraw-Hill Book Co., Inc., New York and London, 1950.
8. Sorenson, Harry A., "Gas Turbines", Ronald Press Co., New York, 1951.
9. Squire, H. B. and K. G. Winter, "The Secondary Flow in a Cascade of Airfoils in a Non-uniform Stream", Journal of the Aeronautical Sciences, Vol. 18, No. 4, April 1951.
10. Weske, John R., "Fluid Dynamic Aspects of Axial Flow Compressors and Turbines", Journal of the Aeronautical Sciences, Vol. 14, November 1947.
11. Kochendorfer, Fred D. and J. Cary Nettles, "An Analytical Method of Estimating Turbine Performance", NACA Report 930, U. S. Government Printing Office, Washington, D.C., 1951.
12. Howell, A. R., "The Aerodynamics of the Gas Turbine", Journal of the Royal Aeronautical Society, Vol. 52, 1948.
13. Kraft, Hans, "Reaction Tests of Turbine Nozzles for Subsonic Velocities", Transactions of the ASME, Vol. 71, October 1949.
14. Keenan, J. H., "Reaction Tests of Turbine Nozzles for Supersonic Velocities", Transactions of the ASME, Vol. 71, October 1949.

15. Emmert, H. D., "Current Design Practices for Gas-Turbine Power Elements", *Transactions of the ASME*, Vol. 72, February, 1950.
16. Reeman, J., "The Turbine for the Simple Jet Propulsion Engine", *Proceedings of the Institution of Mechanical Engineers*, Vol. 153, 1945.
17. Weske, J. R., "Investigations of Blade Characteristics", *Transactions of the ASME*, Vol. 66, July, 1944.
18. Scholz, N., "Systematic Investigations on Secondary Flow Losses in Cascades", Report No. 56/18a, Institute of Fluid Mechanics, Engineering University, Braunschweig, Germany, March 1957.
19. Gerstan, K., "Results of Systematic Investigations on Secondary Flow Losses in Cascades", Part I: Secondary Flow Losses in Compressor Cascades of Profile, NACA 8410, Institute of Fluid Mechanics, Engineering University, Braunschweig, Germany, June, 1955.
20. Markov, N. M., "Calculation of the Aerodynamic Characteristics of Turbine Blading", Associated Technical Services, Inc., New Jersey, 1958.
21. Meldahl, A., "The End Losses of Turbine Blades", *Brown-Boveri Review*, November 1941.
22. Carter, A. D. S., "Three-Dimensional Flow Theories for Axial Compressors and Turbines", *Proceedings of the Institution of Mechanical Engineers*, Vol. 159, 1948.
23. Ainley, D. G., "Performance of Axial Flow Turbines", *Proceedings of the Institution of Mechanical Engineers*, Vol. 159, 1948.
24. Ainley, D. G., and G. C. R. Mathieson, "An Examination of the Flow and Pressure Losses in Blade Rows of Axial Flow Turbines", *Aeronautical Research Council Reports and Memoranda No. 2891*, Ministry of Aviation, Her Majesty's Stationery Office, London, March, 1951.
25. Ainley, D. G., and G. C. R. Mathieson, "A Method of Performance Estimation for Axial Flow Turbines", *Aeronautical Research Council Reports and Memoranda, No. 2974*, Ministry of Aviation, Her Majesty's Stationery Office, London, December, 1951.

26. Trampel, W., "Die Strahlablenkung in der Wollbeaufschlagten Turbine", Report No. 3, Institute of Thermal Turbomachines, Federal Institute of Technology, Leeman Brothers, Zurich, Switzerland, 1956.
27. Hawthorne, W. R. and W. T. Olson, "Design and Performance of Gas Turbine Power Plants", Princeton University Press, 1960.
28. Zweifel, O., "The Spacing of Turbo-Machine Blading, Especially with Large Angular Deflection", Brown-Boveri Review, December 1945.
29. Vavra, M. H., unpublished data.

FIG. 1
EFFICIENCY VS. HEAD COEFFICIENTS

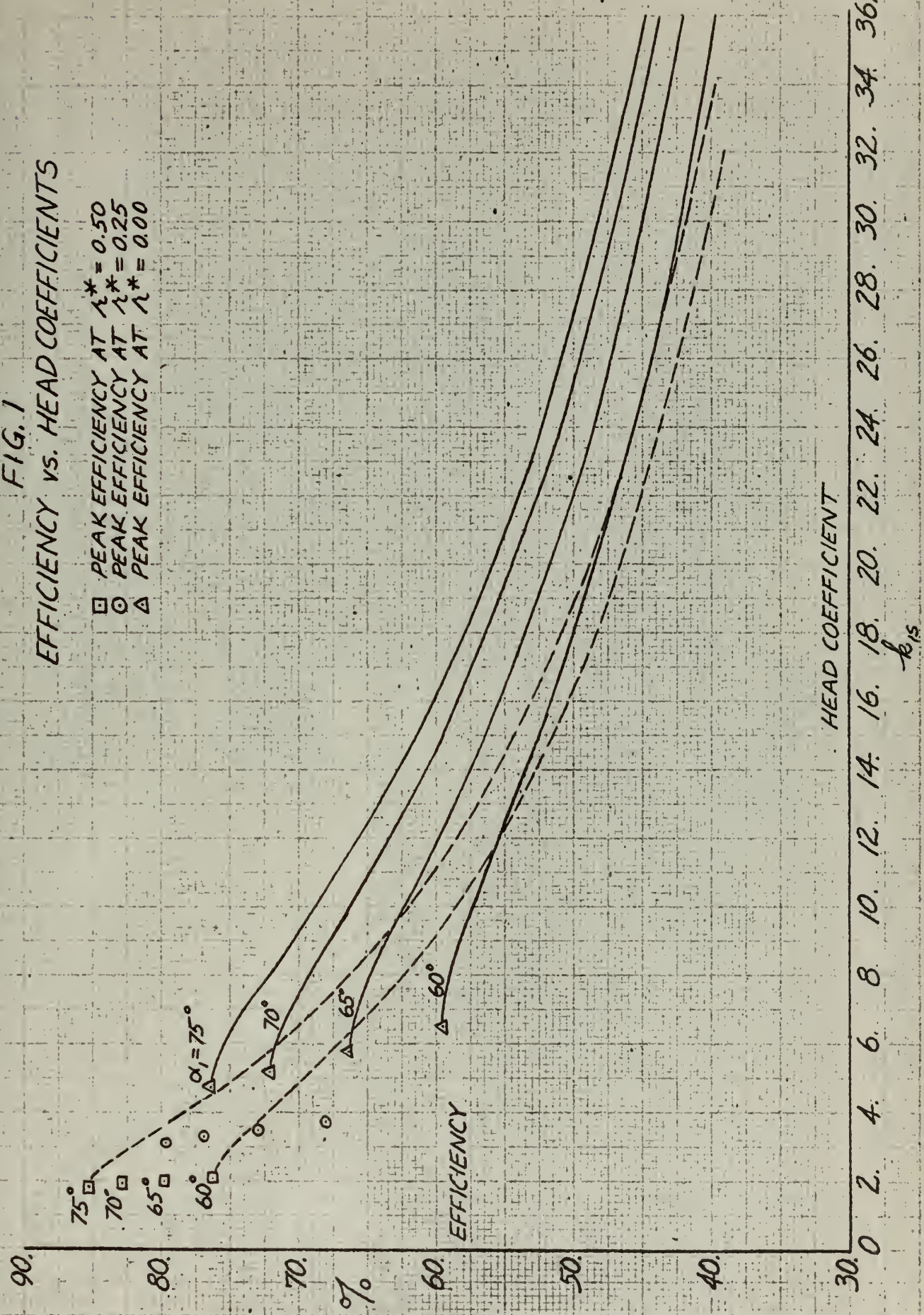


FIG. 2
HIGH HEAD COEFFICIENT DATA
 $\alpha_1 = 60^\circ$

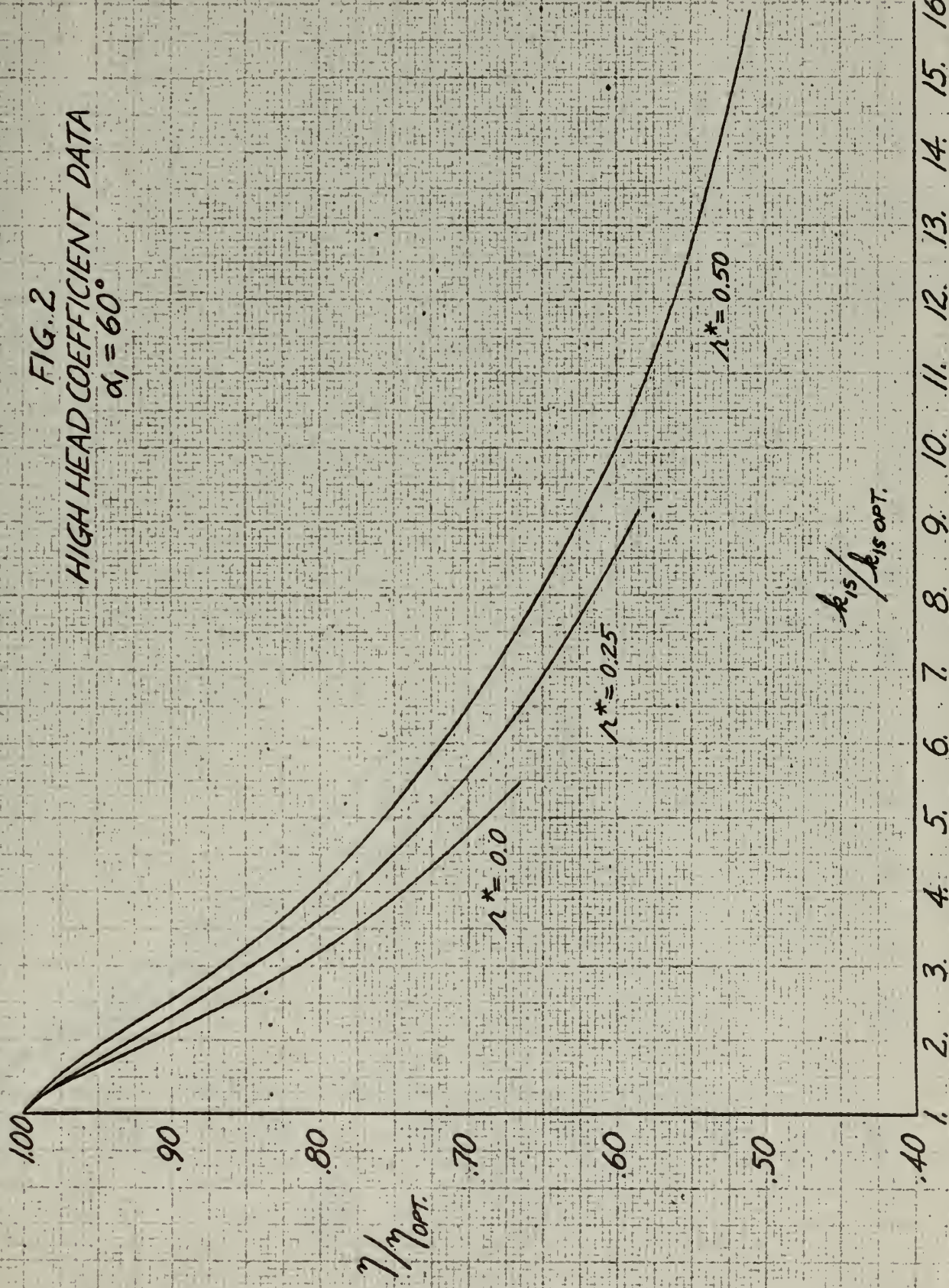


FIG. 3
HIGH HEAD COEFFICIENT DATA
 $\alpha_1 = 65^\circ$

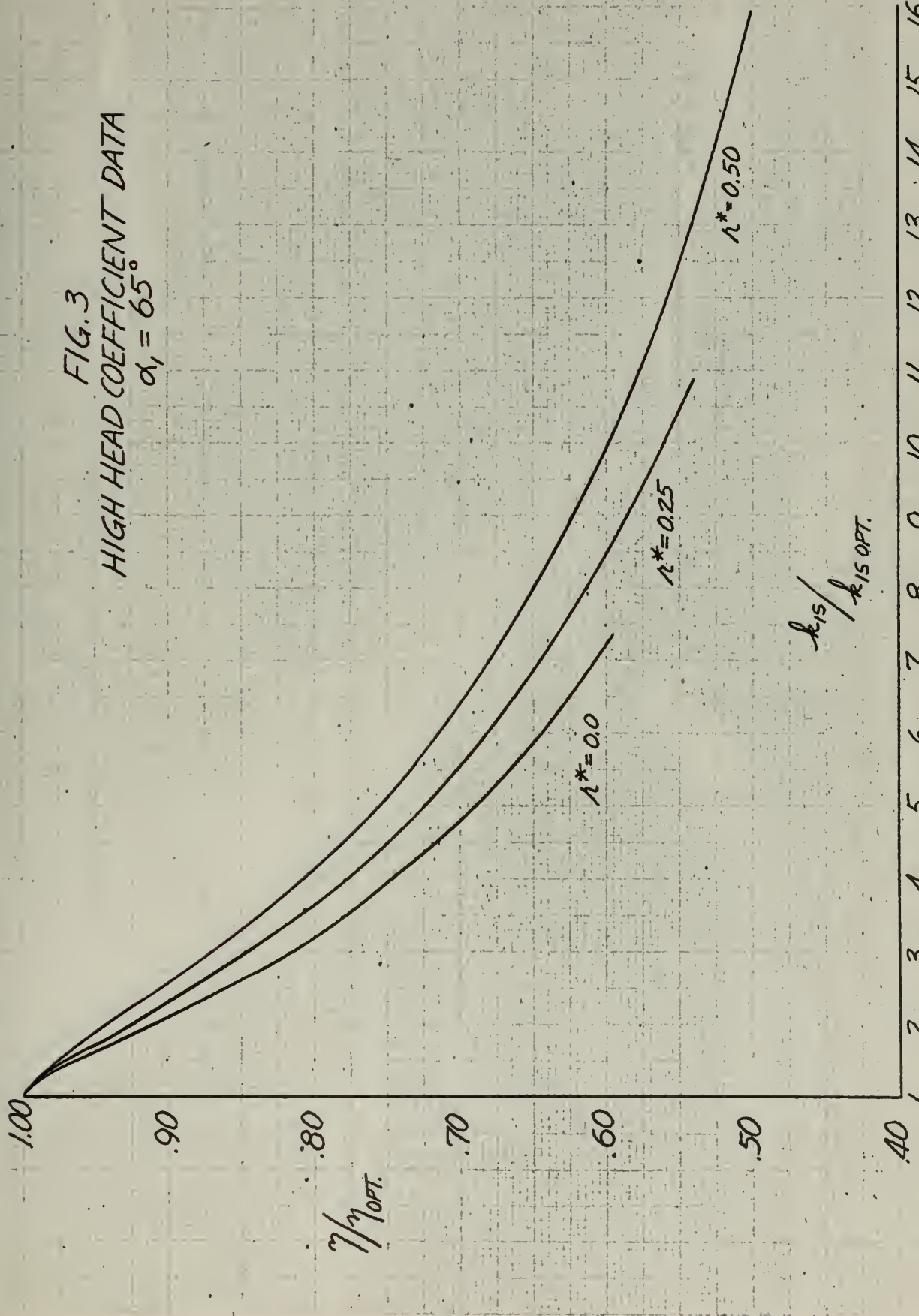


FIG. 4
HIGH HEAD COEFFICIENT DATA
 $\alpha_i = 70^\circ$

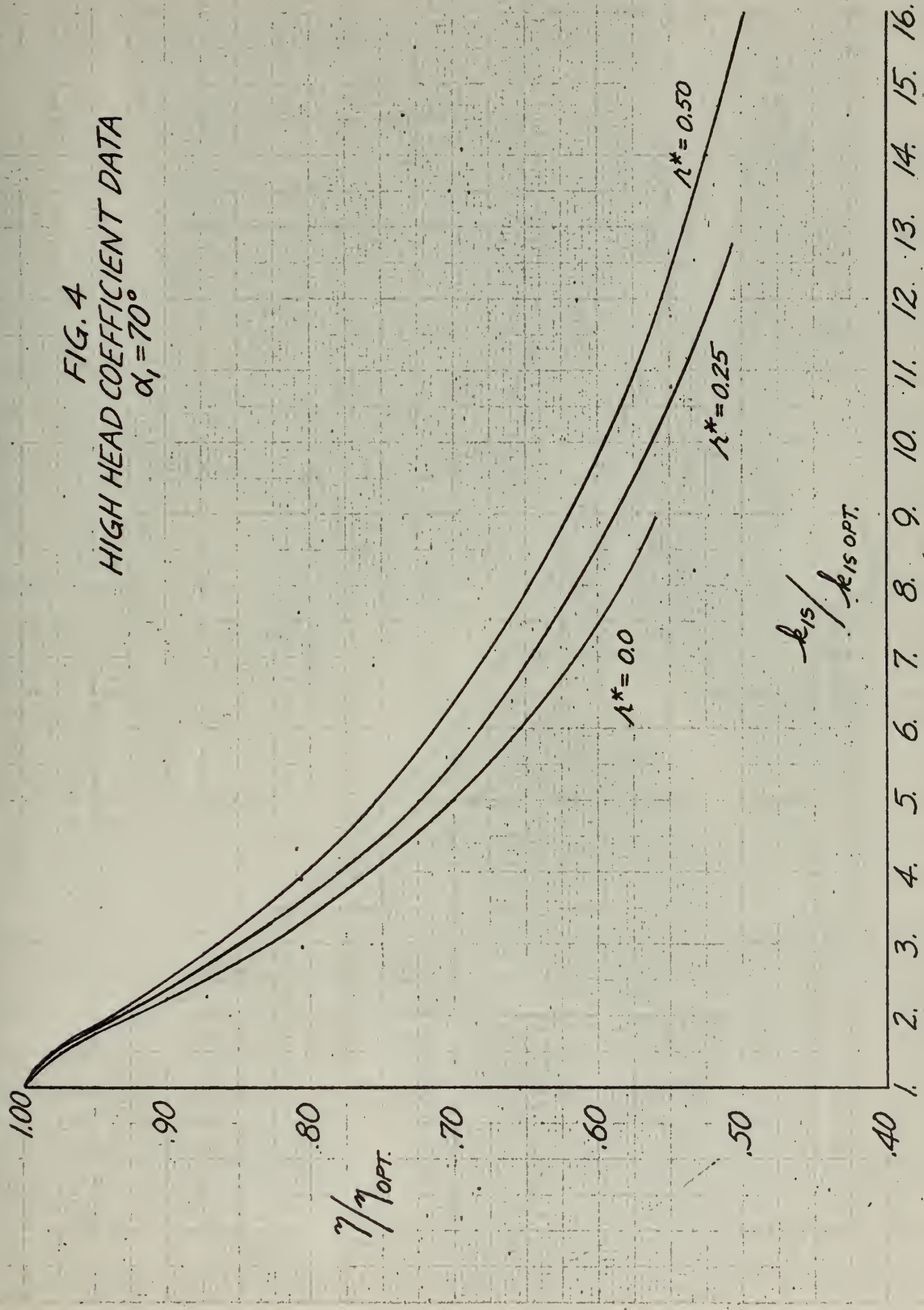


FIG. 5
HIGH HEAD COEFFICIENT DATA
 $\alpha_1 = 75^\circ$

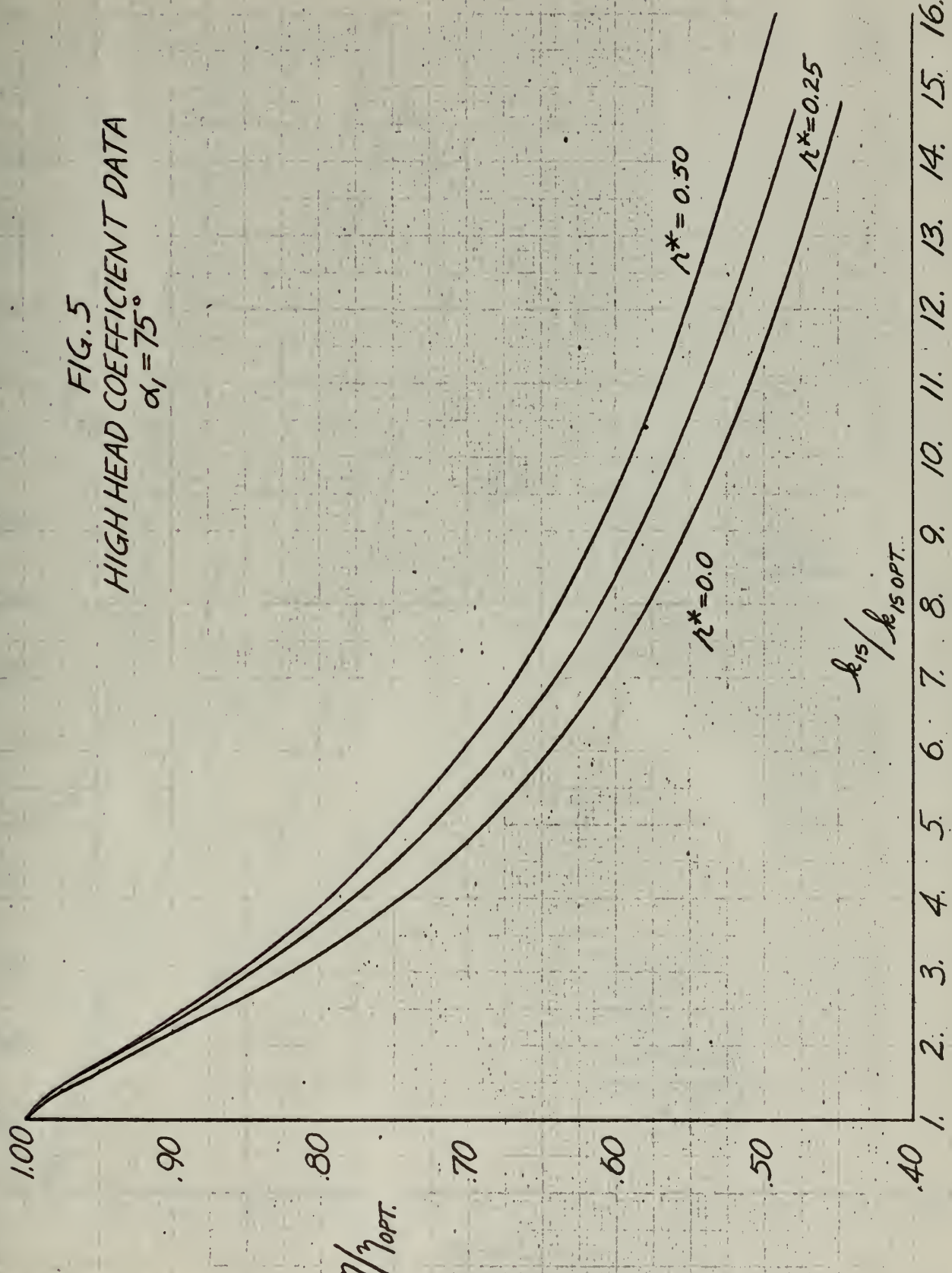


FIG. 9
TIP CLEARANCE
LOSS COEFFICIENTS

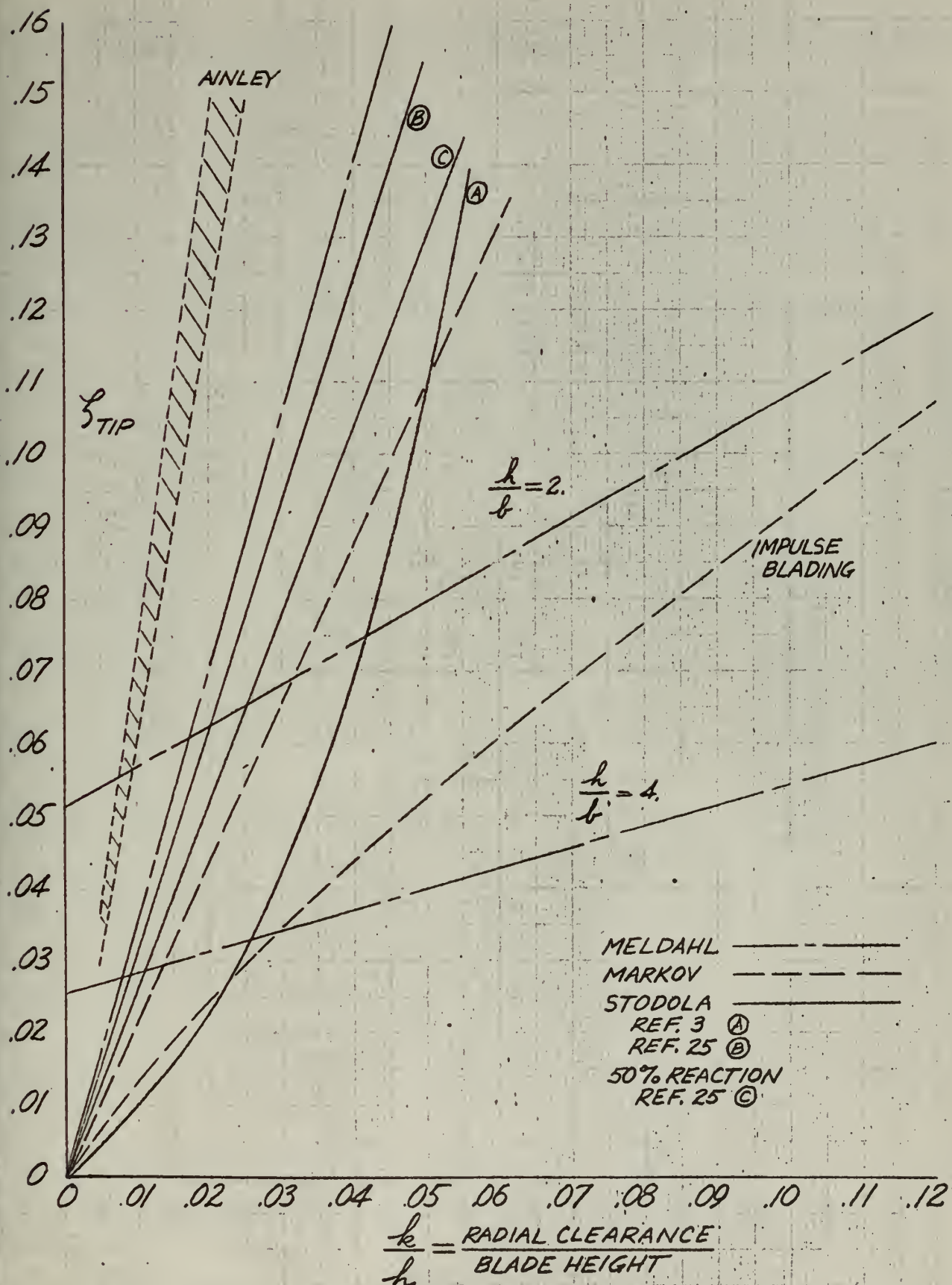


FIG. 10
PROFILE LOSS COEFFICIENTS

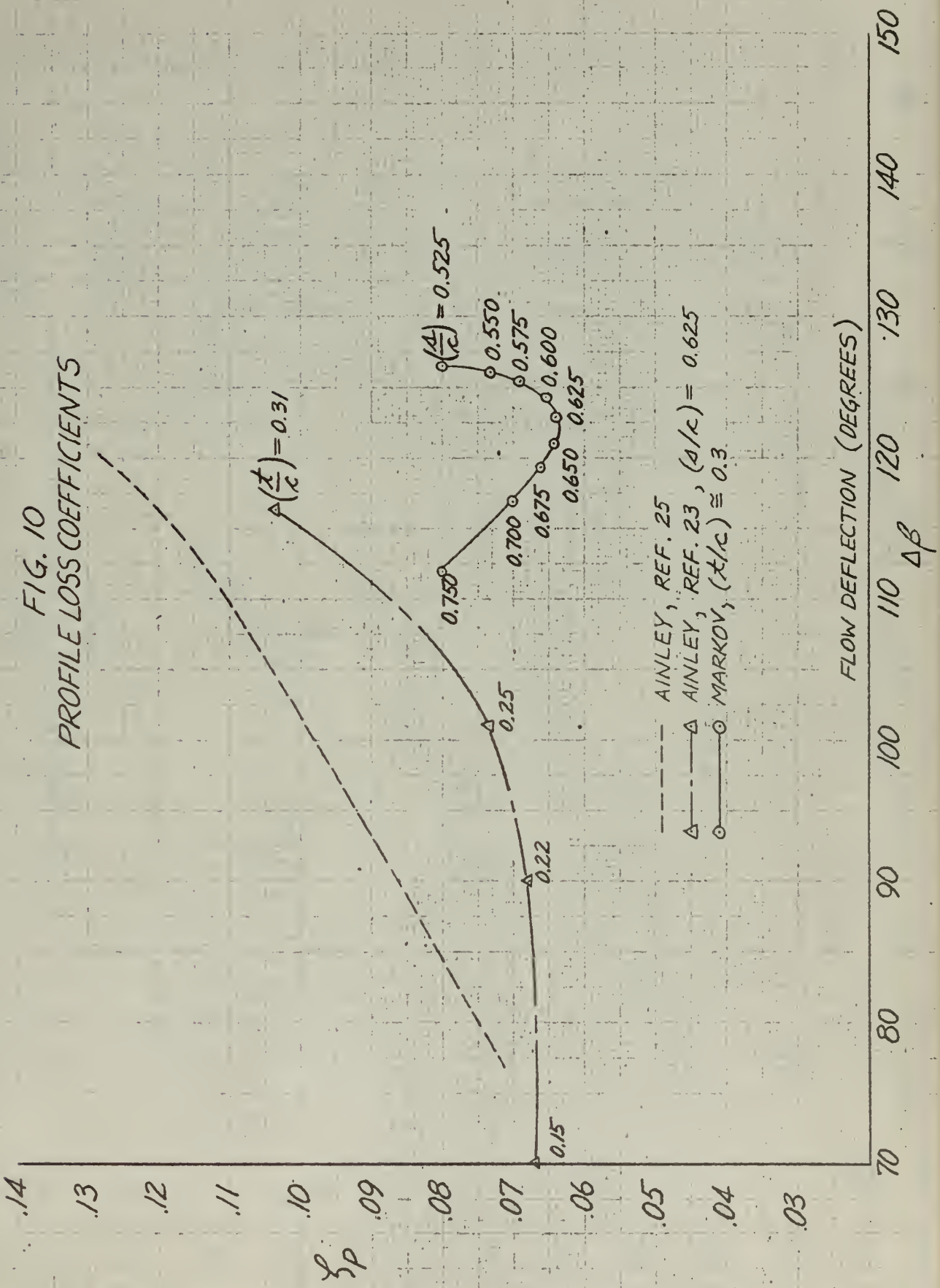
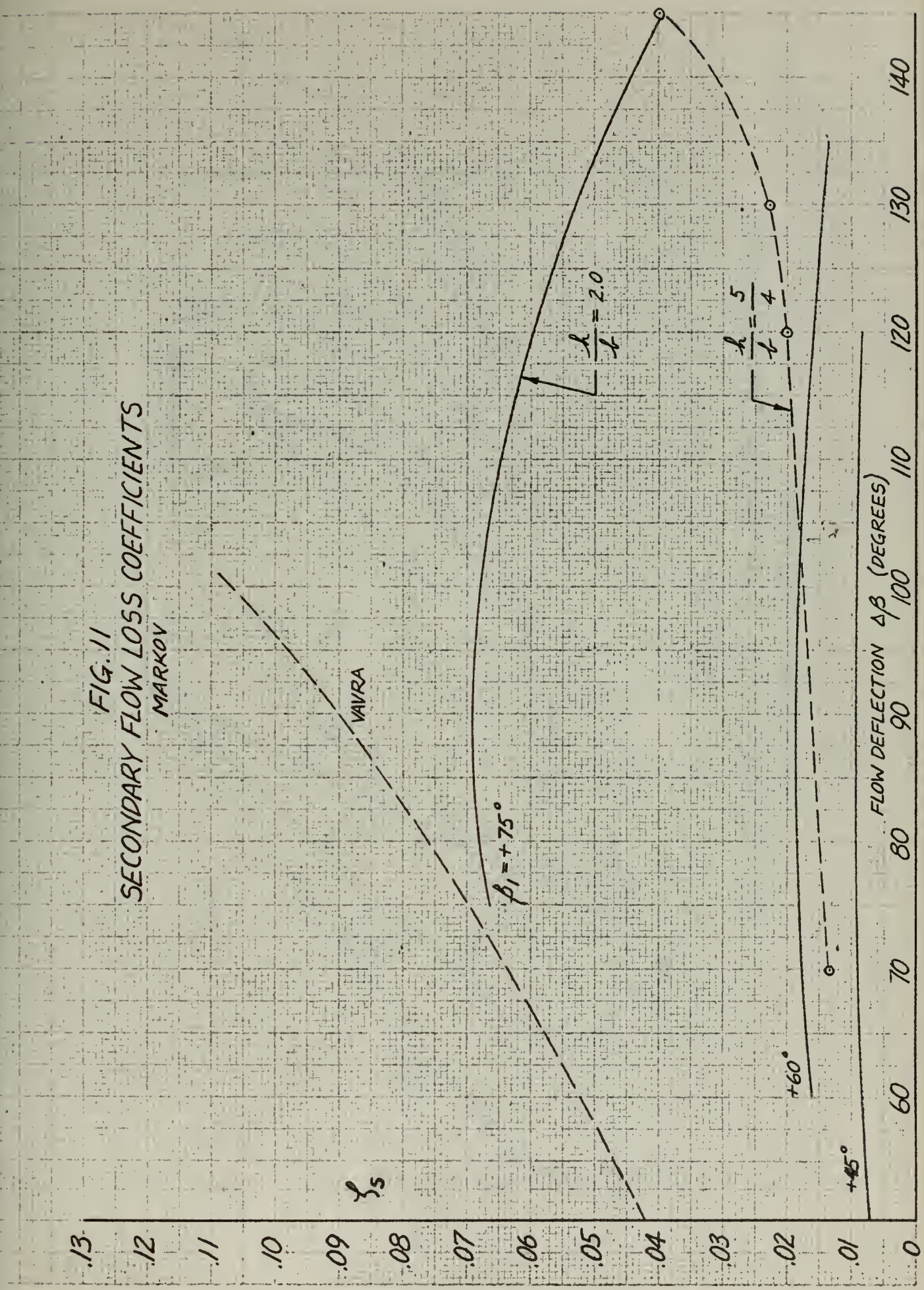


FIG. 11
SECONDARY FLOW LOSS COEFFICIENTS
MARKOV



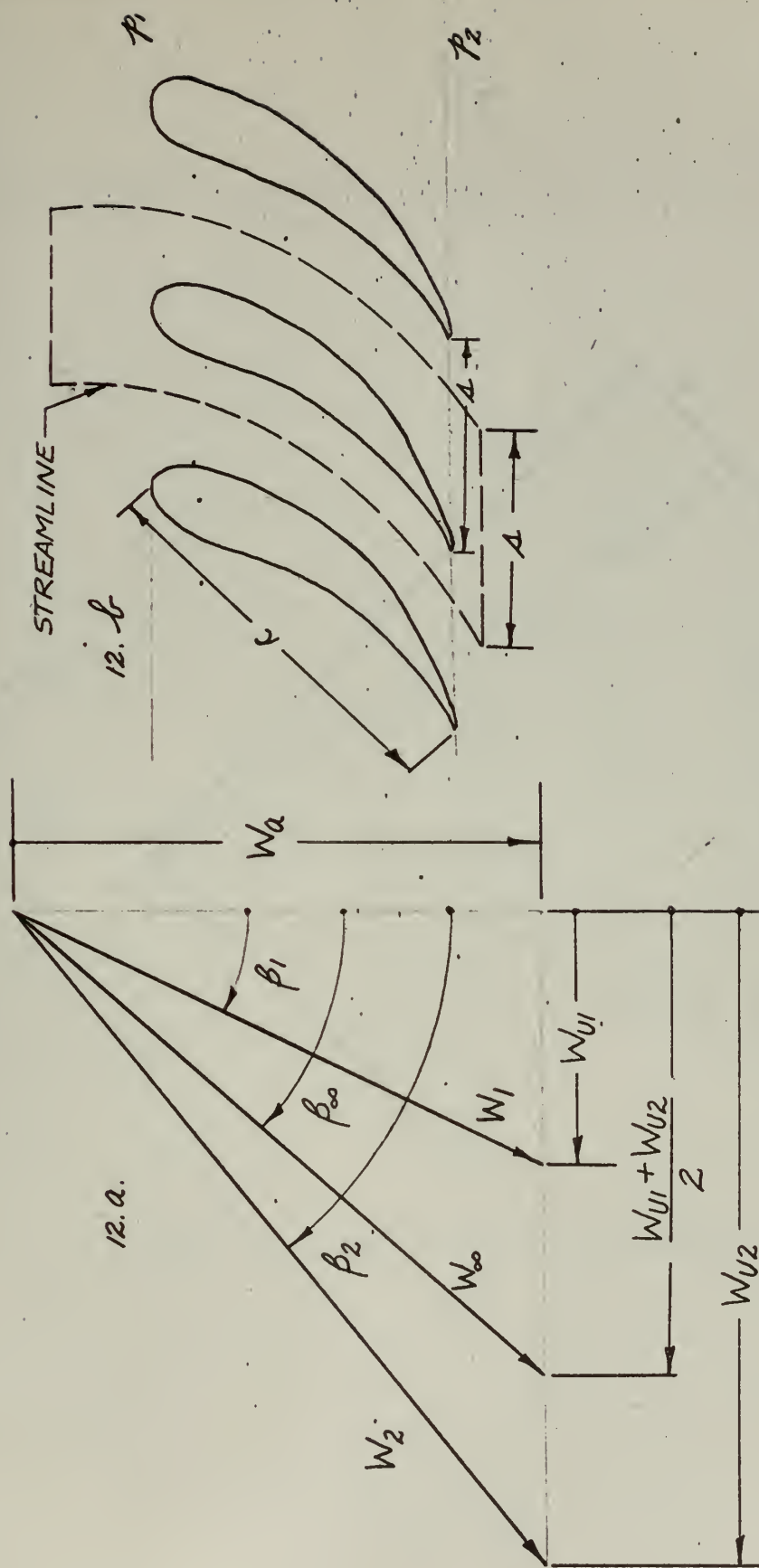


FIG. 12
VECTOR DIAGRAM OF FLOW THROUGH AN ARBITRARY
TURBINE CASCADE

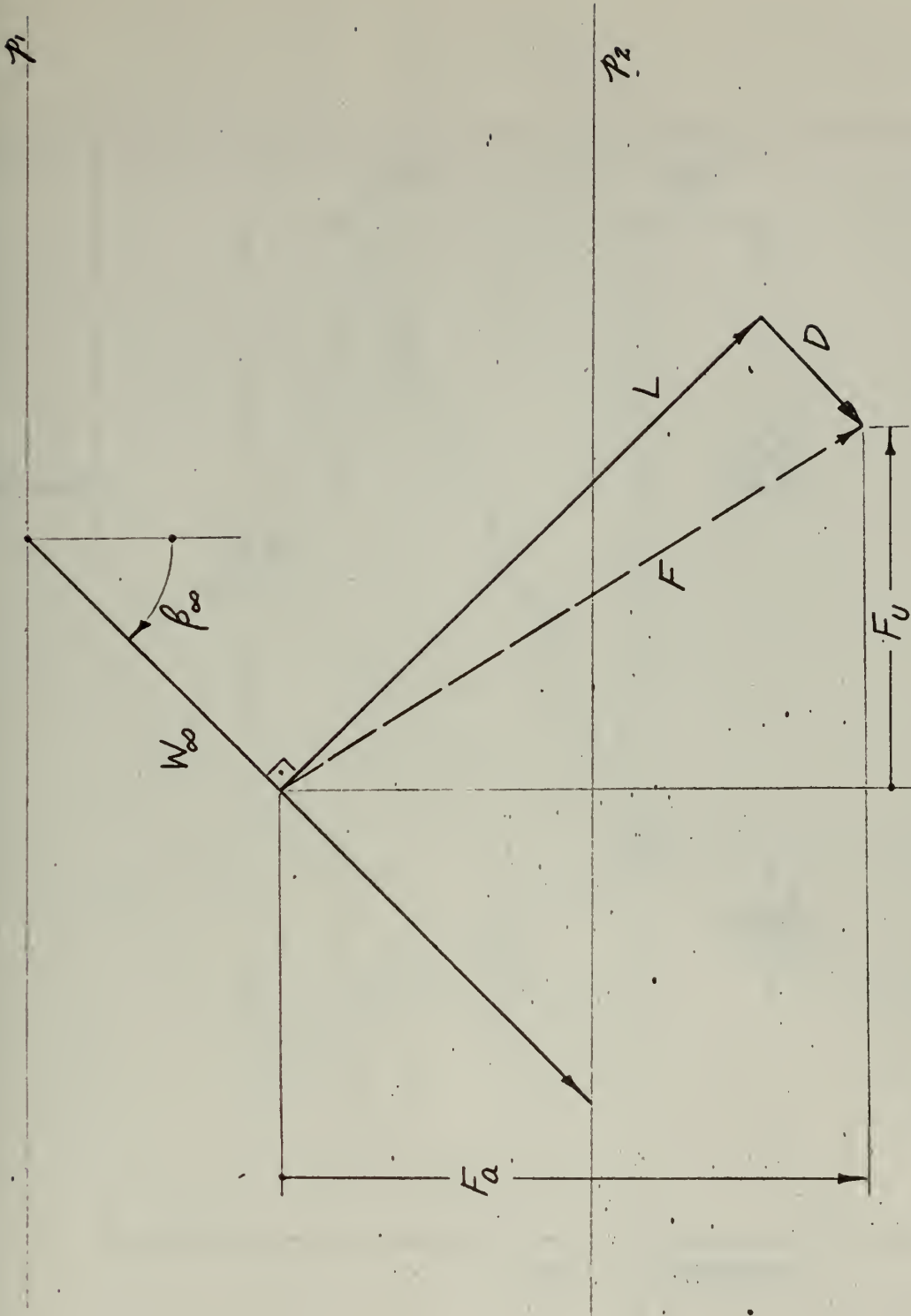


FIG. 13
VECTOR DIAGRAM OF FORCES
ON ONE BLADE

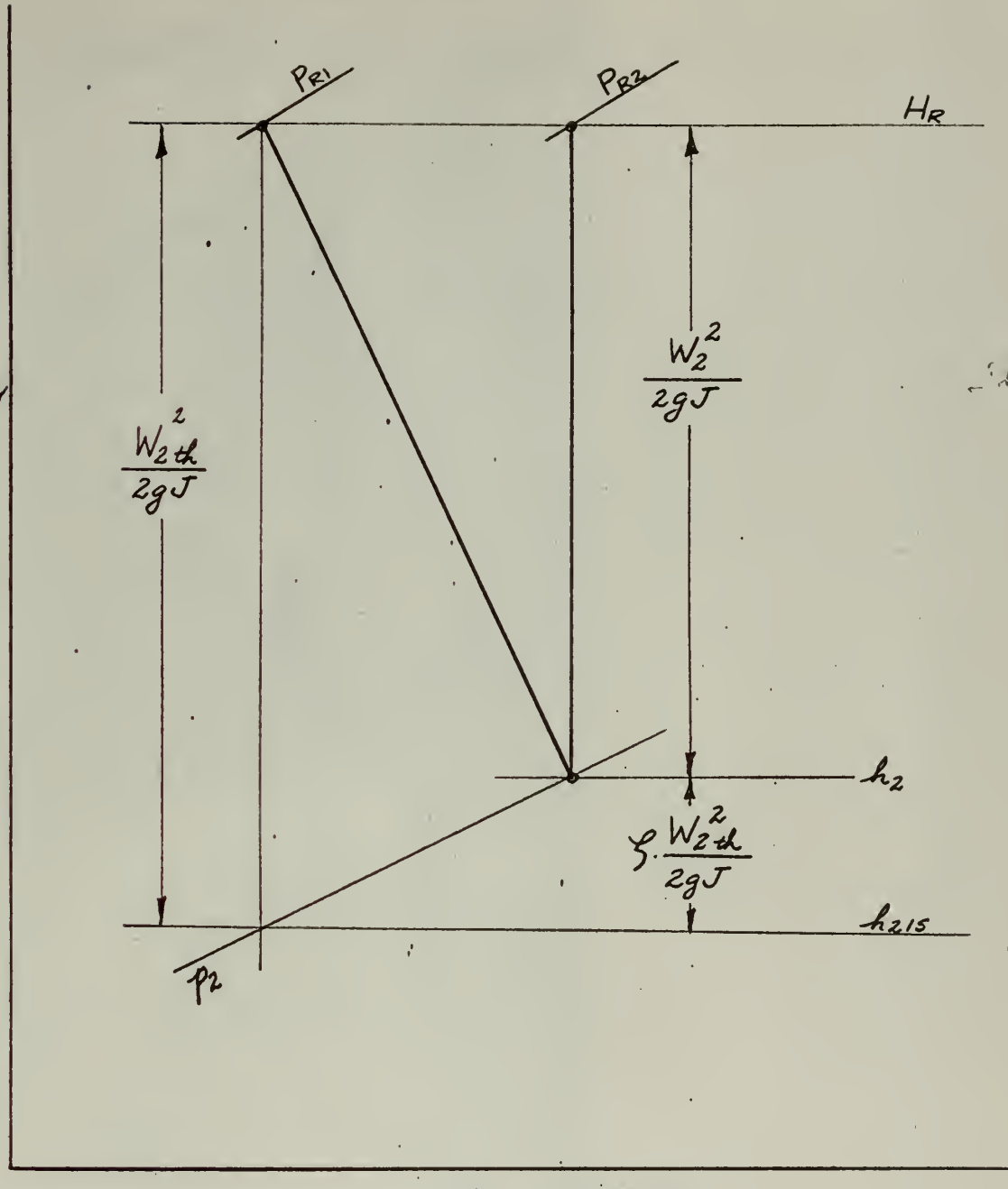
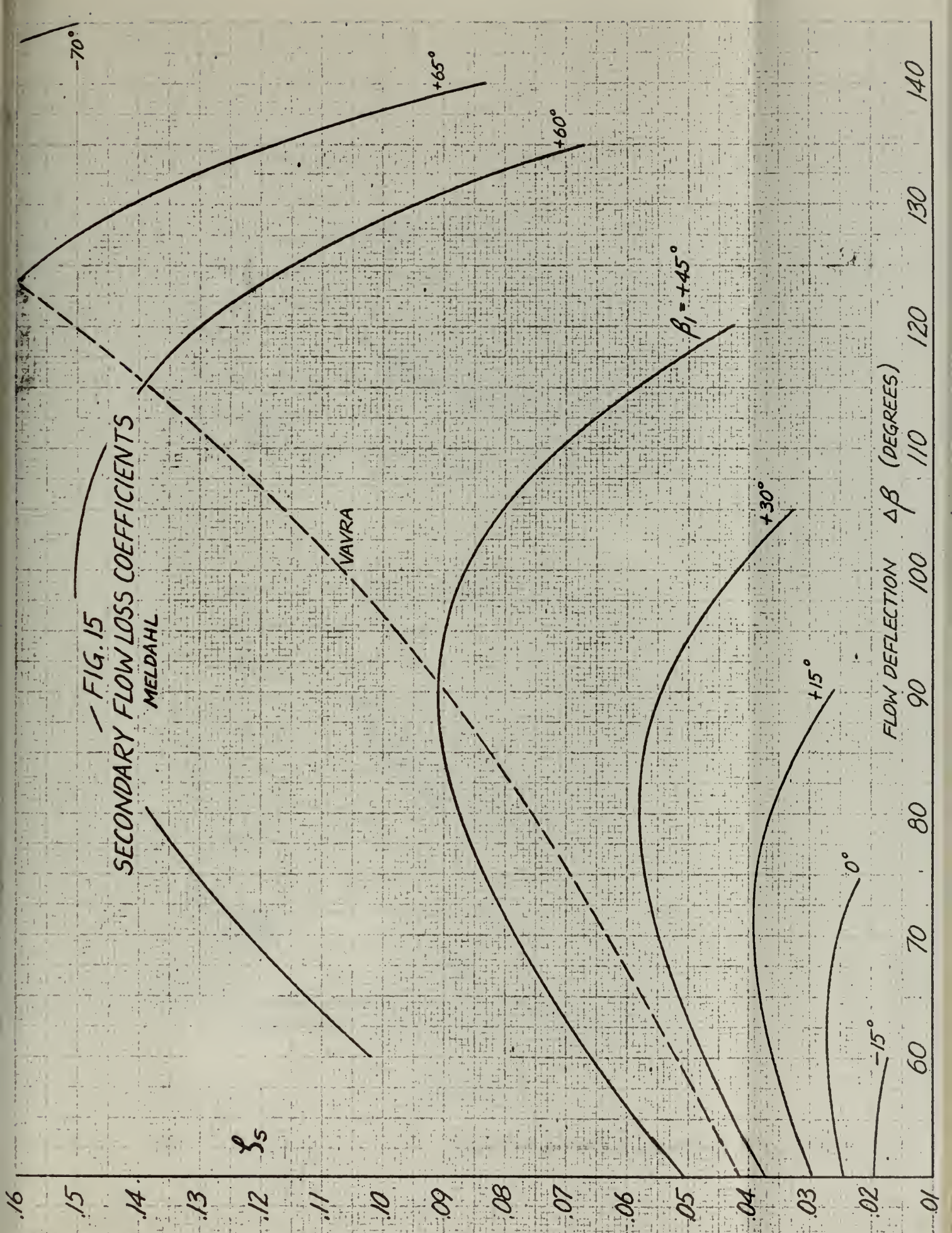
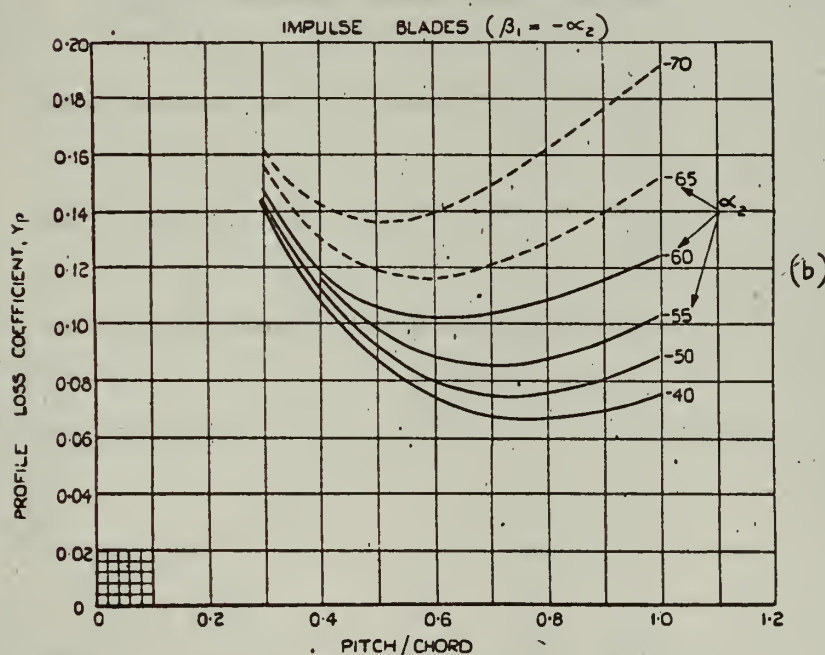
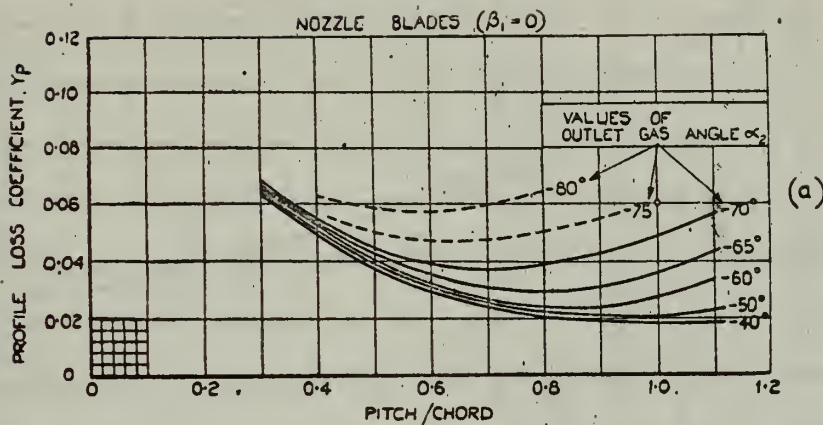


FIG. 14
 H-s DIAGRAM FOR THE RELATIVE FLOW
 IN A ROTOR

FIG. 15
SECONDARY FLOW LOSS COEFFICIENTS
MELDAHL





Profile-loss coefficients for conventional section blades at zero incidence. $t/c = 20$ per cent; $Re = 2 \times 10^5$; $M < 0.6$.

FIG. 16

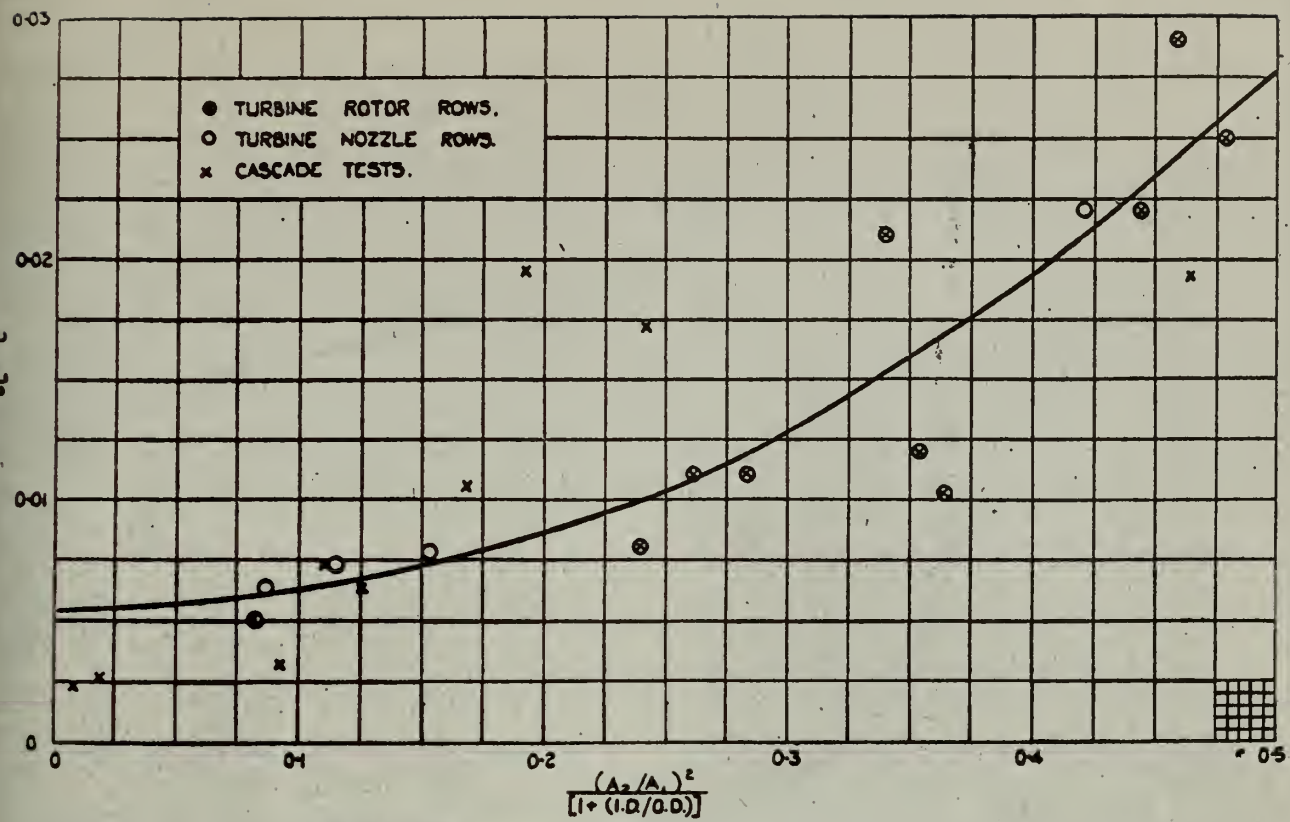


FIG. 17 Secondary losses in turbine blade rows.

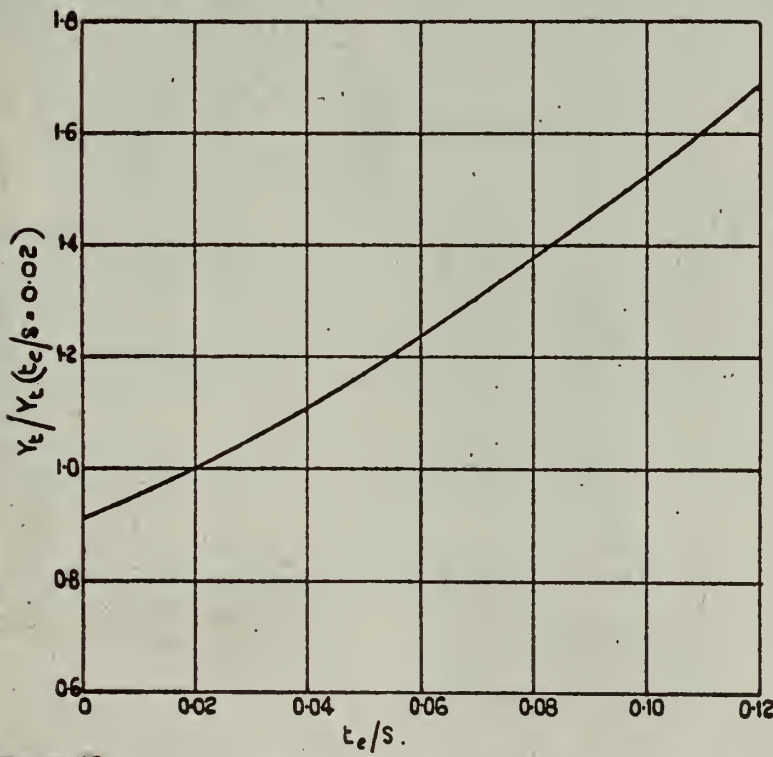


FIG. 19 Effect of trailing-edge thickness on blade loss coefficients.

FIG. 18
SECONDARY FLOW LOSS COEFFICIENTS

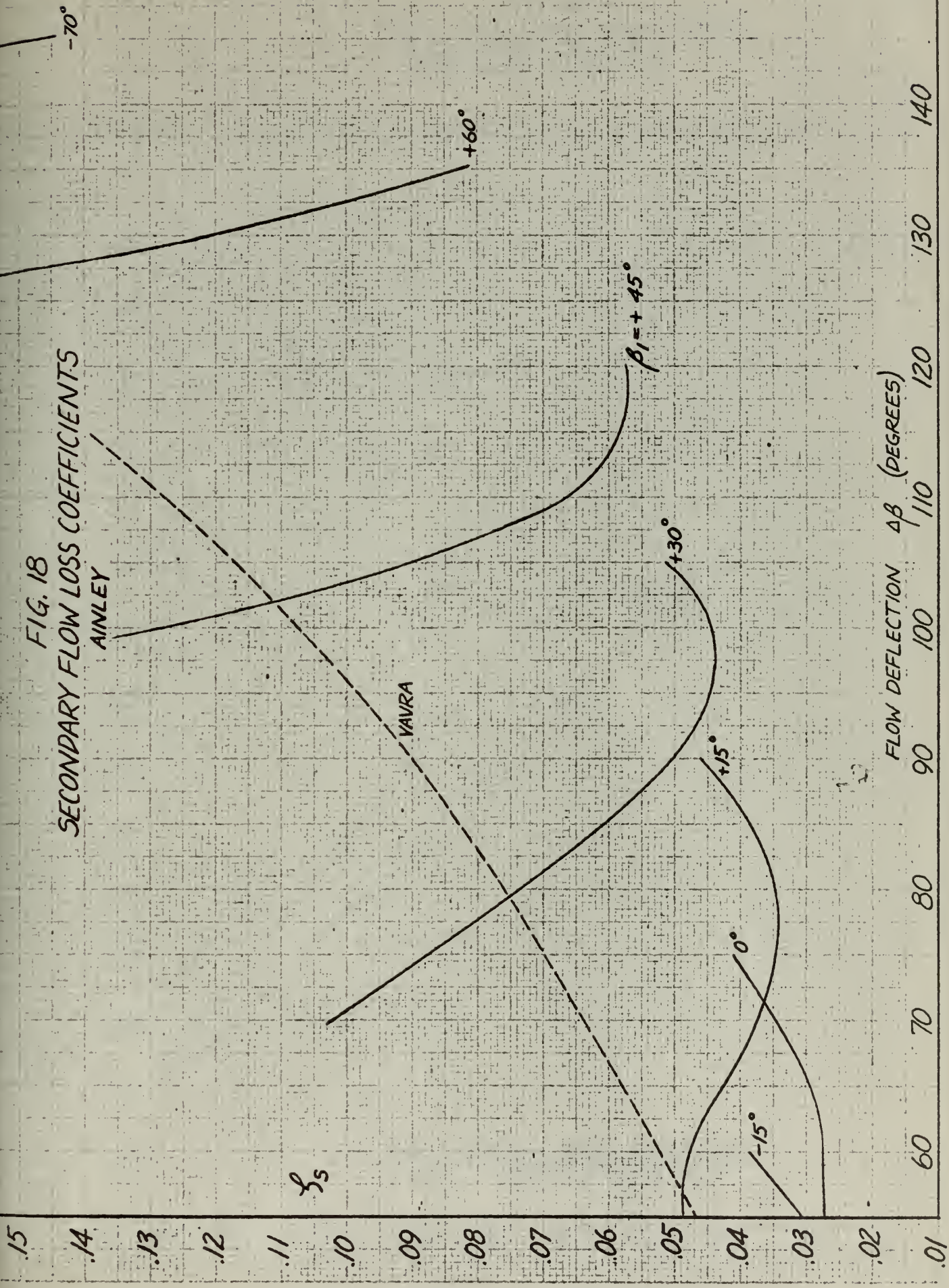


FIG. 20
TRAILING EDGE THICKNESS
LOSS COEFFICIENTS

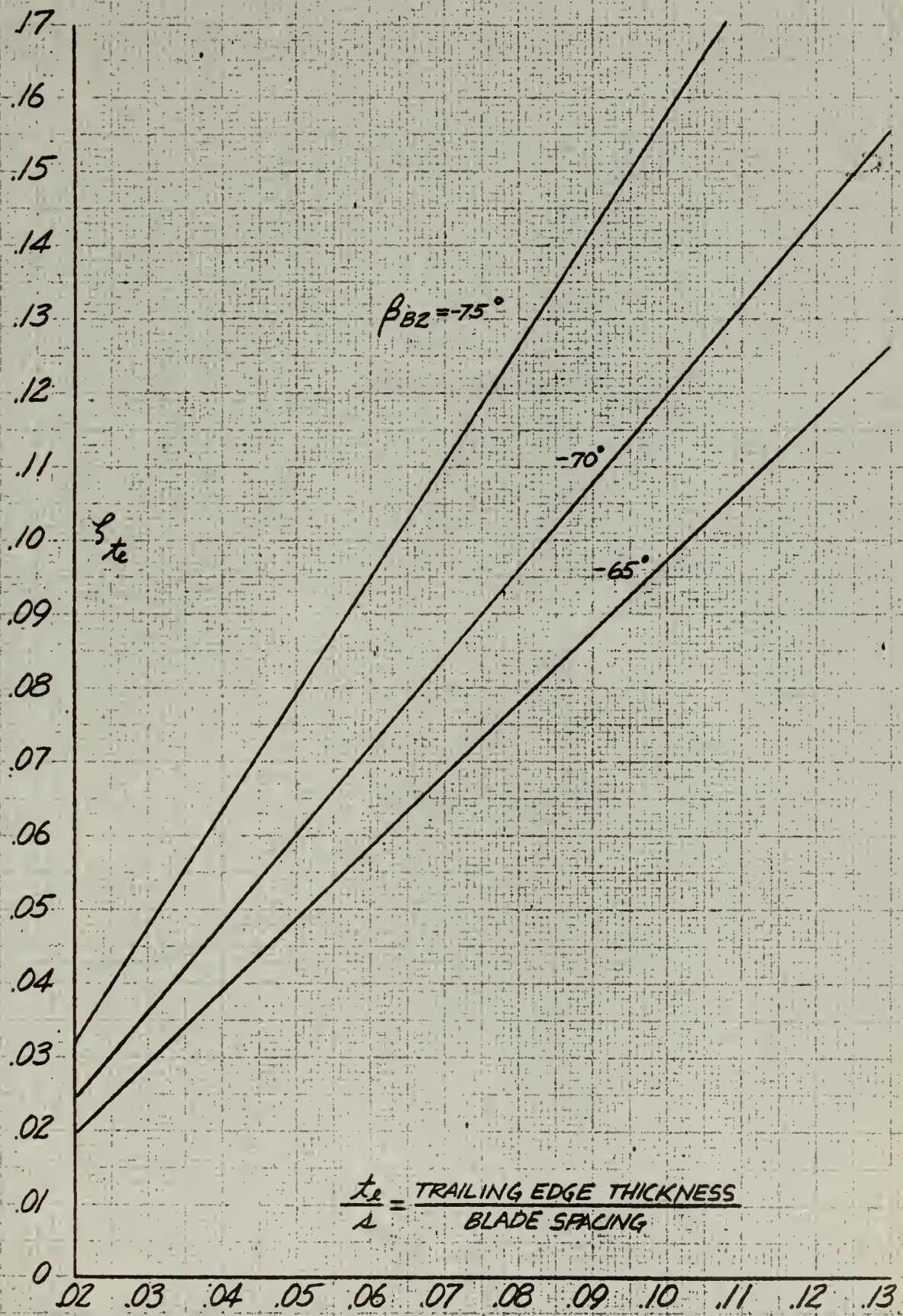


FIG. 21
STATOR LOSS COEFFICIENTS

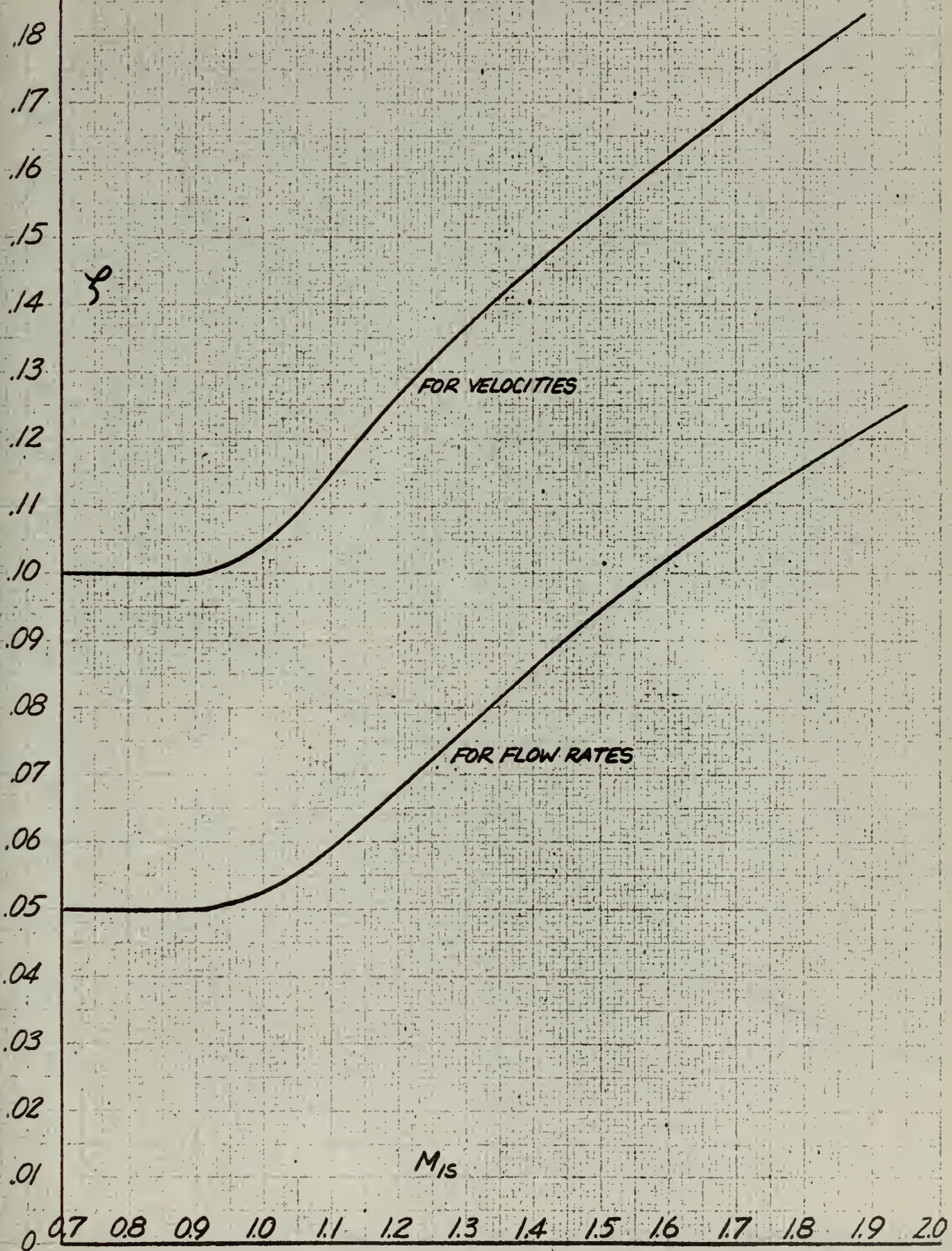


FIG. 22
ROTOR LOSS COEFFICIENTS

.34

.32

.30

.28

.26

.24

.22

.20

.18

.16

.14

.12

.10

.08

.06

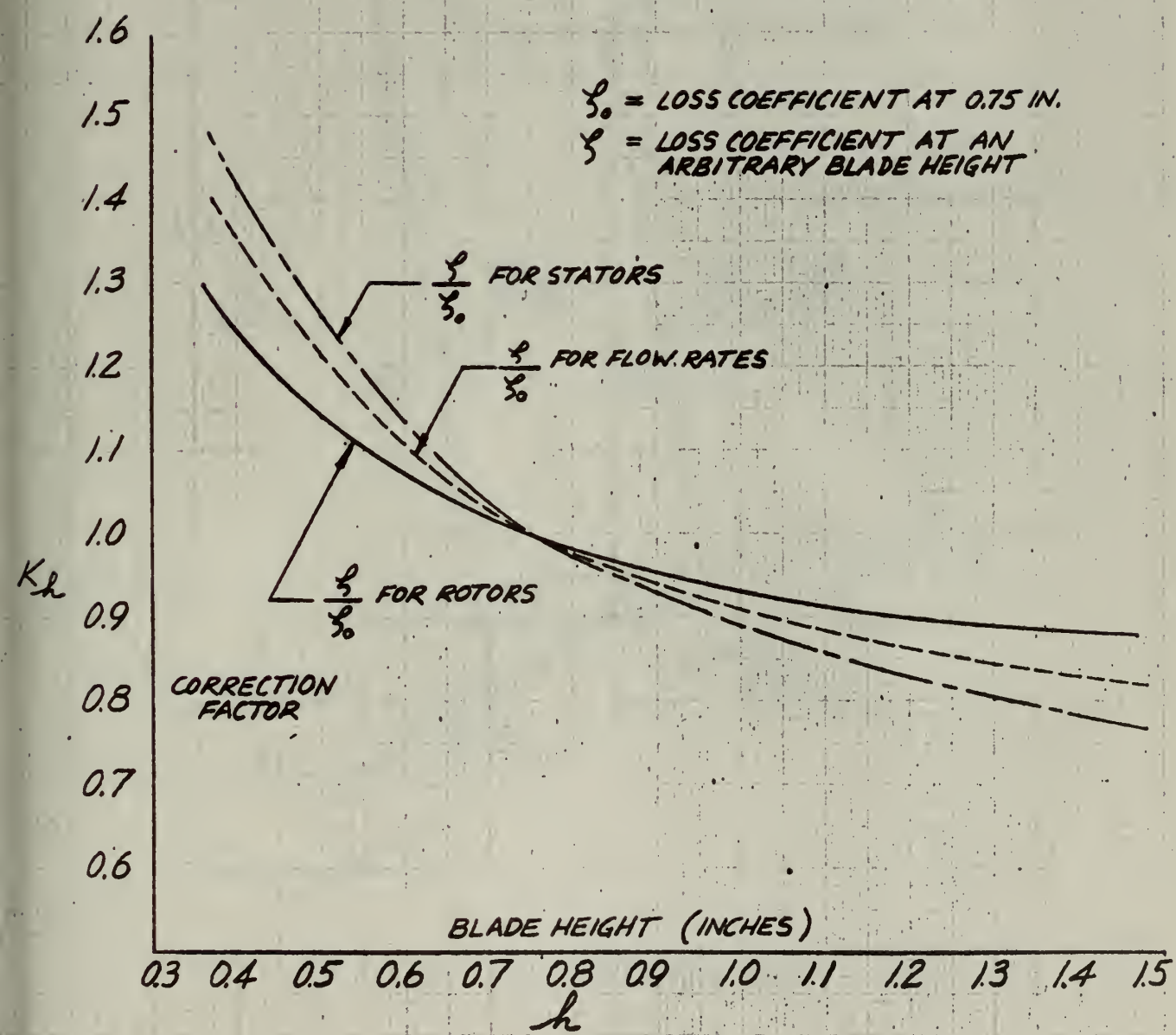
.04

.02

0 0.30 0.32 0.34 0.36 0.38 0.40 0.42 0.44 0.46 0.48 0.50 0.52 0.54 0.56

U_1/V_1

FIG. 23
EFFECT OF BLADE HEIGHT
ON LOSS COEFFICIENTS



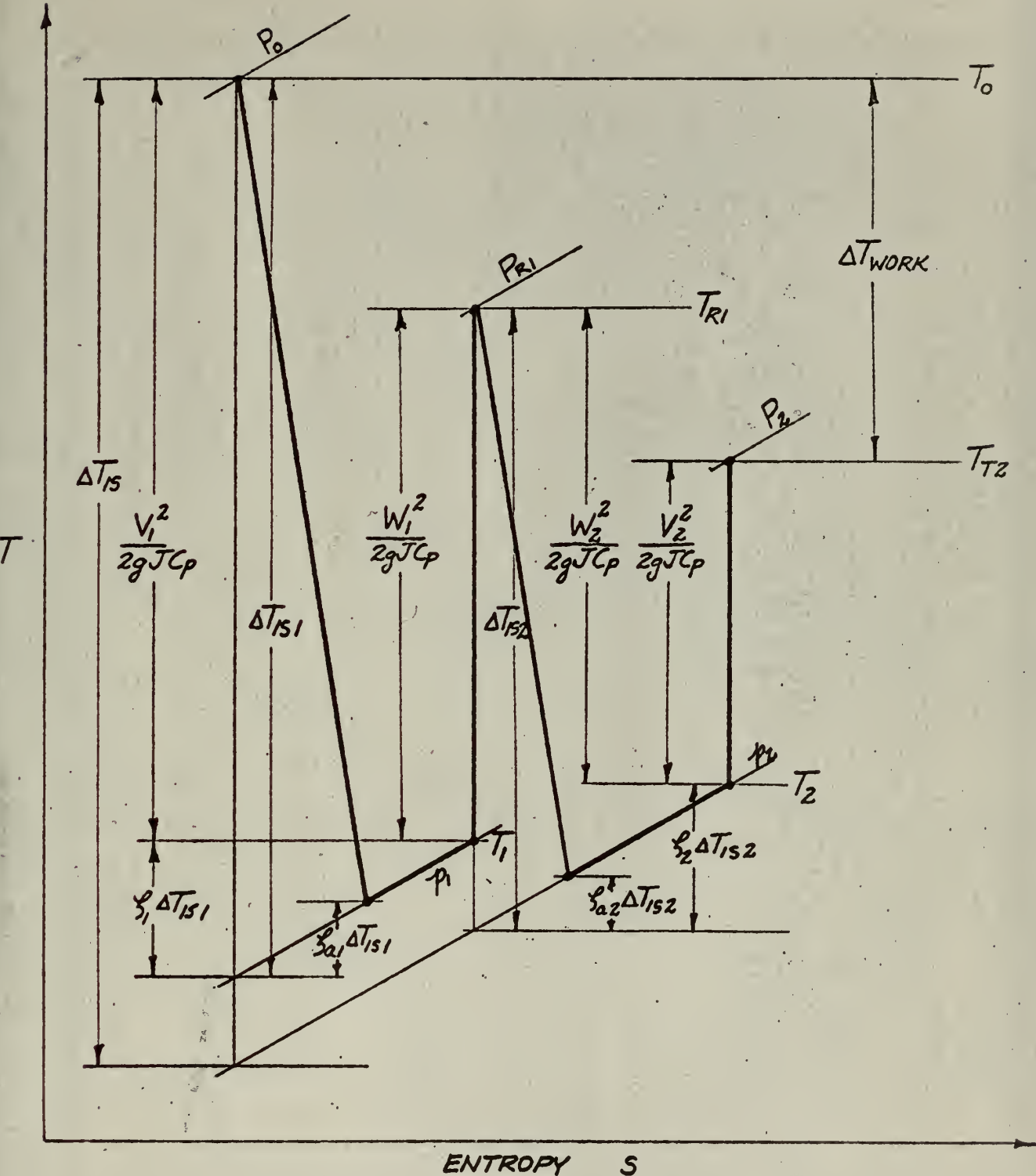


FIG. 24
T-s DIAGRAM OF EXPANSION PROCESS
THROUGH A TURBINE

STATION 0

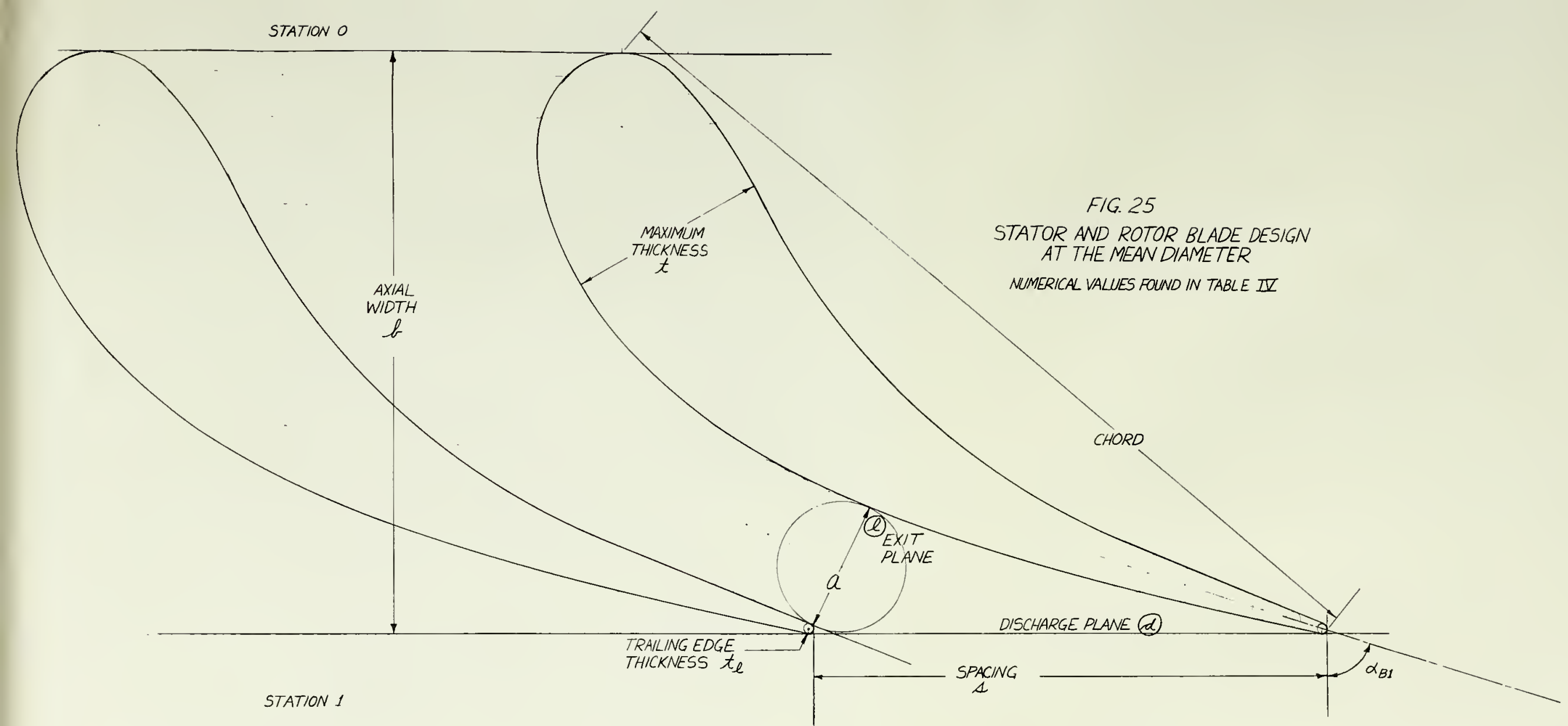
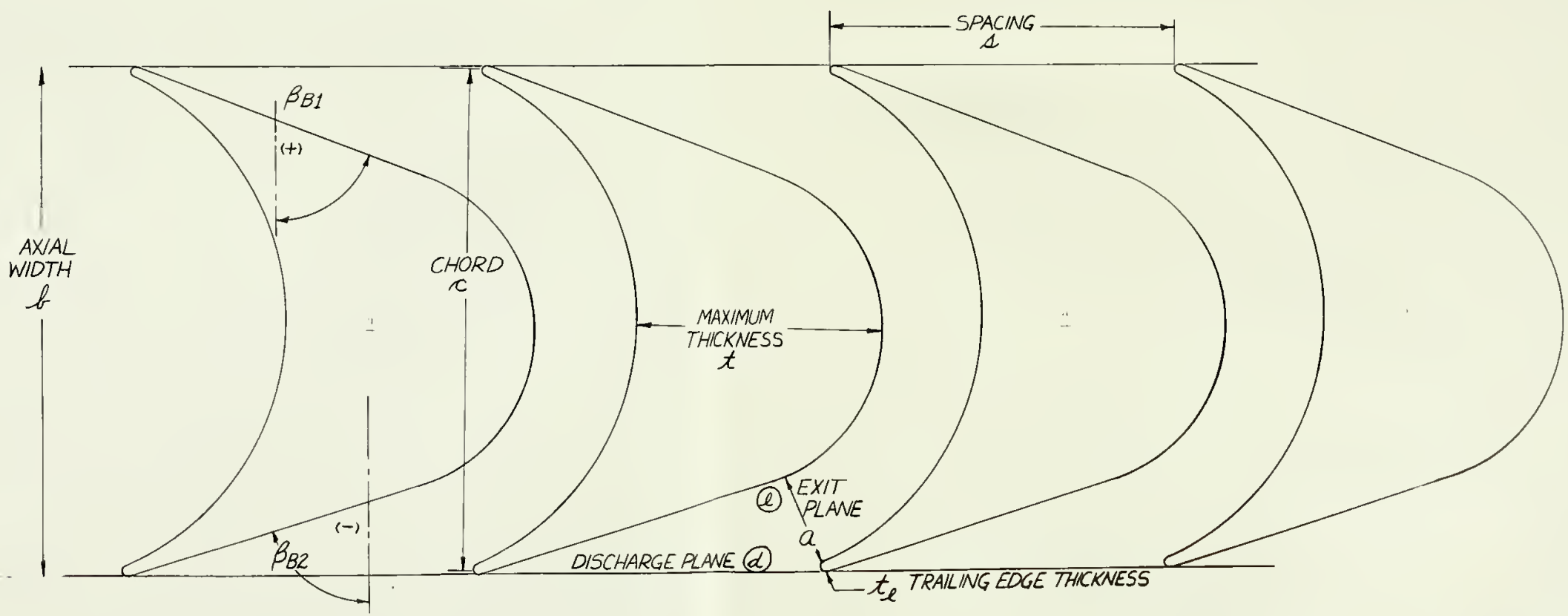


FIG. 25

STATOR AND ROTOR BLADE DESIGN
AT THE MEAN DIAMETER

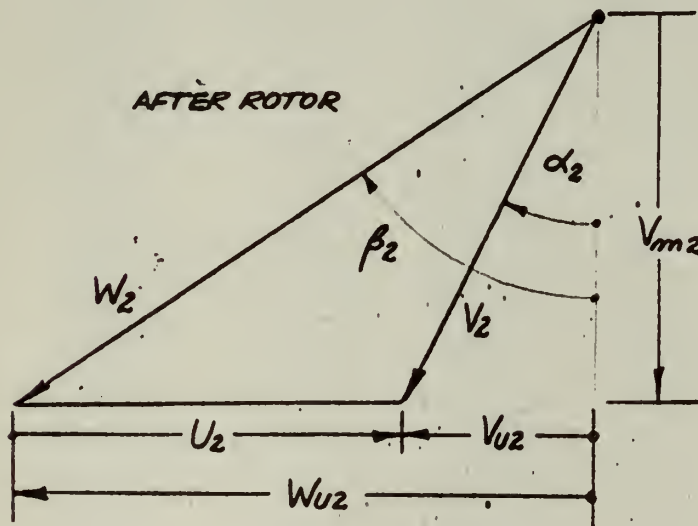
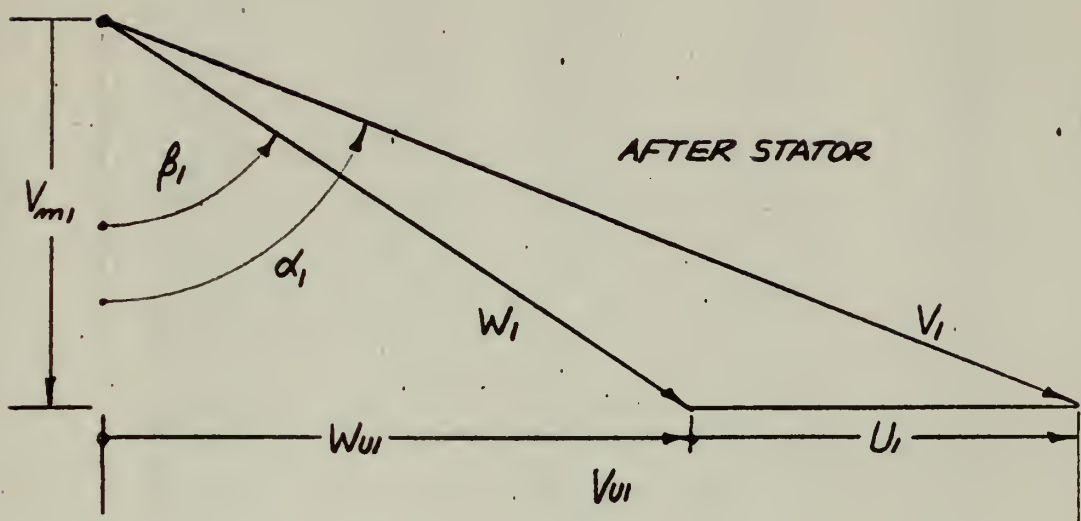
NUMERICAL VALUES FOUND IN TABLE IV

STATION 1



STATION 2

FIG. 26
VELOCITY TRIANGLES FOR TURBINE FLOW



SIGN CONVENTION :

U
 $+V_U$
 $+W_U$

ANGLES



FLW FUNCTI

PRESSURE
RATIO

1.02
1.04
1.06
1.08
1.10
1.12
1.14
1.16
1.18
1.20
1.22
1.24
1.26
1.28
1.30
1.32
1.34
1.36
1.38
1.40
1.42
1.44
1.46
1.48
1.50
1.52
1.54
1.56
1.58
1.60
1.62
1.64
1.66
1.68
1.70
1.72
1.74
1.76
1.78
1.80
1.82
1.84
1.86
1.88
1.90
1.92
1.94
1.96
1.98
2.00
2.05
2.00
2.05
3.00
3.05
3.00
3.05
4.00
4.05
4.00
4.05
5.00
5.05
5.00
5.05
5.50
5.55
5.50
5.55
6.00

PRESSURE RATIO	ZETA =	.000	.025	.050	.075	.100	.125	.150	.175	.200	.225	.250
1.02		.19589	.19340	.19088	.18833	.18574	.18312	.18046	.17776	.17503	.17225	.16942
1.04		.27145	.26797	.26444	.26087	.25725	.25358	.24987	.24610	.24228	.23840	.23446
1.06		.32588	.32165	.31738	.31305	.30857	.30423	.29973	.29518	.29055	.28587	.28111
1.08		.36898	.36415	.35926	.35431	.34931	.34424	.33911	.33392	.32865	.32330	.31788
1.10		.40465	.39930	.39389	.38842	.38289	.37729	.37162	.36588	.36006	.35416	.34817
1.12		.43496	.42915	.42329	.41735	.41136	.40529	.39915	.39293	.38663	.38025	.37378
1.14		.46114	.45493	.44866	.44232	.43591	.42942	.42286	.41623	.40950	.40270	.39579
1.16		.48403	.47746	.47081	.46411	.45732	.45047	.44354	.43652	.42942	.42223	.41494
1.18		.50423	.49732	.49034	.48330	.47618	.46899	.46171	.45436	.44691	.43938	.43174
1.20		.52217	.51496	.50767	.50032	.49289	.48539	.47780	.47013	.46238	.45453	.44658
1.22		.53819	.53069	.52312	.51548	.50777	.49999	.49212	.48416	.47612	.46799	.45975
1.24		.55256	.54479	.53696	.52906	.52109	.51304	.50491	.49669	.48838	.47998	.47148
1.26		.56549	.55748	.54940	.54125	.53304	.52474	.51637	.50791	.49935	.49071	.48196
1.28		.57715	.56891	.56060	.55223	.54378	.53526	.52666	.51797	.50920	.50033	.49136
1.30		.58769	.57924	.57072	.56213	.55347	.54474	.53592	.52703	.51804	.50896	.49978
1.32		.59724	.58858	.57986	.57108	.56222	.55329	.54427	.53518	.52600	.51673	.50735
1.34		.60590	.59705	.58814	.57917	.57012	.56100	.55181	.54253	.53316	.52371	.51416
1.36		.61376	.60473	.59564	.58649	.57727	.56798	.55861	.54916	.53962	.52999	.52027
1.38		.62090	.61170	.60244	.59312	.58373	.57428	.56475	.55513	.54544	.53565	.52577
1.40		.62739	.61802	.60861	.59913	.58959	.57997	.57029	.56052	.55068	.54074	.53071
1.42		.63328	.62377	.61420	.60457	.59437	.58512	.57528	.56538	.55539	.54532	.53515
1.44		.63863	.62898	.61926	.60949	.59966	.58976	.57979	.56975	.55963	.54942	.53912
1.46		.64349	.63370	.62384	.61394	.60397	.59394	.58385	.57368	.56343	.55310	.54268
1.48		.64790	.63797	.62799	.61796	.60736	.59771	.58750	.57721	.56684	.55639	.54586
1.50		.65189	.64184	.63174	.62158	.61137	.60110	.59076	.58036	.56988	.55933	.54868
1.52		.65551	.64533	.63511	.62484	.61451	.60413	.59369	.58318	.57259	.56193	.55119
1.54		.65877	.64848	.63815	.62776	.61733	.60684	.59630	.58568	.57500	.56424	.55340
1.56		.66171	.65131	.64087	.63038	.62208	.61139	.60065	.58985	.57712	.56627	.55534
1.58		.66435	.65384	.64330	.63271	.62208	.61139	.60065	.58985	.57899	.56805	.55703
1.60		.66671	.65610	.64546	.63478	.62405	.61328	.60245	.59156	.58061	.56959	.55849
1.62		.66882	.65812	.64738	.63660	.62579	.61492	.60401	.59304	.58201	.57091	.55974
1.64		.67069	.65990	.64907	.63821	.62730	.61636	.60537	.59432	.58321	.57204	.56079
1.66		.67234	.66145	.65054	.63960	.62862	.61759	.60652	.59540	.58422	.57297	.56166
1.68		.67378	.66281	.65182	.64080	.62973	.61864	.60749	.59630	.58505	.57374	.56237
1.70		.67503	.66399	.65291	.64181	.63058	.61951	.60829	.59703	.58572	.57435	.56291
1.72		.67611	.66498	.65384	.64266	.63146	.62022	.60894	.59761	.58624	.57513	.56332
1.74		.67702	.66582	.65460	.64335	.63208	.62078	.60943	.59805	.58662	.57532	.56373
1.76		.67778	.66651	.65522	.64390	.63257	.62120	.60980	.59835	.58687	.57540	.56376
1.78		.67839	.66705	.65569	.64432	.63292	.62149	.61003	.59853	.58699	.57537	.56368
1.80		.67887	.66746	.65604	.64460	.63314	.62166	.61015	.59860	.58700	.57523	.56350
1.82		.67922	.66775	.65627	.64477	.63326	.62172	.61015	.59855	.58691	.57523	.56323
1.84		.67946	.66793	.65638	.64483	.63326	.62167	.61005	.59841	.58673	.57500	.56323
1.86		.67959	.66799	.65639	.64479	.63316	.62152	.60986	.59817	.58644	.57468	.56287
1.88		.67961	.66796	.65630	.64464	.63297	.62129	.60958	.59784	.58608	.57427	.56242
1.90		.67954	.66783	.65613	.64441	.63269	.62096	.60921	.59744	.58563	.57379	.56191
1.92		.67938	.66762	.65586	.64410	.63234	.62056	.60877	.59695	.58511	.57324	.56133
1.94		.67913	.66732	.65551	.64371	.63190	.62008	.60825	.59640	.58452	.57262	.56067
1.96		.67881	.66695	.65509	.64324	.63139	.61953	.60766	.59578	.58387	.57193	.55996
1.98		.67841	.66650	.65460	.64271	.63081	.61892	.60701	.59510	.58316	.57119	.55919
2.00		.67794	.66598	.65404	.64211	.63018	.61825	.60631	.59436	.58239	.57040	.55838
2.20		.67027	.65794	.64564	.63338	.62114	.60892	.59672	.58453	.57235	.56016	.54796
2.40		.65909	.64649	.63395	.62146	.60902	.59663	.58428	.57195	.55965	.54737	.53511
2.60		.64613	.63334	.62063	.60800	.59544	.58295	.57050	.55812	.54578	.53347	.52120
2.80		.63237	.61945	.60663	.59391	.58128	.56874	.55626	.54387	.53153	.51925	.50701
3.00		.61838	.60538	.59249	.57972	.56706	.55450	.54204	.52966	.51736	.50513	.49297
3.20		.60450	.59144	.57852	.56573	.55307	.54052	.52809	.51576	.50351	.49014	.47929
3.40		.59092	.57783	.56489	.55211	.53947	.52696	.51457	.50230	.49014	.47808</	

MACH	ALFA	GAMMA		
1.000	75	1.370		
PRAT	PRAT1	VELRAT1	DALFA	ZA
1.0000	1.0000	1.0000	- .0000	.0000
.9800	.9800	.9800	.0039	.0000
.9600	.9600	.9600	.0157	.0000
.9400	.9401	.9401	.0355	.0001
.9200	.9201	.9201	.0636	.0001
.9000	.9001	.9001	.1002	.0003
.8800	.8799	.8799	.1460	.0005
.8600	.8601	.8601	.2001	.0008
.8400	.8401	.8401	.2641	.0011
.8200	.8201	.8201	.3380	.0016
.8000	.7999	.7999	.4230	.0021
.7800	.7800	.7800	.5180	.0028
.7600	.7599	.7599	.6250	.0036
.7400	.7399	.7399	.7440	.0045
.7200	.7200	.7200	.8750	.0055
.7000	.7001	.7001	1.0200	.0067
.6800	.6800	.6800	1.1810	.0080
.6600	.6600	.6600	1.3570	.0095
.6400	.6400	.6400	1.5500	.0112
.6200	.6199	.6199	1.7620	.0130
.6000	.6000	.6000	1.9930	.0150
.5800	.5799	.5799	2.2460	.0171
.5600	.5599	.5599	2.5230	.0194
.5400	.5399	.5399	2.8250	.0219
.5200	.5199	.5199	3.1560	.0246
.5000	.4999	.4999	3.5180	.0274

TIME, 1 MINUTES AND 36 SECONDS

FIG. 28
AFTER-EXPANSION AT $\gamma=1.37$ AND $\alpha_i=75^\circ$

BLADING FOR ROTOR DESIGN

DIAMETER	=	23.0000	23.0000	23.0000	23.0000	23.0000
NUMBER OF BLADES	=	74	76	78	80	82
INLET ANGLE	=	20.4000	20.4000	20.4000	20.4000	20.4000
EXIT ANGLE	=	18.4300	18.4300	18.4300	18.4300	18.4300
AXIAL WIDTH	=	1.3750	1.3750	1.3750	1.3750	1.3750
SPACING	=	.9764	.9507	.9264	.9032	.8812
EDGE THICKNESS	=	.0250	.0250	.0250	.0250	.0250
R	=	.7291	.7291	.7291	.7291	.7291
X1	=	.2541	.2541	.2541	.2541	.2541
X2	=	.2305	.2305	.2305	.2305	.2305
Y1	=	.6833	.6833	.6833	.6833	.6833
Y2	=	.6917	.6917	.6917	.6917	.6917
X3	=	.3259	.3259	.3259	.3259	.3259
X4	=	.3096	.3096	.3096	.3096	.3096
RS	=	.4276	.4362	.4443	.4521	.4594
X5	=	.9821	.9562	.9317	.9084	.8863
Y3	=	.7002	.6998	.6994	.6990	.6986
Y4	=	.6748	.6752	.6756	.6760	.6764
X6	=	2.2681	2.2681	2.2681	2.2681	2.2681
Y5	=	.7223	.7223	.7223	.7223	.7223
Y6	=	.6527	.6527	.6527	.6527	.6527
AREA	=	.661387	.649473	.637951	.626808	.616030
DELTA	=	.9850	.9850	.9850	.9850	.9850
CG(XS)	=	.9434	.9361	.9292	.9225	.9160
CG(X7)	=	.9433	.9360	.9290	.9223	.9159
CG(Y7)	=	.6996	.6994	.6993	.6992	.6991
CG(Y8)	=	.6754	.6756	.6757	.6758	.6759
I(X-X)	=	.06302621	.06249739	.06196594	.06143323	.06090044
I(Y-Y)	=	.03595965	.03399491	.03219183	.03053410	.02900724
X(MAX)1	=	.6378	.6305	.6235	.6168	.6104
Y(MAX)1	=	.6619	.6619	.6619	.6619	.6619
X(MAX)2	=	.6259	.6186	.6116	.6049	.5985
Y(MAX)2	=	.6876	.6876	.6876	.6876	.6876
X(MAX)3	=	.4664	.4564	.4470	.4381	.4298

TIME, 0 MINUTES AND 33 SECONDS

FIG. 29

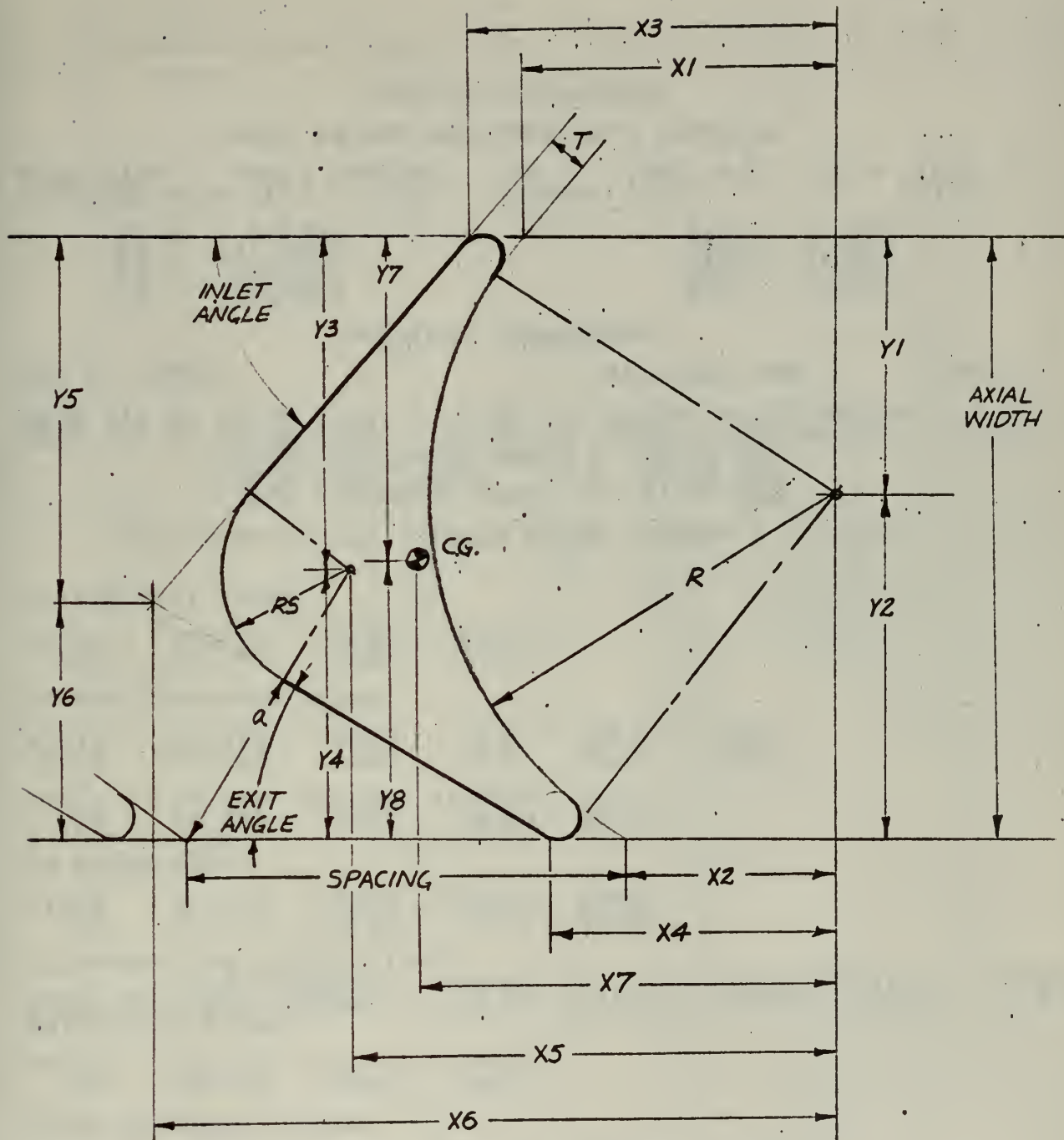


FIG. 30
DIMENSIONS OF ROTOR BLADES

TURBINE PERFORMANCE

INPUT VALUES AND CONSTANTS COMPUTED

FLOW RATE = 100.0 LBM/SEC $P_0 = 1000$ PSIA $T_0 = 1460$ $^{\circ}$ R
 REFERRED FLOW RATE = 3.821 GAMMA = 1.37 $R = 421.50$

$C_1 = 3.6195$	$C_2 = 316.9026$	$C_3 = 0.000010$	$C_4 = 136.3049$	$EXP_1 = .2701$	$EXP_2 = 3.7027$
					$EXP_3 = 2.7027$
					$RTO = 38.21$

PHYSICAL PARAMETERS

RPM = 13000.

REFERRED RPM = 340.226

MEAN DIA AT ROTOR INLET = 23.00 IN STATOR BLADE HEIGHT = 1.165 IN
 MEAN DIA AT ROTOR EXIT = 23.00 IN ROTOR BLADE HEIGHT = 1.465 IN
 STATOR DISCHARGE ANGLE = 75.00 DEG
 ROTOR INLET ANGLE = 69.60 DEG
 ROTOR DISCHARGE ANGLE = -71.57 DEG

LOSS COEFFICIENT THROUGH ROTOR (FLOWS) = .1572

STATOR EXIT PLANE

$M(V_E)$	V_E/RTO	P_E/P_0	T_E/T_0
1.00	121.515	.5380	.8530

STATOR DISCHARGE PLANE

$M(V_1)$	V_1/RTO	P_1/P_0	T_1/T_0	ALFA_1	ZETA_1
1.06	131.612	.4600	.8275	74.78	.0883

$M(W_1)$	W_1/RTO	P_{R1}/P_0	T_{R1}/T_0	BETA_1
.80	99.071	.6955	.9253	69.60

IN ROTOR ENTRY

$M(W_1)$	W_1/RTO	P_{R1}/P_0	T_{R1}/T_0	BETA_1
.80	99.071	.6955	.9253	69.60

FLOW FUNCTION COMPUTATIONS

PHI COMPUTED = .58953 PHI CRITICAL = .60837
 PRESSURE RATIO IMPOSED = 1.512 CRITICAL PRESSURE RATIO = 1.827
 ROTOR EXIT PLANE

$M(W_E)$	W_E/RTO	P_{E2}/P_0	T_{E2}/T_0
.73	90.952	.4600	.8429

ROTOR DISCHARGE PLANE

$M(W_2)$	W_2/RTO	P_2/P_0	T_2/T_0	BETA_2	ZETA_2
.67	84.389	.4600	.8543	-71.57	.2744

$M(V_2)$	V_2/RTO	P_2/P_0	T_2/T_0	ALFA_2
.42	53.105	.4600	.8543	-59.84

RESULTANT POWER AND EFFICIENCY

$V_{U1}(\text{FT/SEC})$	$V_{U2}(\text{FT/SEC})$	$P_2(\text{PSIA})$	$P_{2T}(\text{PSIA})$	T_2	T_{2T}
4852.61	-1754.49	460.	519.	1247.	1288.

OVERALL PRESSURE RATIO = 2.174 HP = 48682. EFFICIENCY = .723

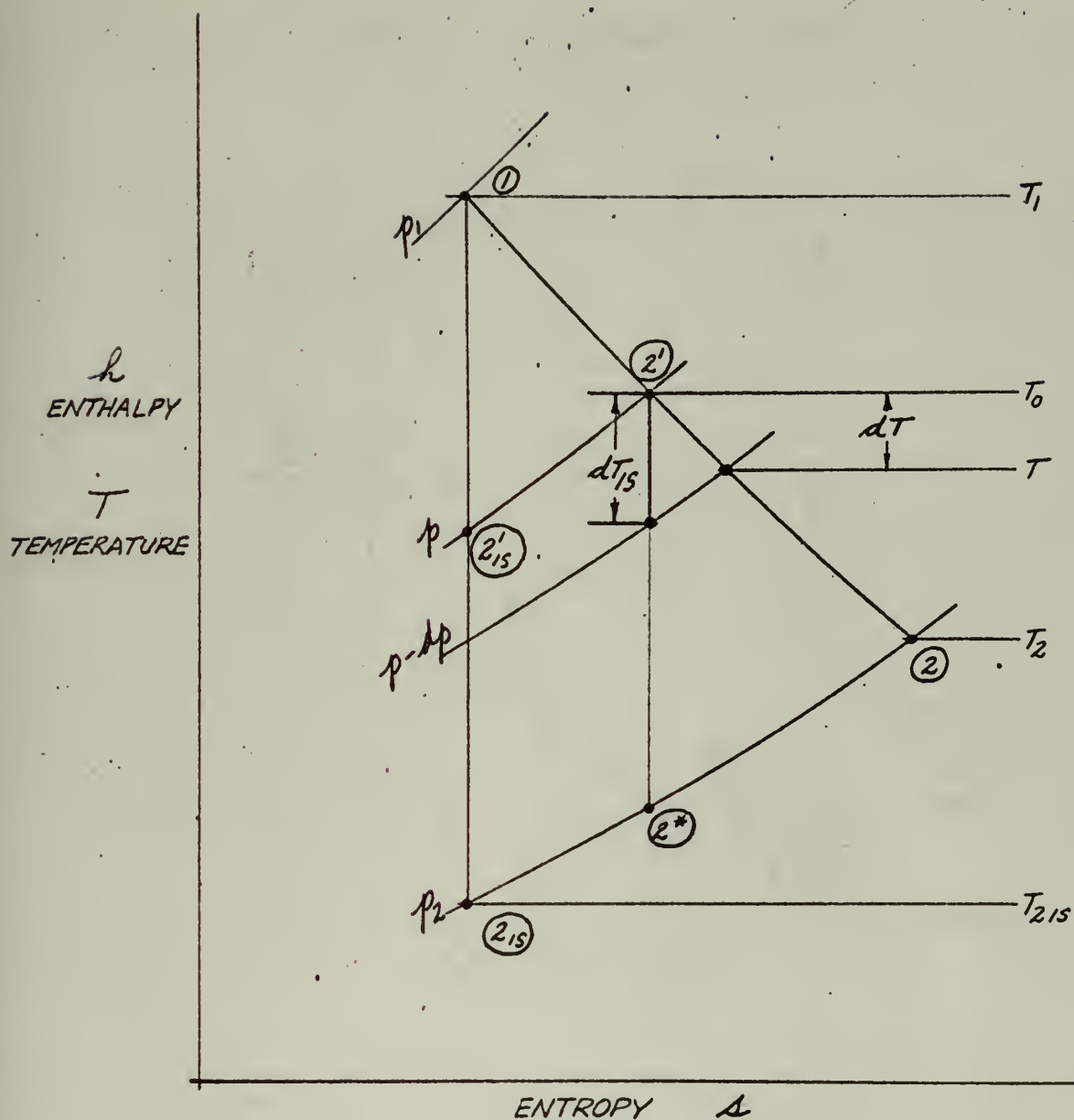


FIG. 32
 $h-s$ DIAGRAM FOR POLYTROPIC EXPANSION

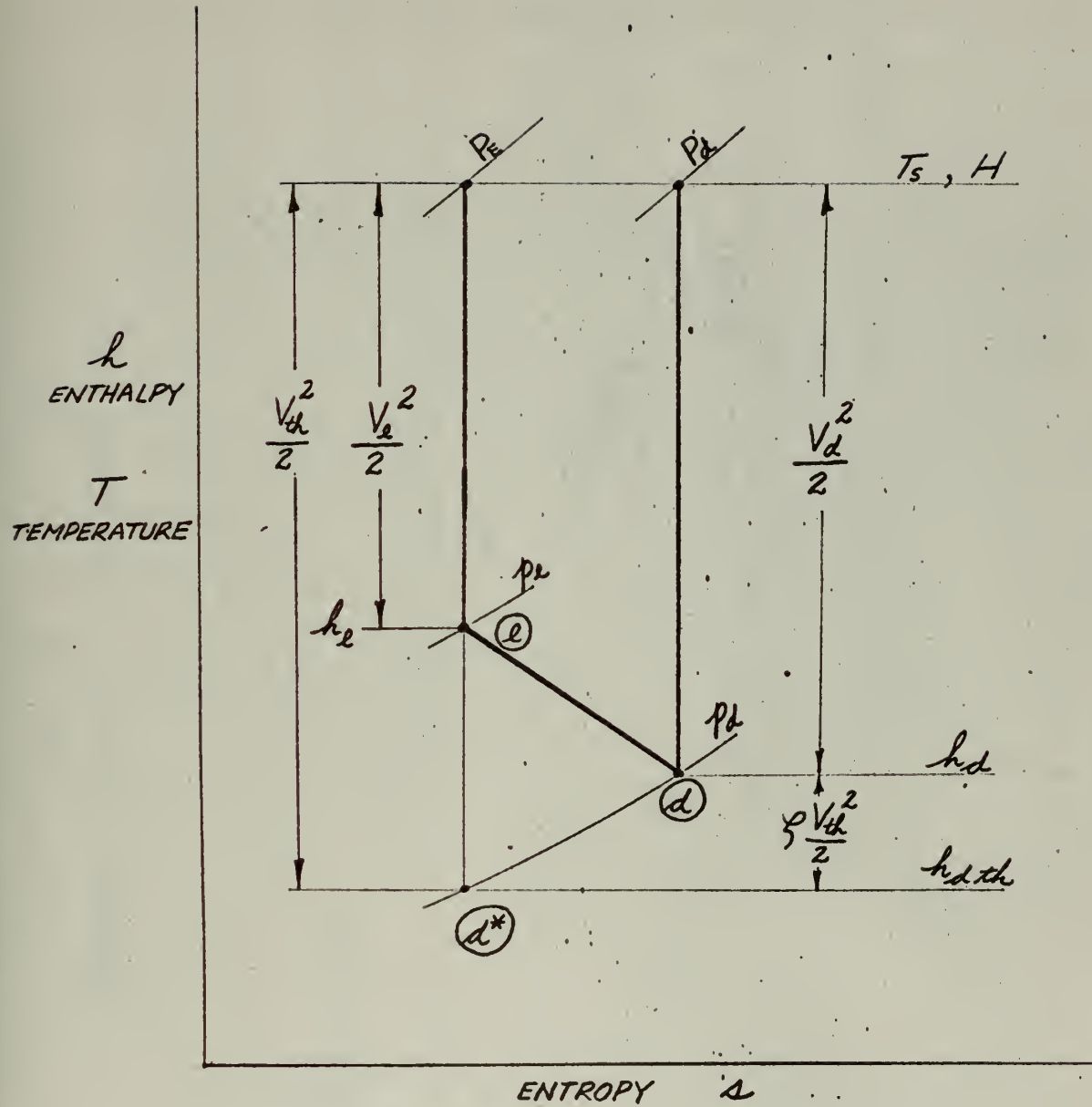


FIG. 34
h-s DIAGRAM FOR AFTER-EXPANSION PROCESS

FIG. 35

TURBINE EFFICIENCY vs. PRESSURE RATIO

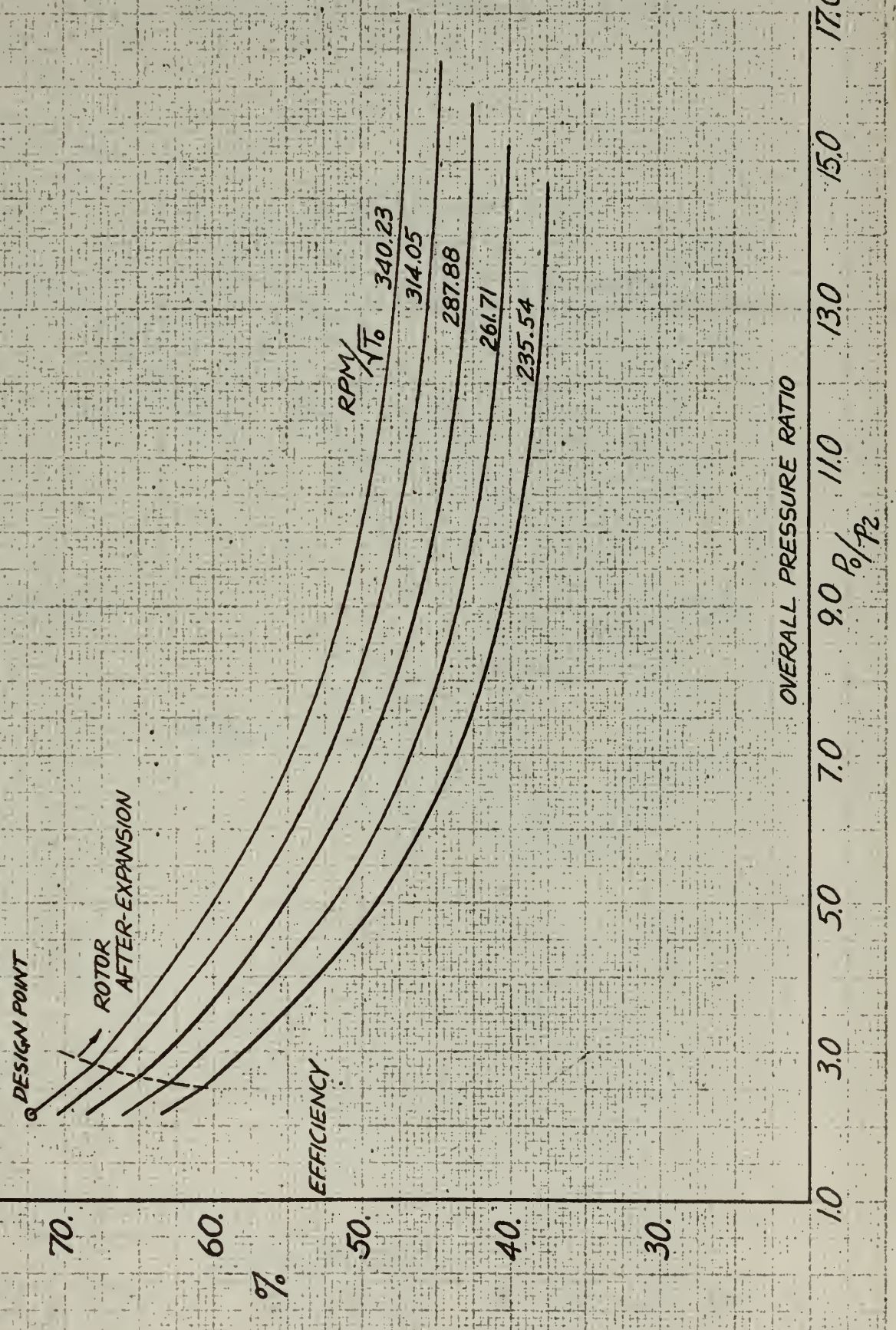


FIG. 36
POWER COEFFICIENT vs. TURBINE EFFICIENCY

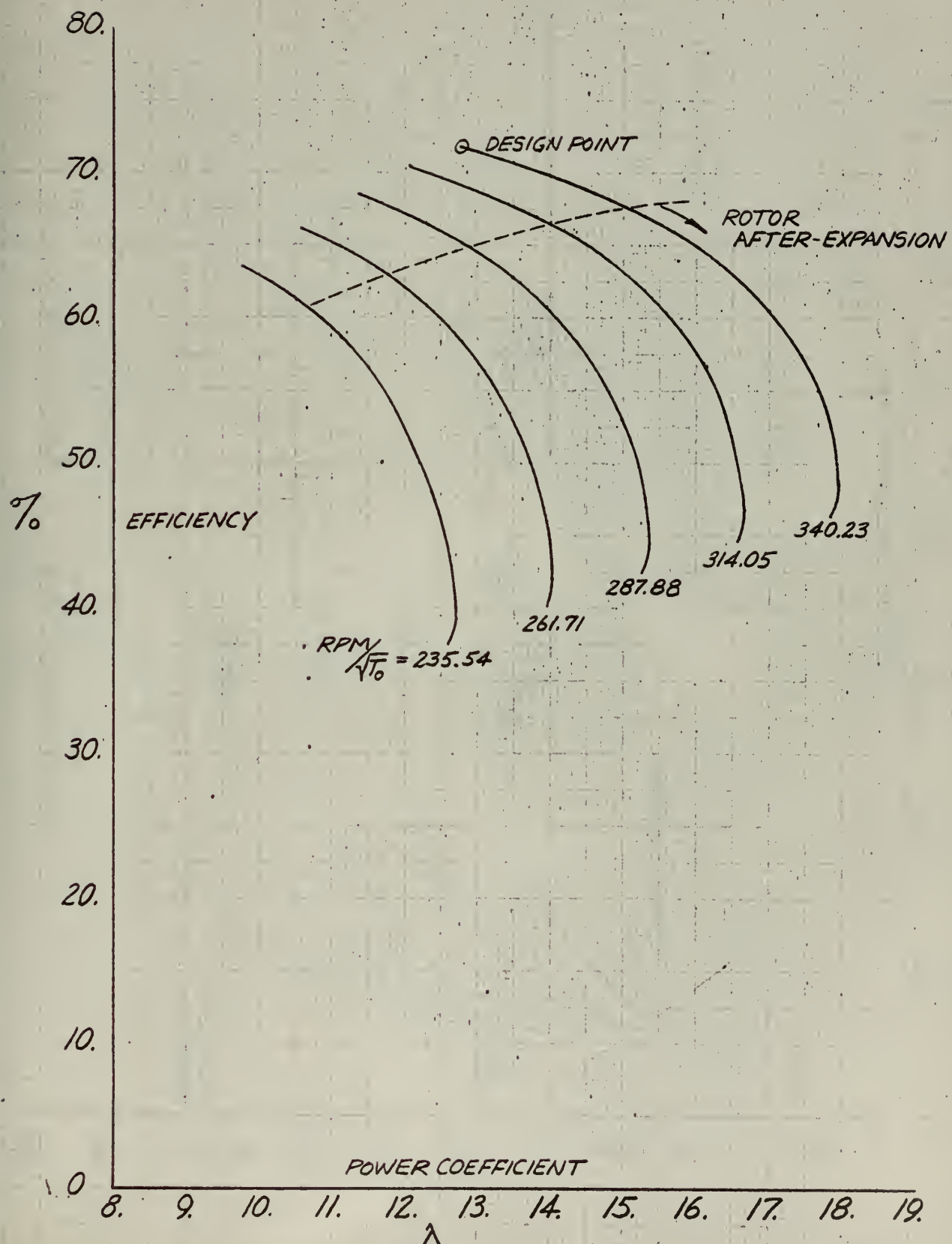


FIG. 37
POWER COEFFICIENT vs. PRESSURE RATIO

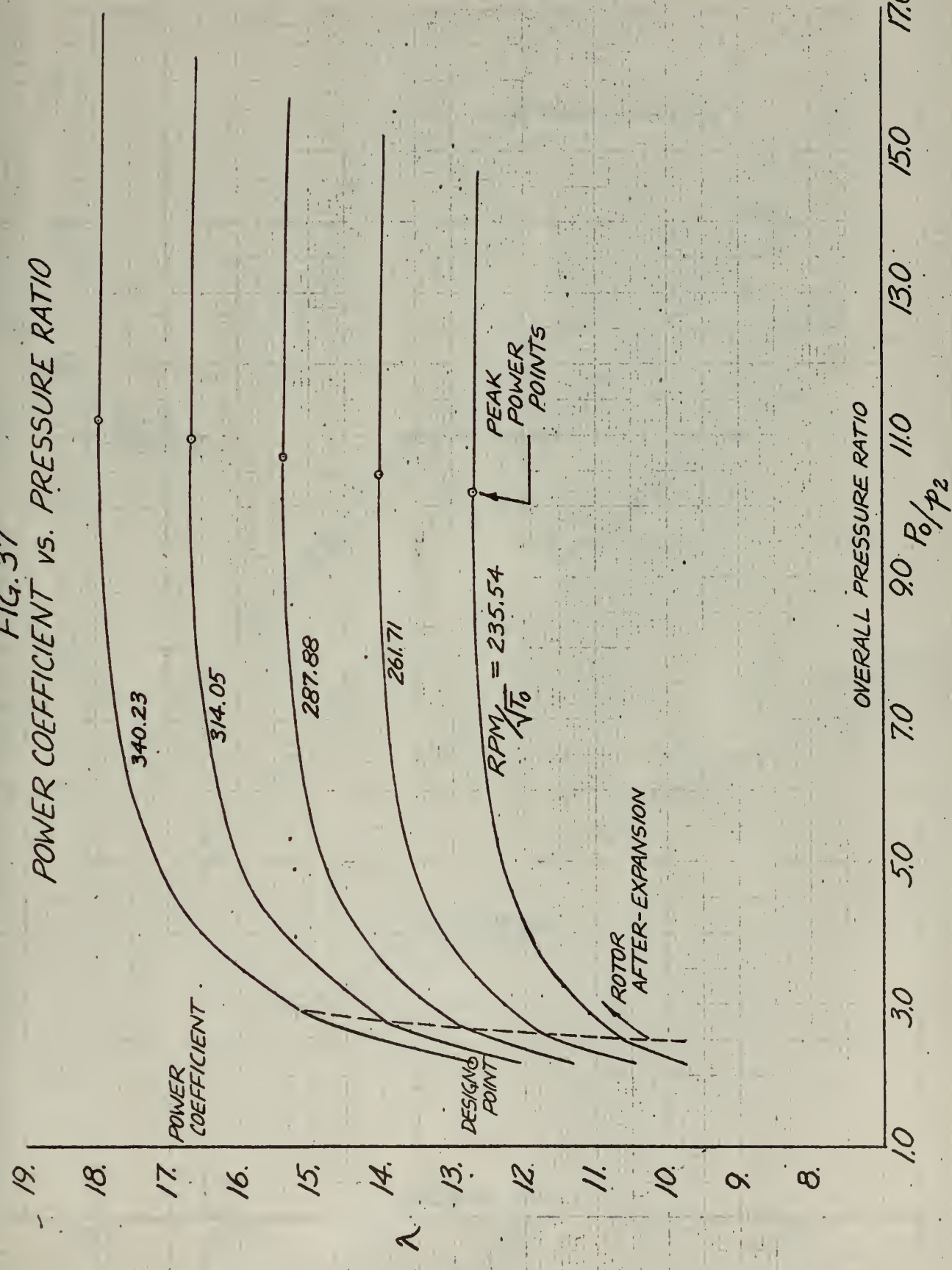


FIG. 38
TURBINE PERFORMANCE MAP.

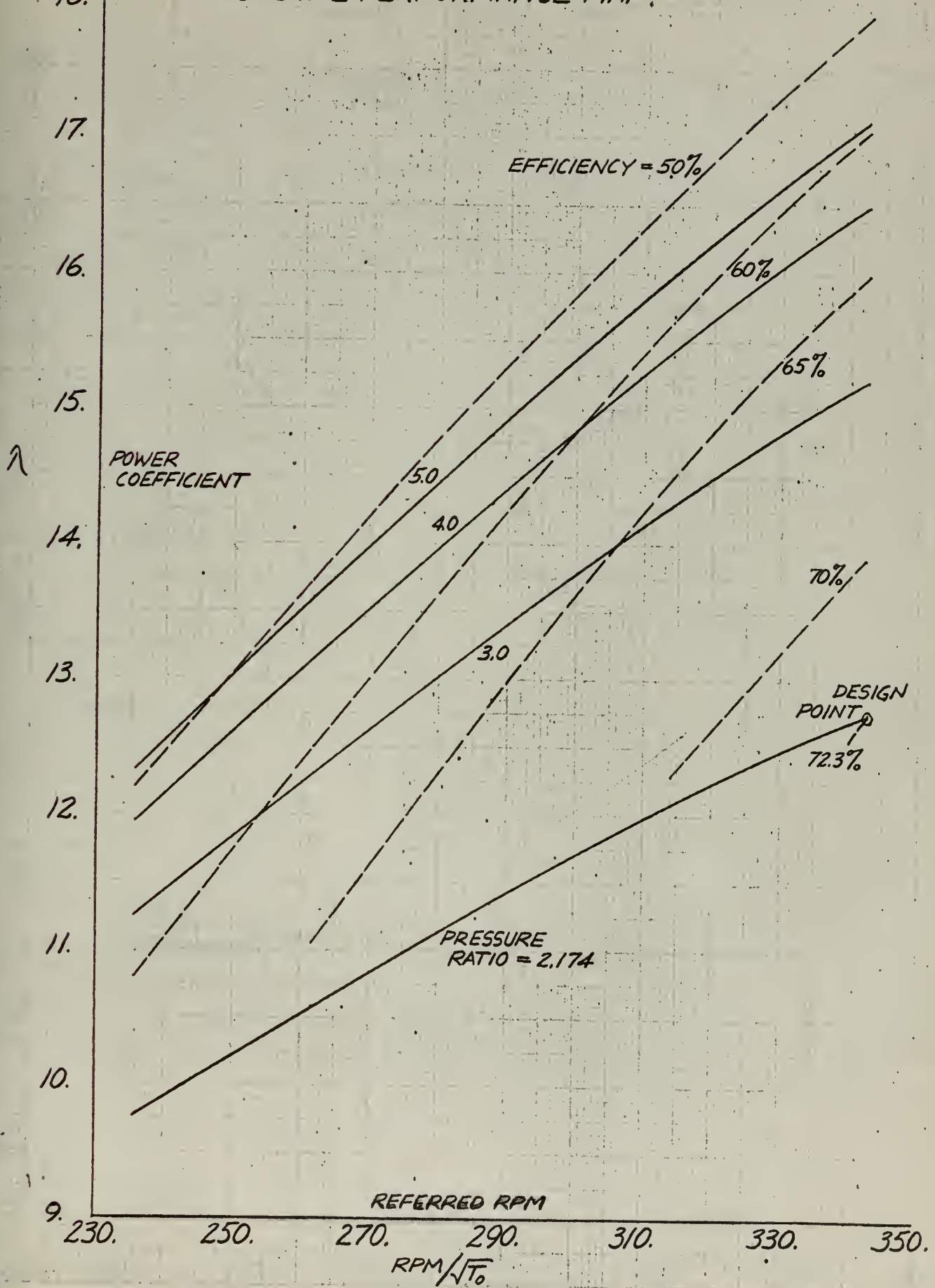
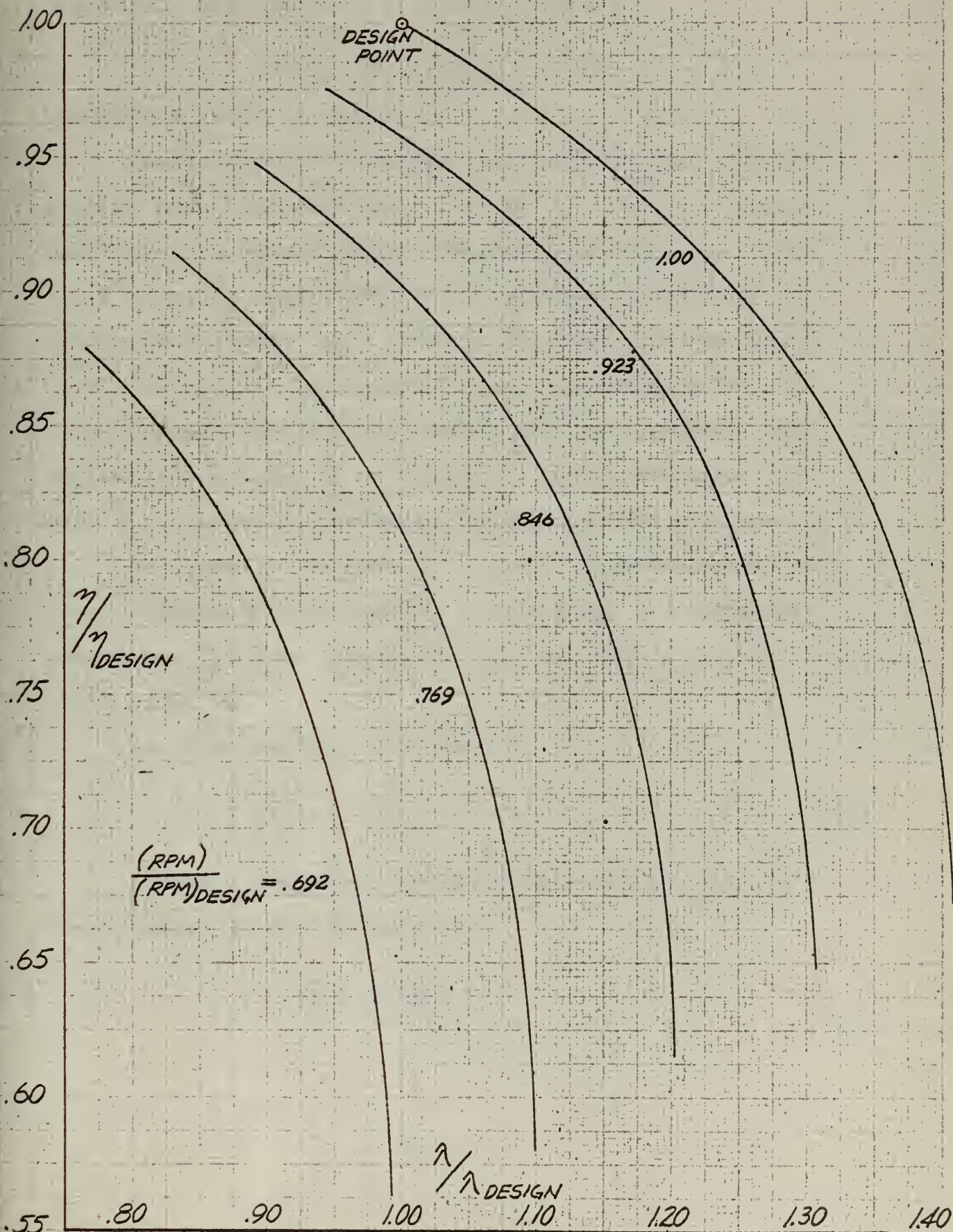


FIG. 39
POWER COEFFICIENT VS. TURBINE EFFICIENCY
REFERRED TO DESIGN POINT



Appendix I. Development of Flow Function Relations

In Fig. 32 is shown the adiabatic expansion process in a turbine from state 1 to state 2.

The fluid proceeds from state 1 to state $2'$ and the isentropic enthalpy drop is represented by process $(1-2'_{is})$. The fluid proceeds from state $2'$ to state 2 and the isentropic enthalpy drop is process $(2'-2^*)$. For the complete process the isentropic enthalpy drop is represented by process $1-2_{is}$. However, the sum of processes $(1-2'_{is}) + (2'-2^*)$ is greater than process $(1-2_{is})$ due to the so-called "reheat factor". The frictional effects raise the temperature, and therefore the enthalpy, of the fluid as it proceeds from state 1 to state $2'$. This increase of enthalpy is then available to do work.

As a result, it is necessary to make a distinction between the loss coefficient ζ for the overall process of Fig. 14 and the loss coefficient ζ_p for the polytropic process from pressure (p) to $(p-dp)$ on Fig. 32.

The polytropic loss coefficient is

$$\zeta_p = 1 - \gamma_p \quad (I,1)$$

Looking at the expansion process in more detail in Fig. 32, the efficiency can also be seen to be

$$\gamma_p = \frac{dT}{dT_{is}} \quad (I,2)$$

From this the relation along the polytropic line is

$$dT_{is} = T_0 \left[1 - \left(\frac{p - dp}{p} \right)^{\frac{\gamma-1}{\gamma}} \right] = T_0 \left[\frac{\gamma-1}{\gamma} \frac{dp}{p} \right] \quad (I, 3)$$

and

$$dT = \gamma_p dT_{is} = T_0 \left[\gamma_p \frac{\gamma-1}{\gamma} \frac{dp}{p} \right]$$

or

$$\frac{dT}{T} = \gamma_p \frac{\gamma-1}{\gamma} \frac{dp}{p} \quad (I, 4)$$

Since, for an adiabatic process

$$p v^n = \text{constant, then} \quad T \propto p^{\frac{\gamma-1}{\gamma}} \quad (I, 5)$$

and for an isentropic process

$$p v^{\gamma} = \text{constant, then} \quad T \propto p^{\frac{\gamma-1}{\gamma}} \quad (I, 6)$$

Comparing these exponents, there is

$$\frac{n-1}{n} = \gamma_p \left(\frac{\gamma-1}{\gamma} \right) = (1 - \gamma_p) \left(\frac{\gamma-1}{\gamma} \right)$$

and

$$n = \frac{\gamma}{\gamma_p (\gamma-1) + 1} \quad (I, 7)$$

To find the relation between the overall loss coefficient and the polytropic loss coefficient, eq. (I,5) can be written between two points on the polytropic expansion line as

$$\frac{T_0}{T} = \left(\frac{P_0}{P} \right)^{\frac{\gamma_p}{\gamma} \frac{n-1}{\gamma}}$$

and

$$T_0 - T = T_0 \left[1 - \left(\frac{P}{P_0} \right)^{\frac{\gamma_p}{\gamma} \frac{n-1}{\gamma}} \right] = \gamma T_0 \left[1 - \left(\frac{P}{P_0} \right)^{\frac{n-1}{\gamma}} \right] \quad (I,8)$$

Solving equation (I,8) for γ and using

$$\zeta = 1 - \gamma$$

the reduced result is

$$\zeta = \frac{\left(\frac{P}{P_0} \right)^{(1-\zeta_p) \frac{n-1}{\gamma}} - \left(\frac{P}{P_0} \right)^{\frac{n-1}{\gamma}}}{1 - \left(\frac{P}{P_0} \right)^{\frac{n-1}{\gamma}}} \quad (I,9)$$

To define a flow function for the mass flow through the blade row, the expression for mass flow rate must be expressed in terms of the pressure ratio and the polytropic exponent. The mass flow is

$$\dot{m} = \frac{A_2 V_2}{\rho_2} \quad (I,10)$$

and following the procedure outlined in Appendix IV for finding the velocity corresponding to a pressure drop the result is

$$V_2^2 = \frac{2x}{\gamma-1} gRT_0 \left[1 - \left(\frac{p}{P_0} \right)^{\frac{n-1}{n}} \right] \quad (IV,4)$$

Along the polytropic line, for an adiabatic process

$$pv^n = \text{constant}$$

or

$$\frac{v}{v_0} = \left(\frac{P_0}{p} \right)^{\frac{1}{n}} \quad (I,11)$$

When equations (IV,4) and (I,11) are substituted into (I,10) the result can be arranged in non-dimensional form to define a flow function ϕ to be

$$\phi = \frac{\dot{m} \sqrt{T_0}}{P_0 A_1} \sqrt{\frac{R}{g}} = \sqrt{\frac{2x}{\gamma-1} \left[\left(\frac{p}{P_0} \right)^{\frac{n}{n}} - \left(\frac{p}{P_0} \right)^{\frac{n+1}{n}} \right]} \quad (I,12)$$

This flow function reaches a maximum at the choked condition for the blade row. To find the corresponding pressure ratio for choked flow, the derivative of the flow function with respect to the pressure ratio will be set equal to zero and the result solved for the pressure ratio.

$$\phi^2 = \frac{2x}{\gamma-1} \left[\left(\frac{1}{r} \right)^{\frac{2}{n}} - \left(\frac{1}{r} \right)^{\frac{n+1}{n}} \right], \quad r = \frac{P}{P_0}$$

Then

$$\frac{d(\phi^2)}{dr} = \frac{2\gamma}{\gamma-1} \left[-\frac{2}{n} r^{-\frac{2}{n}-1} + \frac{n+1}{n} r^{-\frac{n+1}{n}-1} \right]$$

which reduces to

$$\frac{d(\phi^2)}{dr} = \frac{2\gamma}{\gamma-1} r^{-\frac{2+m}{m}} \left[-\frac{2}{n} + \frac{n+1}{n} r^{\frac{1-m}{m}} \right]$$

When set equal to zero, the result is

$$r^{\frac{n-1}{m}} = -\frac{2}{n} \left(\frac{n}{n+1} \right)$$

and

$$\left(\frac{P}{P_{cr}} \right)_{cr} = \left(\frac{2}{n+1} \right)^{\frac{m}{n-1}} \quad (I,13)$$

When the relation for the critical pressure ratio, eq. (I,13), is substituted into eq. (I,12) the critical flow function is obtained as

$$\phi_{cr} = \left(\frac{2}{n+1} \right)^{\frac{1}{m-1}} \sqrt{\frac{2\gamma}{\gamma-1} \left(\frac{n-1}{n+1} \right)} \quad (I,14)$$

Appendix II. After-expansion from a Blade Row

To find relations to express the expansion of a sonic or super-sonic flow out of a blade row, the following model is employed. The cascade is assumed to have infinitely many blades of zero thickness arranged as in Fig. 33 below.

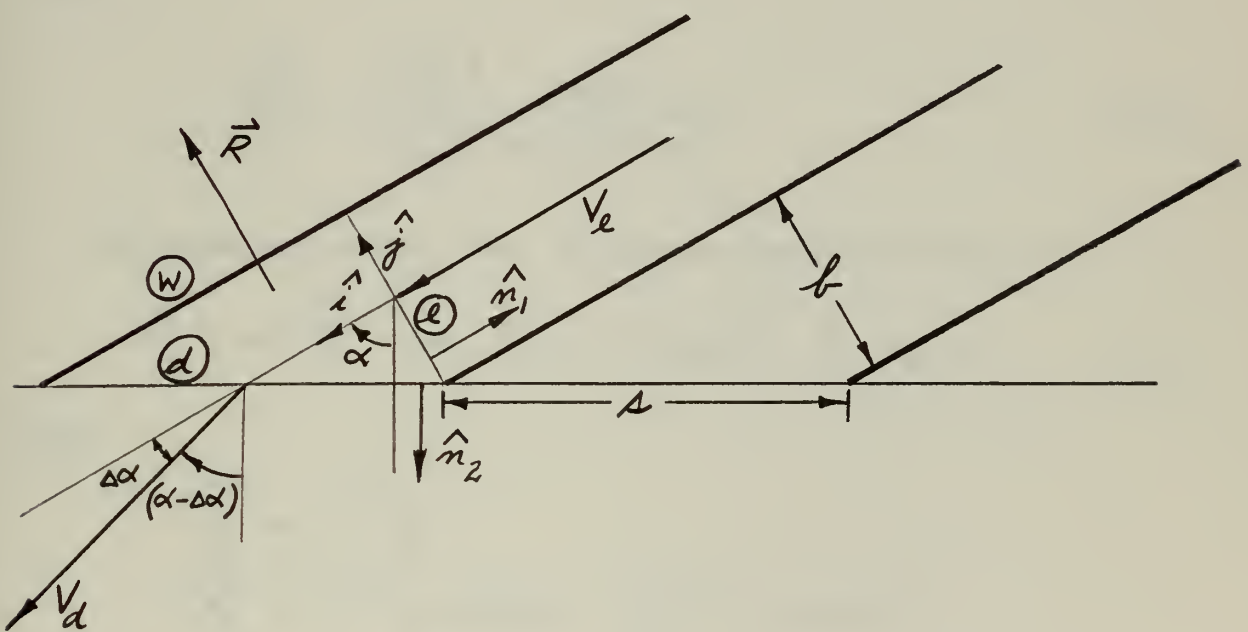


Fig. 33 Relations for After-expansion from a Cascade

A unit height perpendicular to the page is assumed. Also the uniform adiabatic flow is assumed to be frictionless at \textcircled{W} so that \vec{R} is perpendicular to \textcircled{W} . The control area under consideration is bounded by the surfaces \textcircled{W} , \textcircled{e} and \textcircled{d} , i.e., the "wall", the "exit" plane and the "discharge" plane. V_e is sonic or supersonic.

The continuity equation is used to find a relation between the densities,

$$\rho_e V_e b = \rho_d V_d \cos(\alpha - \Delta\alpha) s = m_s$$

$$b = s \cos \alpha$$

and so

$$\frac{\rho_d}{\rho_e} = \left(\frac{V_e}{V_d} \right) \frac{\cos \alpha}{\cos(\alpha - \Delta\alpha)} \quad (II,1)$$

The momentum equation, Ref. 1, ignoring shearing stresses is

$$\vec{R} = m_s \vec{V}_e - m_s \vec{V}_d - \hat{n}_1 \rho_e b - \hat{n}_2 \rho_d s \quad (II,2)$$

where

$$\vec{V}_e = \hat{i} V_e$$

$$\vec{V}_d = \hat{i} V_d \cos \alpha - \hat{j} V_d \sin \alpha$$

$$\hat{n}_1 = -\hat{i}$$

$$\hat{n}_2 = \hat{i} \cos \alpha - \hat{j} \sin \alpha$$

and so

$$\hat{j} R = \hat{i} m_s V_e - m_s V_d (\hat{i} \cos \alpha - \hat{j} \sin \alpha) + \hat{i} \rho_e b - \rho_d s (\hat{i} \cos \alpha - \hat{j} \sin \alpha)$$

Of particular interest are the relations in the \hat{i} direction

$$0 = m_s V_e - m_s V_d \cos \alpha + \rho_e b - \rho_d s \cos \alpha$$

and using

$$m_s = \rho_e V_e b$$

reduces to

$$\frac{\rho_e V_e}{\rho_e} \left[V_e - V_d \cos \Delta \alpha \right] + 1 - \frac{P_d}{\rho_e} = 0$$

Since

$$\frac{P}{\rho} = \frac{a^2}{\gamma} \quad \text{and} \quad M = \frac{V}{a}$$

$$\gamma M_e^2 \left[1 - \frac{V_d}{V_e} \cos \Delta \alpha \right] = \frac{P_d}{\rho_e} - 1 \quad (\text{II,3})$$

Since the process is assumed adiabatic, the total enthalpy remains constant through the control area,

$$h_e + \frac{V_e^2}{2} = h_d + \frac{V_d^2}{2}$$

and

$$h = C_p T = \frac{R}{J} \frac{\gamma}{\gamma-1} T = \frac{\gamma}{\gamma-1} \frac{P}{\rho}$$

and substituting

$$\frac{2\gamma}{\gamma-1} \frac{P_e}{\rho_e} + V_e^2 = \frac{2\gamma}{\gamma-1} \frac{P_d}{\rho_d} + V_d^2$$

(II,4)

Rearranging and substituting in eq. (II,1) and using

$$P_e \gamma = a_e^2 P_e$$

results in

$$\frac{P_d}{P_e} = \frac{V_e}{V_d} \left[\frac{\cos \alpha}{\cos(\alpha - \Delta \alpha)} \right] \left[1 + \frac{\gamma-1}{2} M_e^2 \left(1 - \frac{V_d^2}{V_e^2} \right) \right] \quad (II,5)$$

Then equating eqs. (II,3) and (II,5) and collecting terms results in a quadratic equation in velocity ratio,

$$\left(\frac{V_d}{V_e} \right)^2 \left[\gamma M_e^2 \cos \alpha - \frac{\cos \alpha}{\cos(\alpha - \Delta \alpha)} \left\{ \frac{\gamma-1}{2} M_e^2 \right\} \right] - \left(\frac{V_d}{V_e} \right) \left[\gamma M_e^2 + 1 \right] + \left[\frac{\cos \alpha}{\cos(\alpha - \Delta \alpha)} \left(1 + \frac{\gamma-1}{2} M_e^2 \right) \right] = 0 \quad (II,6)$$

The loss coefficient associated with the flow through the control area can be defined to be

$$\zeta_A = \frac{V_{th}^2 - V_d^2}{V_{th}^2}$$

based on the relations in Fig. 34. Using perfect gas relations and Fig. 34 as a reference, the following relations are obtained for the loss coefficient.

$$\zeta_A \frac{V_{th}^2}{2} = H - h_{dth} - \frac{V_d^2}{2}$$

$$\zeta_A = \frac{2}{V_{th}^2} \left[H - h_{dth} \right] - \left(\frac{V_d}{V_{th}} \right)^2$$

$$H = C_p T_s = \frac{\alpha_s^2}{\gamma - 1} , \quad h_{dth} = C_p T_d^* = \frac{\alpha_d^*}{\gamma - 1} \frac{\alpha_d^*}{\alpha_s}$$

$$\zeta_A = \frac{2}{\gamma - 1} \frac{\alpha_e^2}{V_{th}^2} \left[\left(\frac{\alpha_s}{\alpha_e} \right)^2 - \left(\frac{\alpha_d^*}{\alpha_s} \right)^2 \right] - \left(\frac{V_d}{V_{th}} \right)^2$$

$$\left(\frac{\alpha_s}{\alpha_e} \right)^2 = \frac{T_s}{T_e} = 1 + \frac{\gamma - 1}{2} M_e^2$$

$$\left(\frac{\alpha_d^*}{\alpha_e} \right)^2 = \frac{T_d^*}{T_e} = \left(\frac{p_d}{p_e} \right)^{\frac{\gamma - 1}{\gamma}}$$

$$\zeta_A = \frac{2}{\gamma - 1} \left(\frac{\alpha_e}{V_e} \right)^2 \left(\frac{V_e}{V_{th}} \right)^2 \left[1 + \frac{\gamma - 1}{2} M_e^2 - \left(\frac{p_d}{p_e} \right)^{\frac{\gamma - 1}{\gamma}} \right] - \left(\frac{V_d}{V_e} \right)^2 \left(\frac{V_e}{V_{th}} \right)^2$$

$$\frac{V_{th}^2}{2} = \frac{V_e^2}{2} + h_e - h_{dth} = \frac{V_e^2}{2} + \zeta_p (T_e - T_d^*)$$

$$= \frac{V_e^2}{2} + \frac{R}{J} \frac{\gamma}{\gamma-1} T_e \left[1 - \frac{T_d^*}{T_e} \right]$$

$$V_{th}^2 = V_e^2 + \frac{2}{\gamma-1} a_e^2 \left[1 - \left(\frac{p_d}{p_e} \right)^{\frac{\gamma-1}{\gamma}} \right]$$

$$\left(\frac{V_{th}}{V_e} \right)^2 = 1 + \frac{2}{\gamma-1} \frac{1}{M_e^2} \left[1 - \left(\frac{p_d}{p_e} \right)^{\frac{\gamma-1}{\gamma}} \right]$$

$$\zeta_A = \frac{\frac{2}{\gamma-1} \frac{1}{M_e^2} \left[1 + \frac{\gamma-1}{2} M_e^2 - \left(\frac{p_d}{p_e} \right)^{\frac{\gamma-1}{\gamma}} \right] - \left(\frac{V_d}{V_e} \right)^2}{1 + \frac{2}{\gamma-1} \frac{1}{M_e^2} \left[1 - \left(\frac{p_d}{p_e} \right)^{\frac{\gamma-1}{\gamma}} \right]}$$

$$\zeta_A = 1 - \frac{\left(\frac{V_d}{V_e} \right)^2}{\left[1 + \frac{2}{\gamma-1} \frac{1}{M_e^2} \left\{ 1 - \left(\frac{p_d}{p_e} \right)^{\frac{\gamma-1}{\gamma}} \right\} \right]} \quad (II, 8)$$

The Mach number of flow behind after-expansion is then, using Fig. 34 as reference for relations,

$$M_d = \frac{V_d}{a_d} = \left(\frac{V_d}{V_e} \right) \left(\frac{V_e}{a_e} \right) \left(\frac{a_e}{a_d} \right) \quad (III,9)$$

$$H - h_d = \frac{V_d^2}{2}$$

$$\frac{a_s^2}{\gamma-1} \frac{1}{a_e^2} - \frac{a_d^2}{\gamma-1} \frac{1}{a_e^2} = \frac{V_d^2}{2} \frac{1}{a_e^2}$$

$$\left(\frac{a_s}{a_e} \right)^2 - \left(\frac{a_d}{a_e} \right)^2 = \frac{\gamma-1}{2} \left(\frac{V_d}{a_e} \right)^2$$

Further

$$1 + \frac{\gamma-1}{2} M_e^2 = \left(\frac{a_s}{a_e} \right)^2$$

$$M_e^2 = \frac{V_e^2}{a_e^2}$$

$$\therefore \left(\frac{a_d}{a_e} \right)^2 = 1 + \frac{\gamma-1}{2} M_e^2 - \frac{\gamma-1}{2} \left(\frac{V_d}{a_e} \right)^2$$

$$\left(\frac{a_d}{a_e} \right) = \sqrt{1 + \frac{\gamma-1}{2} M_e^2 \left[1 - \left(\frac{V_d}{V_e} \right)^2 \right]}$$

Substitute into (II,9) above

$$M_d = \left(\frac{V_d}{V_e} \right) M_e \left[\frac{1}{1 + \frac{2 - 1}{2} M_e^2 \left\{ 1 - \left(\frac{V_d}{V_e} \right)^2 \right\}} \right]^{\frac{1}{2}} \quad (II,10)$$

This computation is included in the computer program but is not printed out. It is inserted for ready use if a check is needed.

Appendix III.

MAIN PROGRAM FOR TURBINE PERFORMANCE ANALYSIS

FLOW CHART

FORTRAN NAMES

PROGRAM LISTING

SUBROUTINE AFTER

FLOW CHART

FORTRAN NAMES

PROGRAM LISTING

SUBROUTINE TRNGL

FLOW CHART

FORTRAN NAMES

PROGRAM LISTING

SUBROUTINE BEFORE

FLOW CHART

FORTRAN NAMES

PROGRAM LISTING

SUBROUTINE CURVE

FLOW CHART

FORTRAN NAMES

PROGRAM LISTING

SUBROUTINE CPHI

FLOW CHART

FORTRAN NAMES

PROGRAM LISTING

PROGRAMS TURPLOT AND TURBINE (HIGH HEAD COEFFICIENT DATA)

FORTRAN NAMES

PROGRAM TURPLOT LISTING

PROGRAM TURBINE LISTING

PROGRAM FANNO 3 (FLOW FUNCTION AND ZETA POLYTROPIC)

FORTRAN NAMES

PROGRAM LISTING

PROGRAM FANNO 4 (CHOKED FLOW VALUES OF FANNO 3)

FORTRAN NAMES

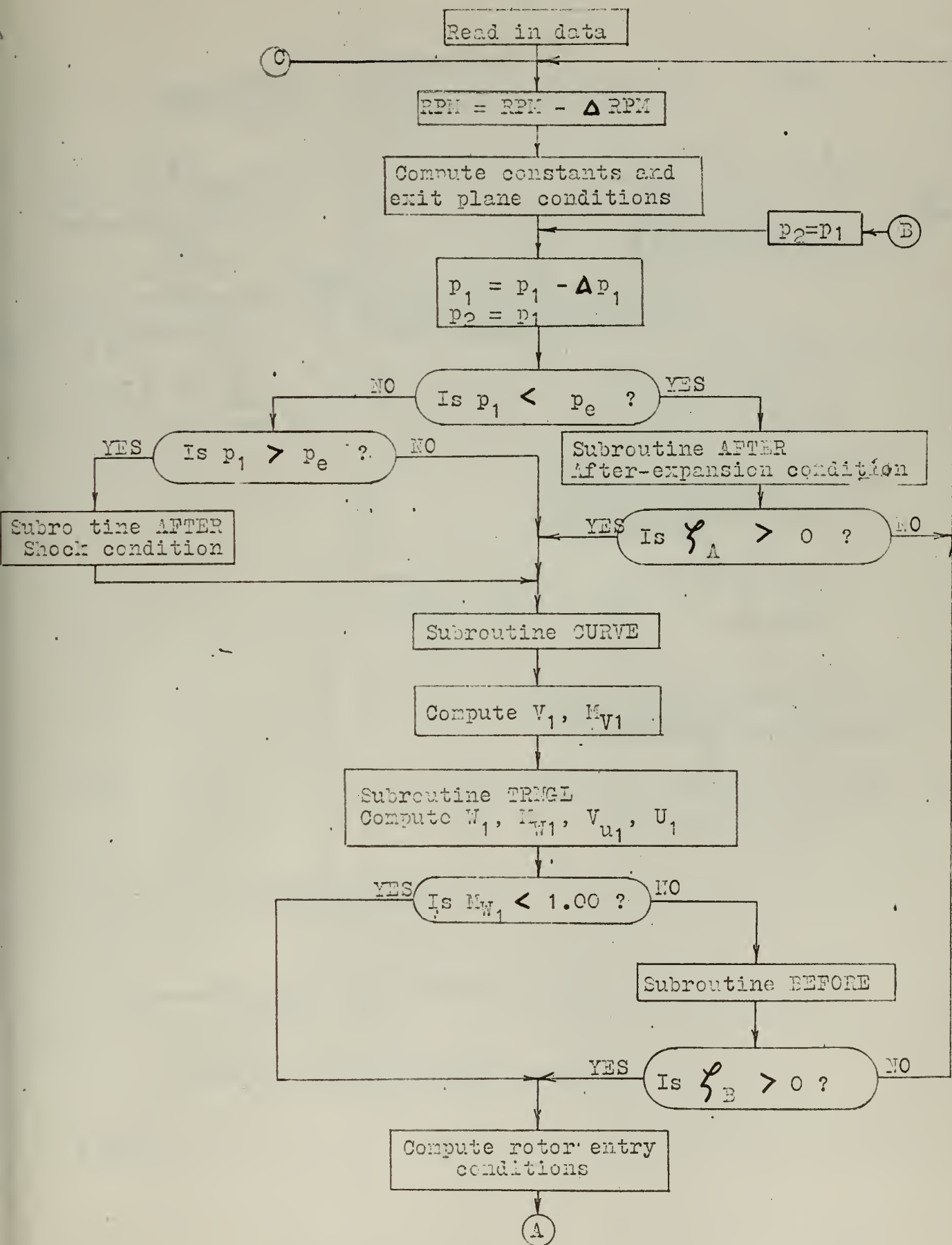
PROGRAM LISTING

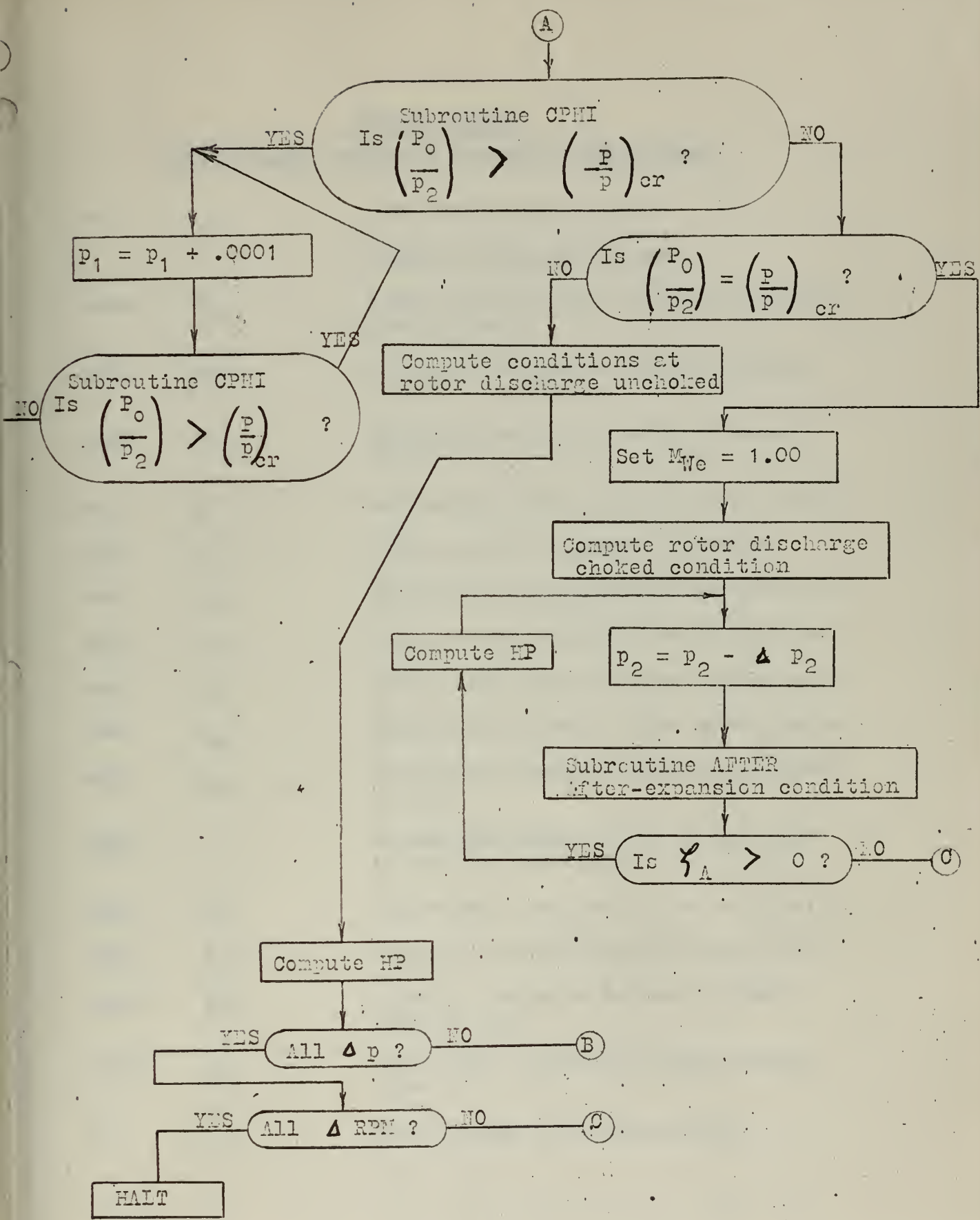
PROGRAM FOR AFTER-EXPANSION COMPUTATIONS

FORTRAN NAMES SAME AS "AFTER" ABOVE

PROGRAM LISTING

MAIN PROGRAM





PROGRAM PERFORM

FORTRAN NAMES, EQUIVALENT SYMBOLS AND DEFINITIONS

AE2	A_{e2}	Area at exit plane of rotor
AJ	J	Mechanical equivalent of heat
ALFAB1	α_{B1}	Undeflected flow angle of absolute velocity leaving stator
ALFA1	α_1	Flow angle of absolute velocity leaving stator
ALFA2	α_2	Flow angle of absolute velocity leaving rotor
AME	M_e	Mach number of flow at exit plane of stator
AMIS	M_{is}	Mach number for isentropic expansion
AMV1	M_{V1}	Mach number of absolute flow leaving stator
AMV2	M_{V2}	Mach number of absolute flow leaving rotor
AMW1	M_{W1}	Relative Mach number of flow entering rotor
AMW2	M_{W2}	Relative Mach number of flow leaving rotor
AMWE	M_{We}	Relative Mach number of flow at exit plane of rotor
AMWEX		Average Mach number of flow at exit plane of rotor for choked flow
BETA1	β_1	Flow angle of relative flow entering rotor
BETA2	β_2	Flow angle of relative flow leaving rotor
BETAB1	β_{B1}	Relative flow angle for zero incidence entering rotor
BETAB2	β_{B2}	Undeflected relative flow angle leaving rotor
CP	C_p	Specific heat at constant pressure

C1		$(\text{Constant } \#1) = \sqrt{R/g}$
C2		$(\text{Constant } \#2) = \sqrt{(2 \gamma gR) / (\gamma - 1)}$
C3		$(\text{Constant } \#3) = (\gamma - 1) / (2 \gamma gR)$
C4		$(\text{Constant } \#4) = \sqrt{\gamma gR}$
DM1	D_{m1}	Mean diameter of blade at rotor entrance
DM2	D_{m2}	Mean diameter of blade at rotor exit
DRPM	ΔRPM	Increment of rpm
DTE	$(\Delta T_e / T_o)$	Temperature drop from inlet to exit plane of stator
DTF	$\Delta T / T_o$	Final temperature difference from total to static temperature after rotor
DTR	$(T_{R1} - T_1)$	Temperature drop between relative total temperature ahead of rotor and static temperature ahead of rotor
DTRAT	$(\Delta T / T_o)$	Temperature drop from inlet to discharge plane of stator
DTE2	$(\Delta T_{e2} / T_o)$	Temperature drop from inlet to exit plane of rotor
DT2	$(\Delta T_2 / T_o)$	Temperature drop from inlet to discharge plane of rotor
EFF	η	Efficiency based on total pressure after rotor
EXP1		Exponent #1 = $(\gamma - 1) / \gamma$
EXP2		Exponent #2 = $\gamma / (\gamma - 1)$
EXP3		Exponent #3 = $1 / (\gamma - 1)$
G	g	Acceleration of gravity
GAM	γ	Specific heat ratio
HKR	K_{hR}	Blade height correction for rotor loss coefficient
HKS	K_{hS}	Blade height correction for stator loss coefficient

HP		Horsepower
HR2	h_{R2}	Rotor blade height
HS1	h_{S1}	Stator blade height
NMAX		Number of data points stored for a particular loss coefficient curve
PE	(p_e / p_o)	Static pressure at exit plane of stator
PE2	(p_{e2} / p_o)	Static pressure at exit plane of rotor
PHIC	ϕ_c	Flow function computed with input γ and ζ
PHICR	ϕ_{cr}	Critical flow function for choked flow in rotor
PPCR	$(P/p)_{cr}$	Critical pressure ratio for choked flow in rotor
PO	p_o	Total pressure ahead of stator
PPRAT	p_{R1} / p_2	Pressure ratio through rotor
PRAT	p_1 / p_e	Pressure ratio between stator exit plane and stator discharge plane
PRATO	p_o / p_2	Overall pressure ratio
PRP	p_{R1} / p_1	Relative pressure ratio
PR1	p_{R1} / p_o	Relative total pressure ahead of rotor
PRIY	p_{R1}^* / p_o	Relative total pressure behind shock in rotor entry
P1	p_1 / p_o	Static pressure between stator and rotor
P2	p_2 / p_o	Static pressure after rotor
P2T	p_2	Static pressure after rotor
R		Gas constant
RFR	$W \sqrt{T_o / p_o}$	Referred flow rate
RPM	$RPM / \sqrt{T_o}$	Referred rpm

RPMA		Actual value of rpm
RTO	$\sqrt{T_o}$	
TE	T_e/T_o	Temperature at exit plane of stator
TEIS	T_{eis}/T_o	Isentropic temperature at exit plane of stator
TE2	T_{e2}/T_o	Temperature at exit plane of rotor
TI		True interval between data points on loss coefficient curves
TO	T_o	Total temperature ahead of stator
T1	T_1/T_o	Static temperature between stator and rotor
T2	T_2/T_o	Static temperature after rotor
T2T	T_2	Static temperature after rotor
TP2	P_2	Total pressure after rotor
TRAT	(T_{1is}/T_o)	Isentropic temperature ratio through stator
TRATR	(T_{2is}/T_{R1})	Isentropic temperature ratio through rotor
TR1	T_{R1}/T_o	Relative total temperature ahead of rotor
TT2	T_{T2}	Total temperature after rotor
T1Y	T_1^*	Static temperature behind shock in rotor entry
U1	$U_1/\sqrt{T_o}$	Peripheral speed of blade at mean diameter at rotor entrance
U2	$U_2/\sqrt{T_o}$	Peripheral speed of blade at mean diameter at rotor discharge
UV	U_1/v_1	Abscissa for rotor loss coefficient data
VE	$v_e/\sqrt{T_o}$	Absolute velocity of flow at exit plane of stator
VM	$v_m/\sqrt{T_o}$	Meridional component of absolute velocity
VU1	$v_{ul}/\sqrt{T_o}$	Peripheral component of absolute velocity leaving stator

VU2	$v_{u2} / \sqrt{T_o}$	Peripheral component of absolute velocity leaving rotor
V1	$v_1 / \sqrt{T_o}$	Absolute flow velocity leaving stator
V2	$v_2 / \sqrt{T_o}$	Absolute flow velocity leaving rotor
WDOT	\dot{w}	Mass flow rate
WE	$w_e / \sqrt{T_o}$	Relative velocity at exit plane of rotor
WM	$w_m / \sqrt{T_o}$	Meridional component of relative velocity
QU1	$w_{u1} / \sqrt{T_o}$	Peripheral component of relative velocity entering rotor
WU2	$w_{u2} / \sqrt{T_o}$	Peripheral component of relative velocity leaving rotor
W1	$w_1 / \sqrt{T_o}$	Relative flow velocity ahead of rotor
W1Y	$w_1^* / \sqrt{T_o}$	Relative flow velocity behind entry shock in rotor
W2	$w_2 / \sqrt{T_o}$	Relative flow velocity behind rotor
YY		Ordinate of loss coefficient curves
ZET	ζ	Loss coefficient for velocity through rotor including after-expansion
ZETAA	ζ_A	After-expansion loss coefficient
ZETAB	ζ_B	Loss coefficient due to rotor entry shock
ZETAS	ζ_S	Stator loss coefficient
ZETAA1	ζ_{a1}	Loss coefficient for flows through stator
ZETAA2	ζ_{a2}	Loss coefficient for flows through rotor
ZETA1	ζ_1	Loss coefficient for velocities through stator
ZETA2	ζ_2	Loss coefficient for velocities through rotor without after-expansion


```

PROGRAM PERFORM
DIMENSION YY(4,50),NMAX(4),TI(4)
COMMON C1,C2,C3,C4,GAM,EXP1,EXP2,EXP3,P0,T0,R
READ 281,P0,T0,GAM,R,WDOT
READ 282,RPMA,DM1,DM2,HS1,HR2,ALFAB1,BETAB1,BETAB2,AE2
READ 283,AME,PE,ZETAA1,ZETAA2,AMIS
DO 118 K = 1,4
READ 284,J,(NMAX(J),TI(J))
NMAX = NMAX(J)
READ 285 (YY(J,I),I=1,NMAX)
118 CONTINUE
AJ = 778.17
G = 32.174
RTO = SQRTF(T0)
RFR = WDOT*RTO/P0
C1 = SQRTF(R/32.174)
C2 = SQRTF(2.*GAM*32.174*R/(GAM-1.))
C3 = (GAM-1.)/(2.*GAM*32.174*R)
C4 = SQRTF(GAM*32.174*R)
EXP1 = (GAM-1.)/GAM
EXP2 = (GAM)/(GAM-1.)
EXP3 = 1./(GAM-1.)
CP = R*GAM/(AJ*(GAM-1.))
PE = PE/P0
TEIS = PE**EXP1
DTE = (1.-TEIS)*(1.-ZETAA1)
TE = 1.-DTE
VE = C2*SQRTF(DTE)
CALL CURVE (1,HS1,HKS,TI,NMAX,YY)
CALL CURVE (2,HR2,HKR,TI,NMAX,YY)
DO 200 J = 1,5
DRPM = 1000.*FLOATF(J-1)
RPMA = 13000.-DRPM
PRINT 250
PRINT 251,WDOT,P0,T0
PRINT 252,RFR,GAM,R
PRINT 253,C1,EXP1
PRINT 254,C2,EXP2
PRINT 255,C3,EXP3
PRINT 256,C4,RTO
RPM = RPMA/RTO
PRINT 257
PRINT 258,RPMA,RPM
PRINT 259,DM1,HS1
PRINT 260,DM2,HR2
PRINT 261,ALFAB1
PRINT 262,BETAB1
PRINT 263,BETAB2
PRINT 264,ZETAA2
ALFAB1 = ALFAB1*3.1415927/180.
BETAB1 = BETAB1*3.1415927/180.
BETAB2 = BETAB2*3.1415927/180.
PRINT 265
PRINT 266,AME,VE,PE,TE
L = 2
DO 198 I = 1,30
P1 = 470.
P1 = P1-FLOATF(I)*10.
P1 = P1/P0
111 CONTINUE
PRAT = P1/PE
P2 = P1
100 IF (P1-PE) 100,101,100
CALL AFTER (AME,PRAT,ALFAB1,ALFA1,ZETAA)
IF (ZETAA) 116,116,103
GO TO 103
101 CONTINUE
ALFA1 = ALFAB1
ZETAA = 0.0
103 CONTINUE
CALL CURVE (3,AMIS,ZETAS,TI,NMAX,YY)
ZETAI = ZETAS*HKS+ZETAA
TRAT = P1**EXP1

```



```

DTRAT = (1.-TRAT)*(1.-ZETA1)
T1 = 1.-DTRAT
V1 = C2*SQRTF(DTRAT)
AMV1 = V1/(C4*SQRTF(T1))
IF (L-3) 119,120,120
120 PRINT 290
L = 1
119 CONTINUE
PRINT 267
AL = ALFA1*180./3.1415927
PRINT 291,AMV1,V1,P1,T1,AL,ZETA1
CALL TRNGL (1,V1,DM1,ALFA1,RPM,VM,VU1,WU1,U1,W1,BETA1)
DTR=C3*W1*W1
TR1=T1+DTR
PRP = (TR1/T1)**EXP2
PR1 = P1*PRP
AMW1 = W1/(C4*SQRTF(T1))
PRINT 269
BE = BETA1*180./3.1415927
PRINT 268,AMW1,W1,PR1,TR1,BE
IF (AMW1-1.0) 104,104,105
104 W1=W1*COSF(BETAB1-BETA1)
PRINT 271
DTR=C3*W1*W1
TR1=T1+DTR
PRP = (TR1/T1)**EXP2
PR1 = P1*PRP
AMW1 = W1/(C4*SQRTF(T1))
BETA1 = BETAB1
BE = BETA1*180./3.1415927
PRINT 268,AMW1,W1,PR1,TR1,BE
GO TO 106
105 CONTINUE
CALL BEFORE (AMW1,BETAB1,BETA1,P1,W1,TR1,T1,W1Y,PR1Y,T1Y,ZETAB)
PRINT 270
W1 = W1Y
AMW1 = W1/(C4*SQRTF(T1Y))
PR1 = PR1Y
BETA1 = BETAB1
BE = BETA1*180./3.1415927
PRINT 268,AMW1,W1,PR1,TR1,BE
IF (ZETAB) 114,106,106
114 PRINT 288
GO TO 198
106 CONTINUE
UV = U1/V1
CALL CURVE (4,UV,ZETAR,TR1,NMAX,YY)
ZETA2 = ZETAR*HKR
PPRAT=PR1/P2
TRATR = 1. / (PPRAT ** EXP1)
DTE2 = (TR1-TRATR*TR1)*(1.-ZETAA2)
TE2 = TR1-DTE2
WE = C2*SQRTF(DTE2)
AMWE = WE/(C4*SQRTF(TE2))
PRINT 272
CALL CPHI (ZETAA2,PPRAT,PHIC,PHICR,PPCR)
PRINT 273,PHIC,P1ICR
PRINT 274,PPRAT,PPCR
IF (PPRAT-PPCR) 107,115,108
107 CONTINUE
DELTA = ABSF(PPRAT-PPCR)
IF (DELTA-.0005) 115,115,122
122 PE2 = P2
PRINT 275
PRINT 266,AMWE,WE,PE2,TE2
PRINT 276
DT2=(TR1-TRATR*TR1)*(1.-ZETA2)
T2 = TR1-DT2
W2=C2*SQRTF(DT2)
AMW2 = W2/(C4*SQRTF(T2))
BETA2=BETAB2
BE2= BETA2*180./3.1415927
PRINT 291,AMW2,W2,P2,T2,BE2,ZETA2

```



```

CALL TRNGL (2,W2,DM2,BETA2,RPM,WM,WU2,VU2,U2,V2,ALFA2)
PRINT 277
AMV2 = V2/(C4*SQRTF(T2))
AL2= ALFA2*180./3.1415927
PRINT 268,AMV2,V2,P2,T2,AL2
GO TO 113
108 CONTINUE
PRINT 286
L = 6
110 P2 = P2+.0001
PPRAT = PR1/P2
CALL CPHI (ZETAA2,PPRAT,PHIC,PHICR,PPCR)
DELTA = ABSF(PPRAT-PPCR)
IF (DELTA-.0005)121,121,110
121 P1 = P2
GO TO 111
115 CONTINUE
AMWE = 1.00
PE2 = P2
PPRAT = PR1/PE2
TRATR = 1./(PPRAT**EXP1)
DTE2 = (TR1-TRATR*TR1)*(1.-ZETAA2)
TE2 = TR1-DTE2
WE = C2*SQRTF(DTE2)
AMWEX= WE/(C4*SQRTF(TE2))
299 FORMAT (100X,F10.3)
PRINT 275
PRINT 266,AMWE,WE,PE2,TE2
DT2=(TR1-TRATR*TR1)*(1.-ZETAA2)
T2 = TR1-DT2
W2=C2*SQRTF(DT2)
BETA2=BETAB2
CALL TRNGL (2,W2,DM2,BETA2,RPM,WM,WU2,VU2,U2,V2,ALFA2)
AMW2 = W2/(C4*SQRTF(T2))
AMV2 = V2/(C4*SQRTF(T2))
PRINT 276
BE2= BETA2*180./3.1415927
PRINT 291,AMW2,W2,P2,T2,BE2,ZETA2
PRINT 277
AL2= ALFA2*180./3.1415927
PRINT 268,AMV2,V2,P2,T2,AL2
L = 3
GO TO 113
112 P2=P2-.01
IF (L-5) 109,123,123
123 PRINT 290
L = 1
109 CONTINUE
PRINT 287
PRAT=P2/PE2
CALL AFTER (AMWE,PRAT,BETAB2,BETA2,ZETAA)
IF (ZETAA) 116,116,117
116 PRINT 289
GO TO 199
117 CONTINUE
PPRAT = PR1/P2
TRATR = 1./(PPRAT**EXP1)
DT2=(TR1-TRATR*TR1)*(1.-(ZETA2+ZETAA))
T2 = TR1-DT2
W2=C2*SQRTF(DT2)
CALL TRNGL (2,W2,DM2,BETA2,RPM,WM,WU2,VU2,U2,V2,ALFA2)
AMW2 = W2/(C4*SQRTF(T2))
AMV2 = V2/(C4*SQRTF(T2))
PRINT 276
BE2= BETA2*180./3.1415927
ZET = ZETA2+ZETAA
PRINT 291,AMW2,W2,P2,T2,BE2,ZET
PRINT 277
AL2= ALFA2*180./3.1415927
PRINT 268,AMV2,V2,P2,T2,AL2
113 CONTINUE
P2T = P2*PO
T2T = T2*T0

```



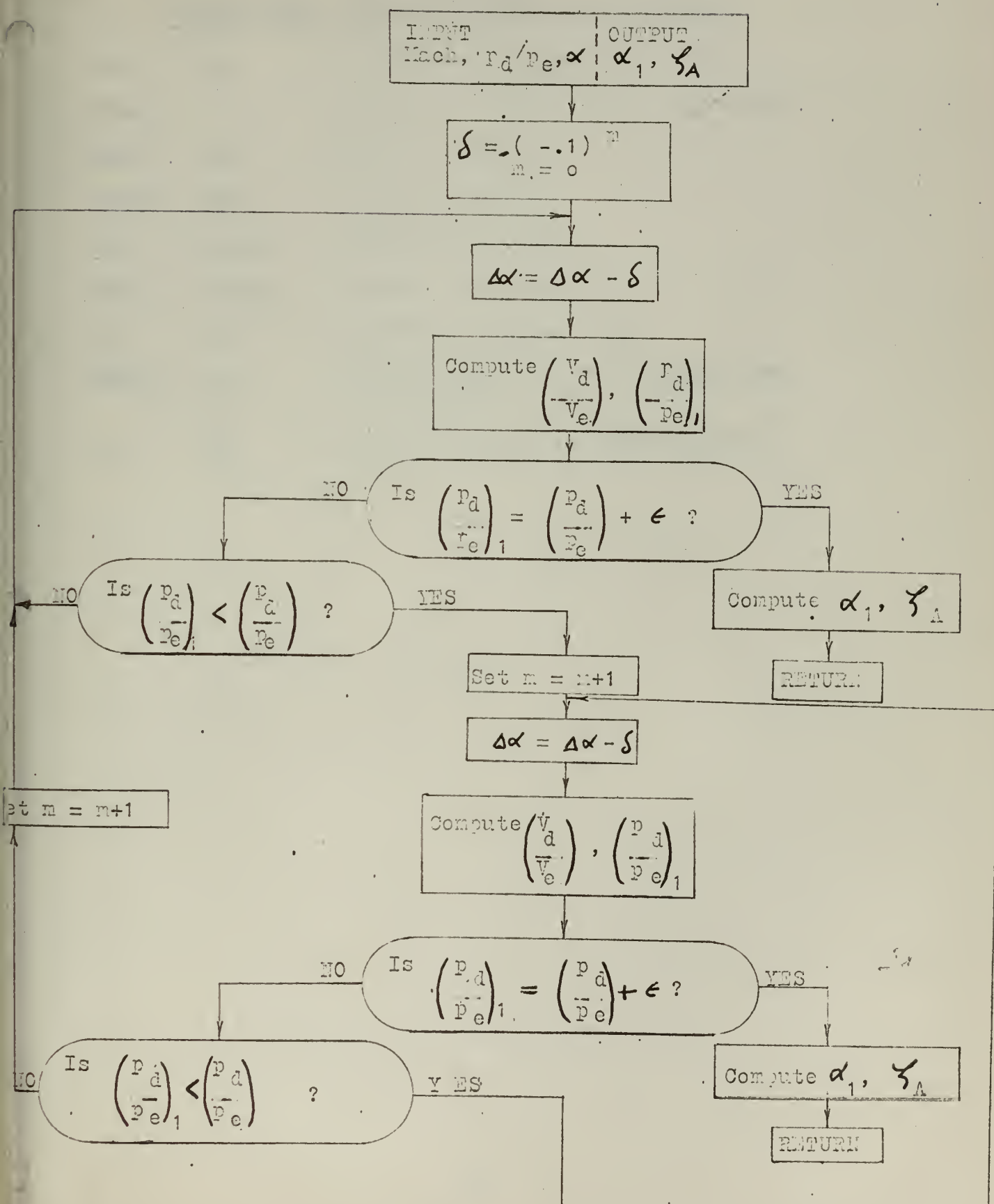
```

DTF = C3*V2*V2
TT2 = T2+DTF
TP2 = P2T*((TT2/T2)**EXP2)
PRATO = 1./P2
TT2 = TT2*T0
DH1 = T0-TT2
DH2 = T0*(1.-(TP2/P0)**EXP1)
EFF = DH1/DH2
VU1T = VU1*RTO
VU2T = VU2*RTO
HP = RTO*WDOT*1.+14*(VU1T*U1-VU2T*U2)/(G*AJ)
PRINT 278
PRINT 279,VU1T,VJ2T,P2T,TP2,T2T,TT2
PRINT 280,PRATO,HP,EFF
L = L+1
IF (AMWE-1.00) 198,112,112
2500FORMAT (1H1,21X19HTURBINE PERFORMANCE//13X35HINPUT VALUES AND CONS
ITANTS COMPUTED /)
2510FORMAT (13H FLOW RATE = F6.1, 17H LB/M SEC PO = F6.0, 13H PSIA.
1T0 = F6.0, 2H R )
2520FORMAT (22H REFERRED FLOW RATE = F5.3,4X8HGAMMA = F4.2,7X5HR =
1 F6.2 /)
253 FORMAT (7X5HC1 = F9.4,21X7HEXP1 = F6.4)
254 FORMAT (7X5HC2 = F9.4,21X7HEXP2 = F6.4)
255 FORMAT (7X5HC3 = F9.4,21X7HEXP3 = F6.4)
256 FORMAT (7X5HC4 = F9.4,21X7HRT0 = F6.2)
257 FORMAT (/20X20H PHYSICAL PARAMETERS /)
258 FORMAT (7H RPM = F7.0,23X15HREFERRED RPM = F12.3/)
2590FORMAT (27H MEAN DIA AT ROTOR INLET = F5.2,27H IN STATOR BLADE HEI
1GHT = F5.3,3H IN )
2600FORMAT (27H MEAN DIA AT ROTOR EXIT = F5.2,27H IN ROTOR BLADE HEIG
1HT = F5.3,3H IN )
261 FORMAT (12X26H STATOR DISCHARGE ANGLE = F6.2,4H DEG )
262 FORMAT (12X26H ROTOR INLET ANGLE = F6.2,4H DEG )
263 FORMAT (12X26H ROTOR DISCHARGE ANGLE = F6.2,4H DEG /)
264 FORMAT (7X41HLOSS COEFFICIENT THROUGH ROTOR (FLONS) = F7.4//)
265 FORMAT (18H STATOR EXIT PLANE//32H M(VE) VE/RTO PE/PO TE/T0)
266 FORMAT (F6.2,F10.3,2F8.4)
2670FORMAT (23H STATOR DISCHARGE PLANE//49H M(V1) V1/RTO P1/PO
1T1/T0 ALFA1 ZETA1 )
268 FORMAT (F6.2,F10.3,2F8.4,F8.2)
269 FORMAT (41H M(W1) W1/RTO PR1/PO TR1/T0 BETA1 )
2700FORMAT (28H IN ROTOR BEHIND ENTRY SHOCK//41H M(W1) W1/RTO PR1/P
10 TR1/T0 BETA1 )
2710FORMAT (15H IN ROTOR ENTRY//41H M(W1) W1/RTO PR1/PO TR1/T0 B
1ETA1 )
272 FORMAT (27H FLOW FUNCTION COMPUTATIONS)
273 FORMAT (10X16H PHI COMPUTED = F6.5,13X15HPHI CRITICAL = F6.5)
2740FORMAT (26H PRESSURE RATIO IMPOSED = F6.3,28H CRITICAL PRESSURE RA
1T10 = F6.3)
275 FORMAT (17H ROTOR EXIT PLANE//32H M(WE) WE/RTO PE2/PO TE2/T0)
2760FORMAT (22H ROTOR DISCHARGE PLANE//49H M(W2) W2/RTO P2/PO T
12/T0 BETA2 ZETA2 )
277 FORMAT (41H M(V2) V2/RTO P2/PO T2/T0 ALFA2 )
2780FORMAT (/15X31H RESULTANT POWER AND EFFICIENCY //
1 3X11HVU1(FT/SEC),2X11HVU2(FT/SEC),3X8HP2(PSIA),2X9HP2T(PSIA),3X
2 2HT2,5X3HT2T)
279 FORMAT (F12.2,F13.2,F11.0,2F10.0,F7.0)
280 FORMAT (3X25HOVERALL PRESSURE RATIO = F6.3,2X5HHP = F6.0,15H EFFI
1CIENCY = F4.3//)
281 FORMAT (5F10.0)
282 FORMAT (9F8.0)
283 FORMAT (5F10.0)
284 FORMAT (I3,I6,F10.0)
285 FORMAT (8F9.0)
286 FORMAT (/48H ROTOR CANNOT SATISFY FLOW FUNCTION, INCREASE P1 /)
287 FORMAT (21H ROTOR AFTEREXPANSION)
288 FORMAT (19H ZETAB IS NEGATIVE. )
289 FORMAT (19H ZETAA IS NEGATIVE. )
290 FORMAT (1H1)
291 FORMAT (F6.2,F10.3,2F8.4,F8.2,F8.4)
198 CONTINUE
199 CONTINUE

```


ALFAB1 = ALFAB1*180./3.1415927
BETAB1 = BETAB1*180./3.1415927
BETAB2 = BETAB2*180./3.1415927
200 CONTINUE
END

SUBROUTINE AFTER



SUBROUTINE AFTER

FORTRAN NAMES, EQUIVALENT SYMBOLS AND DEFINITIONS

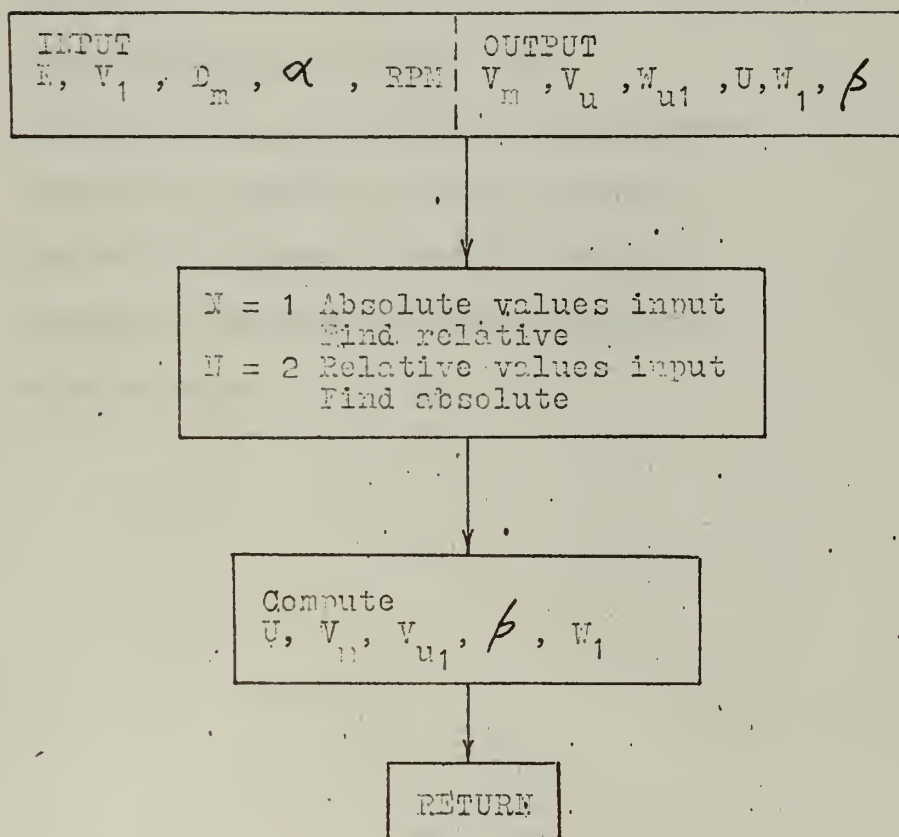
ALFA	α_B	Undeflected flow angle (blade angle)
COSRAT		Cosine ratio of blade angle to flow angle
DALFA	$\Delta\alpha$	$\alpha_B - \alpha_1$ (degrees)
DALFAR	$\Delta\alpha$	$\alpha_B - \alpha_1$ (radius)
PRAT	(p_d/p_e)	Imposed pressure ratio
PRATI	$(p_d/p_e)_1$	Computed pressure ratio
VD	v_d	Velocity at discharge plane
VELRAT	v_d/v_e	Velocity ratio of flow at discharge plane to exit plane
ZA	ζ_A	Loss coefficient due to after-expansion


```

SUBROUTINE AFTER (AME, PRAT, ALFAS, ALFA1, ZA)
COMMON C1,C2,C3,C4,GAM,EXP1,EXP2,EXP3,P0,TO,R
ALFA = ABSF(ALFAS)
EE= (2. / ((GAM-1.) * AME * AME))
DALFA = 0.0
M = 0
400 M = M+1
401 DALFA = (-.1)**(M-1)+DALFA
DALFAR = DALFA*3.1415927/180.
COSRAT = COSF(ALFA)/COSF(ALFA-DALFAR)
AA = GAM*AME*AME*COSF(DALFAR)-COSRAT*(GAM-1.)*AME*AME/2.
BB = -GAM*AME*AME-1.
CC = COSRAT*(1.+(GAM-1.)*AME*AME/2.))
DD = BB*BB-4.*AA*CC
IF (DD) 401,402,402
402 VELRAT = (-BB+SQR(TF(DD))/(2.*AA)
OPRAT1 = (COSRAT*(1.+(GAM-1.)*AME*AME/2.)*(1.-VELRAT*VELRAT)))
1 /VELRAT
IF (PRAT1) 410,411,411
410 PRINT 409,N,AME,PRAT,ALFA,DALFAR
409 FORMAT (72X,I3,4F10.5)
411 CONTINUE
ZA = 1.-(VELRAT*VELRAT)/(1.+EE-EE*(PRAT1**EXP1))
VD = VE*VELRAT
DIFF = ABSF(PRAT1-PRAT)
IF (DIFF-.00001) 408,408,403
403 IF (PRAT1-PRAT) 404,408,401
404 M=M+1
405 DALFA = (-.1)**(M-1)+DALFA
DALFAR = DALFA*3.1415927/180.
COSRAT = COSF(ALFA)/COSF(ALFA-DALFAR)
AA = GAM*AME*AME*COSF(DALFAR)-COSRAT*(GAM-1.)*AME*AME/2.
BB = -GAM*AME*AME-1.
CC = COSRAT*(1.+(GAM-1.)*AME*AME/2.))
DD = BB*BB-4.*AA*CC
IF (DD) 400,406,406
406 VELRAT = (-BB+SQR(TF(DD))/(2.*AA)
OPRAT1 = (COSRAT*(1.+(GAM-1.)*AME*AME/2.)*(1.-VELRAT*VELRAT)))
1 /VELRAT
IF (PRAT1) 412,413,413
412 PRINT 409,N,AME,PRAT,ALFA,DALFAR
413 CONTINUE
ZA = 1.-(VELRAT*VELRAT)/(1.+EE-EE*(PRAT1**EXP1))
VD = VE*VELRAT
DIFF = ABSF(PRAT1-PRAT)
IF (DIFF-.00001) 408,408,407
407 IF (PRAT-PRAT1) 400,408,405
408 CONTINUE
IF (ALFAS) 414,415,415
414 ALFA1 = ALFAS+DALFAR
RETURN
415 ALFA1 = ALFAS - DALFAR
END

```


SUBROUTINE TRIGL



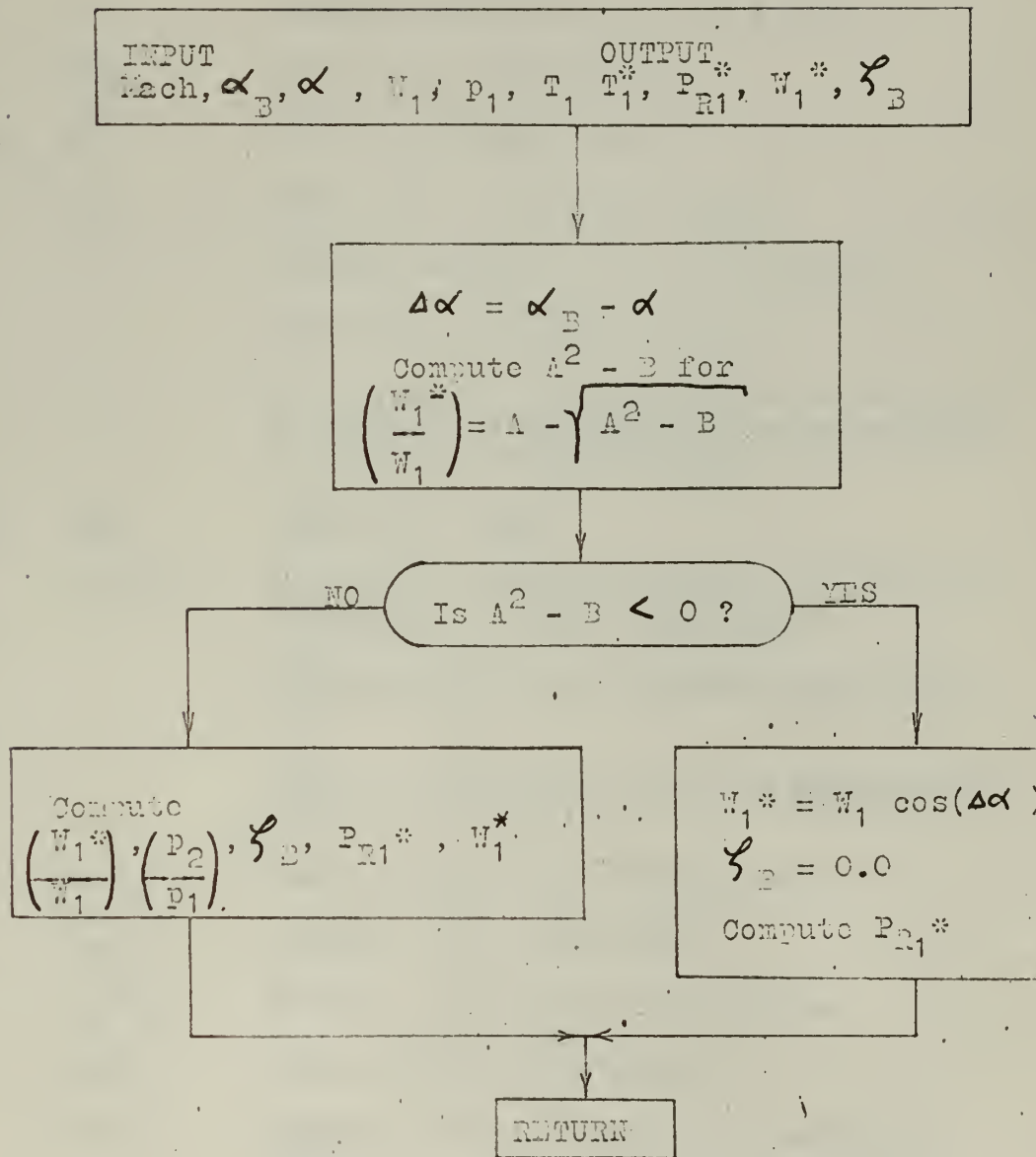
SUBROUTINE TRNGL

FORTRAN NAMES, EQUIVALENT SYMBOLS AND DEFINITIONS

A		Input angle of flow
B		Output flow angle (If $A = \alpha$, $B = \beta$ and if $A = \beta$, $B = \alpha$.)
N		Value selects plus or minus SIGN
U		Peripheral velocity of blade at mean diameter
VM	v_m	Meridional component of absolute velocity
VU1	v_{u1}	Peripheral component of absolute velocity
WU1	w_{u1}	Peripheral component of relative velocity
W1	w_1	Relative velocity


```
SUBROUTINE TRNGL (N,V1,DM,A,RPM,VM,VU1,WU1,U,W1,B)
COMMON C1,C2,C3,C4,GAM,EXP1,EXP2,EXP3,P0,T0,R
SIGN = (-1)**N
U = 3.1415927*RPM*DM/720.
VM = V1*COSF(A)
IF (A) 701,702,702
701 VU1 = -V1*SINF(A)
WU1 = VU1+SIGN*U
B = ATANF(WU1/VM)
W1 = WU1/SINF(B)
702 CONTINUE
VU1 = V1*SINF(A)
WU1 = VU1+SIGN*U
B = ATANF(WU1/VM)
W1 = WU1/SINF(B)
END
```


SUBROUTINE REFORM



SUBROUTINE BEFORE

FORTRAN NAMES, EQUIVALENT SYMBOLS AND DEFINITIONS

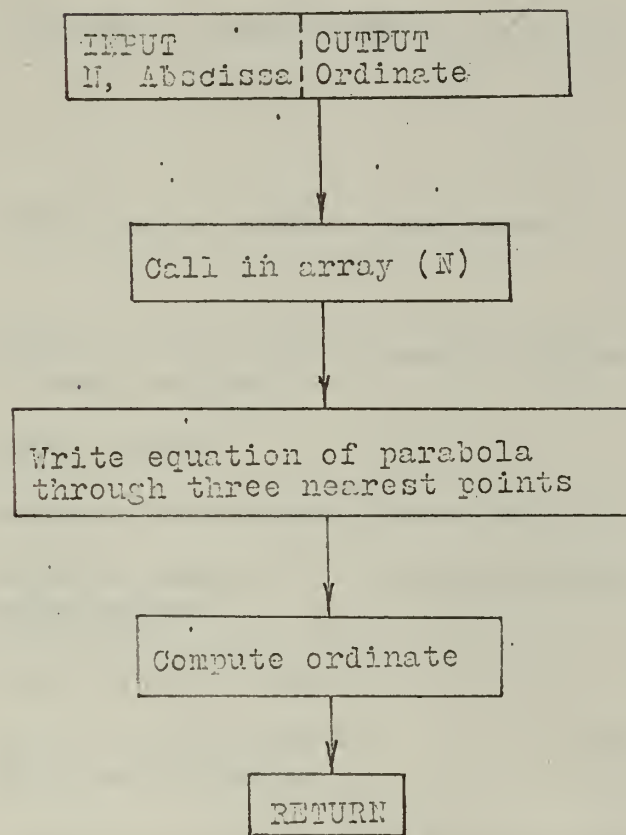
A		Interim computation for velocity ratio
ALFA	α_R	Blade angle entering rotor
ALFAI	α_1	Flow angle ahead of rotor
AMD	M_d	Mach number of flow after shock
B		Interim computation for velocity ratio
CC		Cosine ratio of angles involved
D		$A^2 - B$, used to determine whether shock should be computed, or the component of the velocity in direction of blade be used.
DALFA	$\Delta\alpha$	$\Delta\alpha = \alpha_1 - \alpha_R$
DTR	$(T_{r1} - T_1)$	Temperature difference between relative total temperature and static temperature
FF		Interim computation to find Mach number after shock
GG		Interim computation to find Mach number after shock
PP	p_1/p_1^*	Static pressure ratio through shock
PRP	P_{R1}/p_1	Pressure ratio through shock
PR1Y	P_{R1}^*/p_o	Relative total pressure behind shock
P1Y	p_1^*/p_o	Static pressure behind shock
VV	w_1^*/w_1	Velocity ratio of flow ahead of and behind shock
ZETAB	ζ_B	Loss coefficient of flow due to entry shock


```

SUBROUTINE BEFORE (AM1,ALFA,ALFA1,P1,W1,TR1,T1,W1Y,PR1Y,T1Y,ZETAB)
COMMON C1,C2,C3,C4,GAM,EXP1,EXP2,EXP3,P0,T0,R
DALFA = ALFA1-ALFA
CC = COSF(ALFA1)/COSF(ALFA)
A = (1. / (GAM+1.)) * ((1. / (CC*AM1*AM1)) + GAM*COSF(DALFA))
B = -(1. - (2. / (GAM+1.)) * ((1. / (AM1*AM1)) + GAM))
D = A*A-B
IF (D) 602,601,601
602 W1Y = W1*COSF(ALFA1-ALFA)
ZETAB = 0.0
DTR = C3*W1Y*W1Y
T1Y = TR1-DTR
PRP = (TR1/T1Y)**EXP2
PR1Y = P1Y*PRP
RETURN
601 CONTINUE
VV = A-SQRTF(A*A-B)
PP=CC*((1.+(GAM-1.)*AM1*AM1/2.)*(1./VV)-((GAM-1.)*AM1*AM1*VV/2.))
FF = (GAM-1.)*AM1*AM1/2.
GG = 1.-VV*VV
AMD = VV*AM1*SQRTF(1. / (1.+FF*GG))
ZETAB = 1.-VV*VV-(2. / ((GAM-1.)*AM1*AM1))*(((PP)**EXP1)-1.)
W1Y = W1*VV
P1Y = P1*PP
T1Y = TR1-C3*W1Y*W1Y
PRP = (TR1/T1Y)**EXP2
PR1Y = P1Y*PRP
END

```


SUBROUTINE CURVE



SUBROUTINE CURVE

FORTRAN NAMES, EQUIVALENT SYMBOLS AND DEFINITIONS

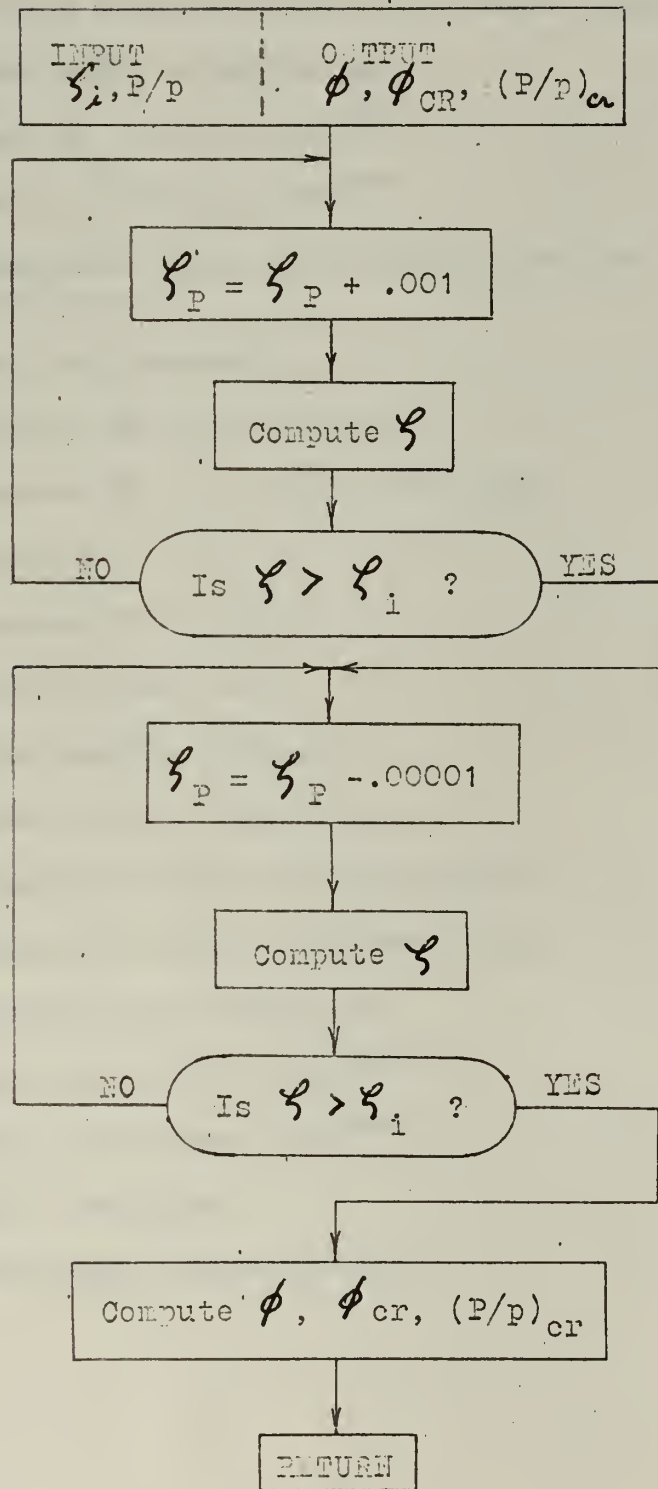
AA	a	}	The terms of equation $ORD = a + bx + cx^2$
BB	b		
CC	c		
I		}	Subscripts for ordinate data points
J			
K			
M			Counter to locate three nearest data points to input abscissa
N			Array selector
NMAX			Number of data points in selected array
ORD			Ordinate computed, i.e., loss coefficient value desired
T1			Data abscissa interval
T2	T1/2		One-half of data interval. Used to select the three nearest points
X			Abscissa in terms of three nearest points
XA			Input abscissa


```

SUBROUTINE CURVE(N,XA1,ORD,TI,NMAX,YY)
DIMENSION YY(4,50),NMAX(4),TI(4),Y(50)
COMMON C1,C2,C3,C4,GAM,EXP1,EXP2,EXP3,PO,TO,R
XA = XA1
NMAX=NMAX(N)
TI=TI(N)
306 DO 306 I = 1,NMAX
      Y(I)= YY(N,I)
      M = XA/TI
      X = TI*FLOATF(M)
      M = M+1
      IF (M-1) 304,300,301
304 PRINT 212
      RETURN
300 I = M
      J = M+1
      K = M+2
      GO TO 305
301 NM = NMAX-1
      IF (M-NM) 302,303,303
303 I = M-1
      J = M
      K = M+1
      GO TO 305
302 DIFR = XA-X
      T2 = TI/2.
      IF (DIFR-T2) 303,303,300
305 CONTINUE
      AA = Y(I)
      CC = 0.5*(Y(K)+Y(I)-2.*Y(J))
      BB = Y(J)-Y(I)-C
      XA = (XA/TI)-FLOATF(I-1)
      ORD = AA+BB*XA+CC*XA*XA
212 FORMAT (36H ABSCISSA WRONG IN SUBROUTINE CURVE )
END
END

```


SUBROUTINE CPHI



SUBROUTINE CPHI

FORTRAN NAMES, EQUIVALENT SYMBOLS AND DEFINITIONS

A		Interim critical pressure ratio while computing
CPHI	ϕ	Compute ϕ , subroutine name
DAB		Name for the term $(p/P)^{\exp 7}$
DAN		Name for the term $(p/P)^{\exp 6}$
DIFF		Difference between given and computed loss coefficient
EN	n	Polytropic exponent
EXP1		Exponent #1 = $(\gamma - 1)/\gamma$
EXP4		Exponent #4 = $(1 - \zeta_p)(\gamma - 1)/\gamma$
EXP6		Exponent #6 = $2/n$
EXP7		Exponent #7 = $(n+1)/n$
GAM	γ	Specific heat ratio
PHI	ϕ	Flow function computed
PHI2	ϕ^2	Flow function, squared
PHICR	ϕ_{cr}	Choked flow value of flow function
PPCR	$(P/P)_{cr}$	Choked flow value of pressure ratio
RC		Computed loss coefficient
RA		Name for the term $(p/P)^{\exp 4}$
RB		Name for the term $(p/P)^{\exp 1}$
ZETA	ζ	Loss coefficient
ZETAP	ζ_p	Polytropic loss coefficient


```

SUBROUTINE CPHI (ZETA,A,PHI,PHICR,PPCR)
COMMON C1,C2,C3,C4,GAM,EXP1,EXP2,EXP3,P0,T0,R
ZETAP = -.001
502 ZETAP = .001+ZETAP
EXP4 = (1.-ZETAP)*(GAM-1.)/GAM
RA = 1./(A**EXP4)
RB = 1./(A**EXP1)
RC = (RA-RB)/(1.-RB)
DIFF = ZETA-RC
IF (DIFF) 501,500,502
501 ZETAP = ZETAP-.00001
EXP4 = (1.-ZETAP)*(GAM-1.)/GAM
RA = 1./(A**EXP4)
RB = 1./(A**EXP1)
RC = (RA-RB)/(1.-RB)
DIFF = ZETA-RC
IF (DIFF) 501,500,500
500 EN = GAM/(1.+ZETAP*(GAM-1.))
EXP6 = 2./EN
EXP7 = (EN+1.)/EN
DAV = 1./(A**EXP6)
DAB = 1./(A**EXP7)
PHI2 = 2.*(GAM/(GAM-1.))*(DAN-DAB)
PHI = SQRTF(PHI2)
PHICR = ((2./(EN+1.))**((1./(EN-1.)))*SQRTF(2.*GAM*(EN-1.)/
((GAM-1.)*(EN+1.)))
PPCR = ((EN+1.)/2.)**(EN/(EN-1.))
END

```


PROGRAMS TURPLOT AND TURBINE

FORTRAN NAMES, EQUIVALENT SYMBOLS AND DEFINITIONS

AKE	k_E	Leaving loss coefficient
AKIS	k_{is}	Head coefficient, eq. 1
ALFA1	α_1	Angle of flow exiting stator (radians), absolute
ALFA2	α_2	Angle of flow leaving rotor (radians), absolute
BETA1	β_1	Flow angle entering rotor (degrees), relative
BETA2	β_2	Flow angle leaving rotor (degrees), relative
DBETA	$\Delta\beta$	$\Delta\beta = \beta_1 - \beta_2$
DETA	$\Delta\gamma$	$\Delta\gamma = \gamma - \gamma_A$
EFF		Reheat factor, defined in Ref. 1
ETA	η	Efficiency
ETAA	η_A	Efficiency assumed
ETAC	η_C	Efficiency computed as an interim step for comparison
EXX	X	Expression defined by eq. 5a
NALFA1	α_1	Angle of flow exiting rotor (degrees), absolute
NPHIE	ϕ_E	Carryover coefficient of kinetic energy into next stage
PHI	ϕ	Velocity coefficient in stator
PHIR	ϕ_R	Carryover coefficient of kinetic energy from stator into rotor
PSI	ψ	Velocity coefficient in rotor

PSIA	ψ_A	Velocity coefficient in rotor computed for comparison
RADRAT	R_2/R_1	Radius ratio through rotor
RBETA1	β_1	Flow angle entering rotor (radians), relative
RBETA2	β_2	Flow angle leaving rotor (radians), relative
RELRAT	w_2/w_1	Ratio of relative velocities
RSTAR	r^*	Degree of reaction, that fraction of the expansion through the stage which occurs in the rotor
VELM1	v_{m1}/u_1	Meridional component of absolute velocity leaving stator/Peripheral velocity of rotor at mean diameter
VELRAT	(v_{m2}/v_{m1})	Velocity ratio of meridional components
WSQR1	w_1^2	The relative velocity entering rotor, squared
WSQR2	w_2^2	The relative velocity leaving rotor, squared
XSQR	x^2	Expression defined by eq. 5a


```

PROGRAM TURPLOT
DO 50 NALFA1 = 60,75,5
N = 1
DO 50 I = 1,12
RSTAR=-.05+{FLOAT F(I))*.05
IF(N-2)21,22,22
21 PRINT 40
N = N+1
GO TO 23
22 N = 1
PRINT 47
23 CONTINUE
NPHIE = 0
RADRAT = 1.00
VELRAT = 1.00
PHI = 0.95
PHIR = 0.95
EFF = 0.0
ETAC = .40
PSI = .99
ALFA1 = FLOAT(NALFA1)*3.1415927/180.
AKIS = 2.0
J = 1
13 AKIS = AKIS + 2.0
J = J + 1
170RBETA1 = ATANF(TANF(ALFA1) - ((1.0)/(PHI*COSF(ALFA1)*SQRTF
1 (1. - RSTAR)*SQRTF(AKIS)))
BETA1 = RBETA1*180./3.1415927
12 CONTINUE
0XSQR = (RSTAR*(1.+EFF)) + ((PHI*PHI)*(1.-RSTAR)*(PHIR-(VELRAT*
1 VELRAT*COSF(ALFA1)*COSF(ALFA1)/(PSI*PSI)))) - (2.*PHIR*PHI
2 *SINF(ALFA1)*SQRTF(1.-RSTAR)/SQRTF(AKIS)) + ((PHIR+RADRAT*
3 RADRAT-1.)/AKIS)
19 EXX = SQRTF(XSQR)
RBETA2=ATANF(-PSI*EXX/(PHI*VELRAT*COSF(ALFA1)*SQRTF(1.-RSTAR)))
BETA2 = RBETA2*180./3.1415927
20 DBETA = BETA1-BETA2
PSIA = 0.99 - .000228*DBETA - 4.97/(180.-DBETA)
DPSI = ABSF(PSI - PSIA)
IF (.0000001-DPSI) 10,11,11
10 PSI = PSIA
GO TO 12
11 PSI = PSIA
OETA = (2./SQRTF(AKIS))*((PHI*SINF(ALFA1)*SQRTF(1.-RSTAR))-
1 (RADRAT*RADRAT/SQRTF(AKIS))+(PSI*EXX*RADRAT))
OAKE = AKIS*((PHI*PHI*(1.-RSTAR)*COSF(ALFA1)*COSF(ALFA1)*VELRAT*
1 VELRAT)+((PSI*PSI)*XSQR)-(2.*PSI*EXX*RADRAT/SQRTF(AKIS)))
2 +((RADRAT*RADRAT)/AKIS))
VELM1 = PHI*SQRTF(1.-RSTAR)*SQRTF(AKIS)*COSF(ALFA1)
OALFA2 = ATANF(((RADRAT/SQRTF(AKIS))-(PSI*EXX))/(PHI*VELRAT*
1 COSF(ALFA1)*SQRTF(1.-RSTAR)))
ALFA2 = ALFA2*180./3.1415927
0WSQR1 = 1.+(AKIS*PHI*PHI*(1.-RSTAR))-2.*SQRTF(AKIS)*PHI*
1 SQRTF(1.-RSTAR)*SINF(ALFA1)
0WSQR2 = (PSI*PSI*AKIS)*(((1.+EFF)*RSTAR)+(PHIR*PHI*PHI*
1 (1.-RSTAR))-(2.*PHIR*PHI*SQRTF(1.-RSTAR)*SINF(ALFA1))/
2 (SQRTF(AKIS))+(PHIR+RADRAT*RADRAT-1.)/AKIS)
RELRAT = SQRTF(WSQR2)/SQRTF(WSQR1)
IF (J-6) 14,14,15
15 PRINT 47
J=2
140PRINT 41,NALFA1,NPHIE,RADRAT,VELRAT,PHI,PHIR,PSI,RSTAR,AKIS,
1 ETA,AKE,VELM1,RELRAT,BETA1,BETA2,ALFA2
IF (ETA-ETAC) 50,50,13
400FORMAT(/118H1 A1 PE R2/R1 VM2/VM1 PHI PHIR PSI R*)
1 KIS ETA KE VM1/U1 W2/W1 BETA1 BETA2 ALFA2 /
410FORMAT ( 13,I6,F7.1,F9.1,F8.2,F7.2,2F7.3,F8.3,F9.5,2F7.3,
1 F8.3,2F8.2,F7.2 )
47 FORMAT (/)
50 CONTINUE
END
END

```



```

PROGRAM TURBINE
DO 50 N=1,4
NALFA1 = 80 - (5*N)
PRINT 40
DO 50 I=1,12
RSTAR=-.05+(FLOATF(I))*.05
IF (I-7) 18,20,13
20 PRINT 40
18 CONTINUE
J = 1
K = 1
NPHIE = 0
ALFA1 = FLOATF(NALFA1)*3.1415927/180.
RADRAT = 1.00
VELRAT = 1.00
PHI = 0.95
PHIR = 0.95
AKIS=8.0
EFF = 0.0
PSI = .99
ETAA = 0.0
170 RBETA1 = ATANF(TANF(ALFA1) - ((1.0) / (PHI*COSF(ALFA1)*SQRTF
1 (1. - RSTAR)*SQRTF(AKIS)))
BETA1 = RBETA1*180./3.1415927
12 CONTINUE
0XSQR = (RSTAR*(1.+EFF))+((PHI*PHI)*(1.-RSTAR)*(PHIR-(VELRAT*
1 VELRAT*COSF(ALFA1)+COSF(ALFA1)/(PSI*PSI)))-(2.*PHIR*PHI
2 *SINF(ALFA1)*SQRTF(1.-RSTAR)/SQRTF(AKIS))+((PHIR+RADRAT*
3 RADRAT-1.)/AKIS))
EXX = SQRTF(XSQR)
RBETA2=ATANF(-PSI*EXX/(PHI*VELRAT*COSF(ALFA1)*SQRTF(1.-RSTAR)))
BETA2 = RBETA2*180./3.1415927
DBETA = BETA1-BETA2
PSIA = 0.99 - .000228*DBETA - 4.97/(180.-DBETA)
DPSI = ABSF(PSI-PSIA)
IF (.0000001-DPSI) 10,11,11
10 PSI = PSIA
K = K+1
IF (K-1000) 12,12,45
11 PSI = PSIA
0ETA = (2./SQRTF(AKIS))*((PHI*SINF(ALFA1)*SQRTF(1.-RSTAR))-*
1 (RADRAT+RADRAT/SQRTF(AKIS))+(PSI*EXX*RADRAT))
IF (ETA-ETAA) 13,14,14
13 DETA = ABSF(ETA-ETAA)
IF (.0000001-DETA) 15,16,16
14 CONTINUE
ETAA = ETA
DKIS = (-1)**J
AKIS = AKIS+DKIS
GO TO 17
15 J = J+1
IF (J-5) 14,14,43
43 PRINT 44
GO TO 50
45 PRINT 46
GO TO 50
16 CONTINUE
OAKE = AKIS*((PHI*PHI*(1.-RSTAR)*COSF(ALFA1)*COSF(ALFA1)*VELRAT*
1 VELRAT)+(PSI*PSI*XSR)-(2.*PSI*EXX*RADRAT/SQRTF(AKIS))
2 +(RADRAT+RADRAT/AKIS))
VELM1 = PHI*SQRTF(1.-RSTAR)*SQRTF(AKIS)*COSF(ALFA1)
OALFA2 = ATANF(((RADRAT/SQRTF(AKIS))-(PSI*EXX))/(PHI*VELRAT*-
1 COSF(ALFA1)*SQRTF(1.-RSTAR)))
ALFA2 = ALFA2*180./3.1415927
0WSQR2 = (PSI*PSI*AKIS)*(((1.+EFF)*RSTAR)+(PHIR*PHI*PHI*-
1 (1.-RSTAR))-(2.*PHIR*PHI*SQRTF(1.-RSTAR)*SINF(ALFA1))/
2 (SQRTF(AKIS))+(PHIR+RADRAT*RADRAT-1.)/AKIS)
0WSQR1 = 1.+(AKIS*PHI*PHI*(1.-RSTAR))-2.*SQRTF(AKIS)*PHI*-
1 SQRTF(1.-RSTAR)*SINF(ALFA1)
REL RAT = SQRTF(WSQR2)/SQRTF(WSQR1)
OPRINT 41,NALFA1,VPHIE,RADRAT,VELRAT,PHI,PHIR,PSI,RSTAR,AKIS,
1 ETA,AKE,VELM1,REL RAT,BETA1,BETA2,ALFA2
L = 1

```



```

19 CONTINUE
  ETAR = ETA-.005
24 AKIS=AKIS+.1
  K=1
  ORBETA1 = ATANF(TANF(ALFA1) - (( 1.0 ) / ( PHI*COSF(ALFA1)*SQRTF
  1 ( 1. - RSTAR)*SQRTF(AKIS)))) )
  BETAI = RBETA1*130./3.1415927
22 CONTINUE
  OXSQR = (RSTAR*(1.+EFF))+((PHI*PHI)*(1.-RSTAR)*(PHIR-(VELRAT*
  1 VELRAT*COSF(ALFA1)*COSF(ALFA1)/(PSI*PSI)))-(2.*PHIR*PHI*
  2 *SINF(ALFA1)*SQRTF(1.-RSTAR)/SQRTF(AKIS))+((PHIR+RADRAT*
  3 RADRAT-1.)/AKIS))
  EXX = SQRTF(XSQR)
  RBETA2=ATANF(-PSI*EXX/(PHI*VELRAT*COSF(ALFA1)*SQRTF(1.-RSTAR)))
  BETAI = RBETA2*130./3.1415927
  DBETA = BETAI-BETAI
  PSIA = 0.99 - .000228*DBETA - 4.97/(180.-DBETA)
  DPSI = ABSF(PSI-PSIA)
  IF (.0000001-DPSI) 21,25,25
21 PSI=PSIA
  K=K+1
  IF (K-1000) 22,22,45
25 PSI=PSIA
  OETA = (2./SQRTF(AKIS))*((PHI*SINF(ALFA1)*SQRTF(1.-RSTAR))-
  1 (RADRAT*RADRAT/SQRTF(AKIS))+(PSI*EXX*RADRAT))
  IF (ETA-ETAR) 23,24,24
23 CONTINUE
  M=1
55 AKIS=AKIS-.001
  M=M+1
  IF (1000-M) 51,35,35
35 CONTINUE
  ORBETA1 = ATANF(TANF(ALFA1) - (( 1.0 ) / ( PHI*COSF(ALFA1)*SQRTF
  1 ( 1. - RSTAR)*SQRTF(AKIS)))) )
  BETAI = RBETA1*130./3.1415927
  OXSQR = (RSTAR*(1.+EFF))+((PHI*PHI)*(1.-RSTAR)*(PHIR-(VELRAT*
  1 VELRAT*COSF(ALFA1)*COSF(ALFA1)/(PSI*PSI)))-(2.*PHIR*PHI*
  2 *SINF(ALFA1)*SQRTF(1.-RSTAR)/SQRTF(AKIS))+((PHIR+RADRAT*
  3 RADRAT-1.)/AKIS))
  EXX = SQRTF(XSQR)
  RBETA2=ATANF(-PSI*EXX/(PHI*VELRAT*COSF(ALFA1)*SQRTF(1.-RSTAR)))
  BETAI = RBETA2*130./3.1415927
  DBETA = BETAI-BETAI
  PSIA = 0.99 - .000228*DBETA - 4.97/(180.-DBETA)
  DPSI = ABSF(PSI-PSIA)
  IF (.0000001-DPSI) 36,38,38
36 PSI=PSIA
  GO TO 35
38 PSI=PSIA
  OETA = (2./SQRTF(AKIS))*((PHI*SINF(ALFA1)*SQRTF(1.-RSTAR))-
  1 (RADRAT*RADRAT/SQRTF(AKIS))+(PSI*EXX*RADRAT))
  IF (ETA-ETAR) 55,26,26
260 AKE = AKIS*((PHI*PHI*(1.-RSTAR)*COSF(ALFA1)*COSF(ALFA1)*VELRAT*.
  1 VELRAT)+((PSI*PSI)*XSQR)-(2.*PSI*EXX*RADRAT/SQRTF(AKIS)))
  2 +((RADRAT*RADRAT)/AKIS))
  VELM1 = PHI*SQRTF(1.-RSTAR)*SQRTF(AKIS)*COSF(ALFA1)
  OALFA2 = ATANF(((RADRAT/SQRTF(AKIS))-(PSI*EXX))/(PHI*VELRAT*.
  1 COSF(ALFA1)*SQRTF(1.-RSTAR)))
  ALFA2 = ALFA2*180./3.1415927
  OWSQR2 = (PSI*PSI*AKIS)*(((1.+EFF)*RSTAR)+(PHIR*PHI*PHI*.
  1 (1.-RSTAR))-(2.*PHIR*PHI*SQRTF(1.-RSTAR)*SINF(ALFA1))/
  2 (SQRTF(AKIS))+((PHIR+RADRAT*RADRAT-1.)/AKIS))
  OWSQR1 = 1.+((AKIS*PHI*PHI*(1.-RSTAR))-2.*SQRTF(AKIS)*PHI*.
  1 SQRTF(1.-RSTAR)*SINF(ALFA1))
  RELRAT = SQRTF(WSQR2)/SQRTF(WSQR1)
  OPRINT 41,NALFA1,VPHIE,RADRAT,VELRAT,PHI,PHIR,PSI,RSTAR,AKIS,
  1 ETA,AKE,VELM1,RELRAT,BETAI,BETA2,ALFA2
  L=L+1
  IF(L-3) 19,42,42
42 PRINT 47
  GO TO 50
51 PRINT 52
  GO TO 50

```



```
400 FORMAT(118H1 A1 PE R2/R1 VM2/VM1 PHI PHIR PSI R*
1 KIS ETA KE VM1/U1 W2/W1 BETA1 BETA2 ALFA2 /)
410 FORMAT (13,16,F7.1,F9.1,F8.2,F7.2,2F7.3,F8.3,F9.5,2F7.3,
1 F8.3,2F8.2,F7.2)
44 FORMAT (135H FIVE ITERATIONS OF AKIS COMPLETED)
46 FORMAT (134H 1000 ITERATIONS OF PSI COMPLETED)
52 FORMAT (35H 1000 ITERATIONS OF AKIS COMPLETED )
47 FORMAT (///)
48 FORMAT (1H1)
50 CONTINUE
END
END
```


PROGRAM FANNO3

FORTRAN NAMES, EQUIVALENT SYMBOLS AND DEFINITIONS

A	P/p	Pressure ratio
DAB		Name for the term $(p/P)^{\exp 2}$
DAN		Name for the term $(p/P)^{\exp 1}$
EE		Reheat factor defined by $(\xi_p - \xi)/(1 - \xi)$
EN	n	Polytropic exponent. See Appendix I
EXP1		Exponent #1 = $(2/n)$
EXP2		Exponent #2 = $(n+1)/n$
EXP3		Exponent #3 = $(1 - \xi_p)(\gamma - 1)/\gamma$
EXP4		Exponent #4 = $(\gamma - 1)/\gamma$
GAM	γ	Specific heat ratio
PH1	ϕ	Flow function
PH12	ϕ^2	Flow function squared. Intermediate step in finding
RA		Name for the term $(p/P)^{\exp 3}$
RB		Name for the term $(p/P)^{\exp 4}$
R		Computed loss coefficient to be used for determining p . $R = (RA - RB)/(1 - RB)$
ZETA	ξ	Loss coefficient = $1 - \gamma$
ZETAP	ξ_p	Polytropic loss coefficient defined in Appendix I


```

PROGRAM FANNO3
DIMENSION PHI(11),ZETA(11),ZETAP(11),EE(11)
DO 22 I = 125,140
XI = I
GAM = XI/100.
100FORMAT (26H1FLOW FUNCTION FOR GAMMA = F5.2//  

19H PRESSURE )
3100FORMAT (30H1 ZETA POLYTROPIC FOR GAMMA = F5.2//  

19H PRESSURE )
2100FORMAT (32H1 REHEAT FACTOR *E* FOR GAMMA = F5.2//  

19H PRESSURE )
      WRITE OUTPUT TAPE 3,10,GAM
      WRITE OUTPUT TAPE 4,310,GAM
      WRITE OUTPUT TAPE 5,210,GAM
      DO 11 M = 1,11
11 ZETA(M) = -.025+.025*FLOATF(M)
12 FORMAT (18H RATIO ZETA = 11F9.3//)
      WRITE OUTPUT TAPE 3,12,ZETA
      WRITE OUTPUT TAPE 4,12,ZETA
      WRITE OUTPUT TAPE 5,12,ZETA
      A = 1.02
13 CONTINUE
      DO 111 N = 1,11
      ZETA(N) = -.025+.025*FLOATF(N)
      ZETAP(N) = -.001
102 ZETAP(N) = +.001+ZETAP(N)
      EXP3 = (1.-ZETAP(N))*(GAM-1.)/GAM
      EXP4 = (GAM-1.)/GAM
      RA = 1./(A**EXP3)
      RB = 1./(A**EXP4)
      R = (RA-RB)/(1.-RB)
      DIFF = ZETA(N)-R
      IF (DIFF) 101,100,102
101 ZETAP(N) = -.00001+ZETAP(N)
      EXP3 = (1.-ZETAP(N))*(GAM-1.)/GAM
      EXP4 = (GAM-1.)/GAM
      RA = 1./(A**EXP3)
      RB = 1./(A**EXP4)
      R = (RA-RB)/(1.-RB)
      DIFF = ZETA(N)-R
      IF (DIFF) 101,100,100
100 EN = GAM/(1.+ZETAP(N)*(GAM-1.))
      EXP1 = 2./EN
      EXP2 = (EN+1.)/EN
      DAN = 1./(A**EXP1)
      DAR = 1./(A**EXP2)
      PHI2 = 2.*((GAM/(GAM-1.))*(DAN-DAB))
      PHI(N) = SQRTF(PHI2)
111 EE(N) = (ZETAP(N)-ZETA(N))/(1.-ZETA(N))
      WRITE OUTPUT TAPE 3,15,A,PHI
      WRITE OUTPUT TAPE 4,15,A,ZETAP
      WRITE OUTPUT TAPE 5,15,A,EE
15 FORMAT (F6.2,13X,11F9.5)
      IF (A-1.99) 17,19,19
17 A = A+.02
      GO TO 13
19 IF (5.9-A) 22,20,20
20 A = A+.20
21 GO TO 13
22 CONTINUE
400 FORMAT (8F12.5)
END
END

```


PROGRAM FANNO4

FORTRAN NAMES, EQUIVALENT SYMBOLS AND DEFINITIONS

A		Interim critical pressure ratio while computing
CPHI		Compute ϕ , subroutine name
DAB		Name for the term $(p/P)^{\exp 6}$
DAN		Name for the term $(p/P)^{\exp 5}$
DIFF		Difference between given and computed loss coefficient
EN	n	Polytropic exponent
EXP1		Exponent #1 = $(\gamma - 1)/\gamma$
EXP4		Exponent #4 = $(1 - \xi_p) (\gamma - 1)/\gamma$
EXP5		Exponent #5 = $2/n$
EXP6		Exponent #6 = $(n+1)/n$
GAM	γ	Specific heat ratio
PH	$(P/p)_{cr}$	Critical pressure ratio name for storing away and printing
PHI	ϕ	Flow function assumed for comparison
PHI2	ϕ^2	Flow function, squared
PHIC	ϕ_c	Flow function computed in subroutine based on γ and ξ
PHICR	ϕ_{cr}	Choked flow value of flow function
PPCR	$(P/p)_{cr}$	Choked flow value of pressure ratio
PR	P/p	Pressure ratio
R		Computed loss coefficient
RA		Name for the term $(p/P)^{\exp 4}$
RB		Name for the term $(p/P)^{\exp 1}$

Z	ζ_p	Polytropic loss coefficient name for storing away and printing
ZETA	ζ	Loss coefficient
ZETAP	ζ_p	Polytropic loss coefficient


```

PROGRAM FANNO4
DIMENSION ZETA(11),PR(11),PH(11),Z(11)
PRINT 400
DO 499 J=1,11
499 ZETA(J)=-.025+.025*FLOAT(J)
PRINT 401,ZETA
DO 490 I = 125,140
XI=I
GAM= XI/100.
DO 498 K=1,11
A = 1.8
PHI=0.2
497 CONTINUE
CALL CPHI (GAM,ZETA(K),A,PHIC,PHICR,PPCR,ZETAP)
IF (PHIC-PHI) 494,493,495
495 CONTINUE
PHI = PHIC
A = PPCR
GO TO 497
494 DIFF = ABSF(PHIC-PHI)
IF (DIFF-.0000001) 493,493,496
496 CONTINUE
PHI = PHIC
A = PPCR
GO TO 497
493 CONTINUE
PR(K) = PPCR
PH(K) = PHICR
Z(K) = ZETAP
498 CONTINUE
IF(I=133) 492,491,492
491 PRINT 400
PRINT 401,ZETA
492 PRINT 402,GAM
PRINT 412,PH
PRINT 403,PR
PRINT 404,Z
4000 FORMAT (90H1 CHOCHED FLOW VALUES OF THE FLOW FUNCTION, PRESSURE RAI
110 AND POLYTROPIC LOSS COEFFICIENT //)
401 FORMAT (11X7HZETA = 11F9.3//)
402 FORMAT (7H GAMMA= F4.2)
412 FORMAT (18H PHI = 11F9.5//)
403 FORMAT (18H (PO/P)C = 11F9.5//)
404 FORMAT (18H ZETAP = 11F9.5//)
490 CONTINUE
END
SUBROUTINE CPHI (GAM,ZETA,A,PHIC,PHICR,PPCR,ZETAP)
ZETAP = -.001
500 ZETAP=0.001+ZETA
EXP4=(1.-ZETAP)*(GAM-1.)/GAM
EXP1 = (GAM-1.)/GAM
RA = 1./(A**EXP4)
RB = 1./(A**EXP1)
R = (RA-RB)/(1.-RB)
IF(ZETA-R) 501,502,500
501 ZETAP=-.00001+ZETAP
EXP4=(1.-ZETAP)*(GAM-1.)/GAM
EXP1 = (GAM-1.)/GAM
RA = 1./(A**EXP4)
RB = 1./(A**EXP1)
R = (RA-RB)/(1.-RB)
IF(ZETA-R) 501,502,502
502 EN=GAM/(1.+ZETAP*(GAM-1.))
EXP5 = 2./EN
EXP6 = (EN+1.)/EN
DAN = 1./(A**EXP5)
DAB = 1./(A**EXP6)
PHI2 = 2.*((GAM/(GAM-1.))*(DAN-DAB))
PHIC = SQRTF(PHI2)
OPHICR=((2./(EN+1.))**((1./(EN-1.)))*SQRTF((2./EXP1)*((EN-1.)/
1.(EN+1.))))
PPCR = ((EN+1.)/2.)*((EN/(EN-1.))
END

```



```

PROGRAM AFTER
AME = 1.37
NALFA = 75
ALFA = FLOATF(NALFA)*3.1415927/180.
GAMMA = 1.37
EXP = (GAMMA - 1.)/GAMMA
EE = (2. / ((GAMMA - 1.)*AME*AME))
PRINT 409
PRINT 410,AME,NALFA,GAMMA
PRINT 404
DO 500 L = 1,26
PRAT = 1.02 - .02*FLOATF(L)
DALFA = 0.0
M = 0
100 M = M+1
101 DALFA = (-.1)**(M-1)+DALFA
DALFAR = DALFA*3.1415927/180.
COSRAT = COSF(ALFA)/COSF(ALFA-DALFAR)
AA = GAMMA*AME*AME*COSF(DALFAR)-COSRAT*(GAMMA-1.)*AME*AME/2.
BB = -GAMMA*AME*AME-1.
CC = COSRAT*(1.+(GAMMA-1.)*AME*AME/2.1)
DD = BB*BB-4.*AA*CC
IF (DD) 101,200,200
200 VELRAT1 = (-RB+SQRTF(DD))/(2.*AA)
OPRAT1 = (COSRAT*(1.+(GAMMA-1.)*AME*AME/2.1)*(1.-VELRAT1*VELRAT1))
1 /VELRAT1
ZA = 1.-(VELRAT1*VELRAT1)/(1.+EE-EE*(PRAT1**EXP))
DIFF = ABSF(PRAT1-PRAT)
IF (DIFF-.0001) 300,300,102
102 IF (PRAT1-PRAT) 103,300,101
103 M = M+1
104 DALFA = (-.1)**(M-1)+DALFA
DALFAR = DALFA*3.1415927/180.
COSRAT = COSF(ALFA)/COSF(ALFA-DALFAR)
AA = GAMMA*AME*AME*COSF(DALFAR)-COSRAT*(GAMMA-1.)*AME*AME/2.
BB = -GAMMA*AME*AME-1.
CC = COSRAT*(1.+(GAMMA-1.)*AME*AME/2.1)
DD = BB*RB-4.*AA*CC
IF (DD) 100,105,105
105 VELRAT1 = (-RB+SQRTF(DD))/(2.*AA)
OPRAT1 = (COSRAT*(1.+(GAMMA-1.)*AME*AME/2.1)*(1.-VELRAT1*VELRAT1))
1 /VELRAT1
ZA = 1.-(VELRAT1*VELRAT1)/(1.+EE-EE*(PRAT1**EXP))
DIFF = ABSF(PRAT1-PRAT)
IF (DIFF-.0001) 300,300,106
106 IF (PRAT-PRAT1) 100,300,104
300 PRINT 412,PRAT,PRAT1,VELRAT1,DALFA,ZA,AMD,AMA
GO TO 500
401 FORMAT (20H B2-4AC IS NEGATIVE /)
4020 FORMAT (60H A B C COSRAT GAMMA
1 AME )
403 FORMAT (6F10.6/)
404 FORMAT (46H PRAT PRAT1 VELRAT1 DALFA ZA /)
405 FORMAT (/E20.10)
406 FORMAT (F7.4,4F10.4)
409 FORMAT (25H1 MACH ALFA GAMMA /)
410 FORMAT (F10.3,I5,F10.3 /)
411 FORMAT (66H PRAT PRAT1 VELRAT1 DALFA ZA
1 MD MA /)
412 FORMAT (7F10.4)
500 CONTINUE
END
END

```


Appendix IV. Critical Mach Number of Flow Undergoing Polytropic Expansion.

The critical pressure ratio for a flow undergoing a polytropic expansion, as developed in Appendix I, is

$$\left(\frac{P}{P_{cr}}\right) = \left(\frac{n+1}{2}\right)^{\frac{m}{m-1}} \quad (I,13)$$

To find the maximum velocity corresponding to this pressure ratio it must be recalled that, for a polytropic process

$$pv^n = \text{constant} \quad (IV,1)$$

$$p\left(\frac{RT}{p}\right)^n = p^{1-n}T^n = \text{constant}$$

$$T = C p^{\frac{n-1}{n}} \quad (IV,2)$$

where C is a constant

Therefore

$$\left(\frac{T}{T_0}\right) = \left(\frac{p}{P_0}\right)^{\frac{n-1}{n}}$$

$$T = T_0 \left(\frac{P_0}{p}\right)^{-\frac{n-1}{n}} \quad (IV,3)$$

Using the T-s diagram of Fig. 24 as a reference, it can be seen that

$$T_0 - T = T_0 \left[1 - \left(\frac{p}{P_0}\right)^{\frac{n-1}{n}} \right]$$

and

$$\frac{V^2}{2gJ} = \zeta_p(T_0 - T) = \frac{R}{J} \frac{\gamma}{\gamma-1} T_0 \left[1 - \left(\frac{P}{P_0} \right)^{\frac{m-1}{m}} \right] \quad (\text{IV,4})$$

For the critical velocity then, using (I,13)

$$V_{cr}^2 = 2gR \frac{\gamma}{\gamma-1} T_0 \left[1 - \left\{ \frac{1}{\left(\frac{m+1}{2} \right)^{\frac{m}{m-1}}} \right\}^{\frac{m-1}{m}} \right]$$

which reduces to

$$V_{cr}^2 = 2gRT_0 \frac{\gamma}{\gamma-1} \left(\frac{m-1}{m+1} \right) \quad (\text{IV,5})$$

The acoustic velocity is

$$a^2 = \gamma gRT = \gamma gRT_0 \left(\frac{P}{P_0} \right)^{\frac{m-1}{m}} = \gamma gRT_0 \left(\frac{m+1}{2} \right)^{\left(\frac{m}{m-1} \right) \left(-\frac{m-1}{m} \right)}$$

which reduces to

$$a^2 = \gamma gRT_0 \left(\frac{2}{m+1} \right) \quad (\text{IV,6})$$

Therefore

$$M_{cr}^2 = \frac{V_{cr}^2}{a^2} = \frac{m-1}{\gamma-1} \quad (\text{IV,7})$$

Also developed in Appendix I was the relation for the polytropic exponent n , in terms of the polytropic loss coefficient, as

$$n = \frac{\gamma}{\xi_p(\gamma-1) + 1} \quad (I,7)$$

Making this substitution, and collecting terms

$$\frac{n-1}{\gamma-1} = \frac{1-\xi_p}{\xi_p \gamma - \gamma - 1} \quad (IV,8)$$

and

$$M_{cr} = \sqrt{\frac{1-\xi_p}{1+\xi_p(\gamma-1)}} \quad (IV,9)$$

For example, for $\gamma = 1.37$ and $\xi_p = 0.10$, $M_{cr} = .931$,
and for $\xi_p = 0.20$, $M_{cr} = .854$.

DUDLEY KNOX LIBRARY



3 2768 00033249 8